University of Southern Queensland

Faculty of Engineering & Surveying

Carbon Nanotubes (CNT) as Potentially a More Effective Material for Photovoltaic (PV) Converters

A dissertation submitted by

Craig Gardner

in fulfilment of the requirements of

ENG4112 Research Project

towards the degree of

Bachelor of Engineering (Electrical / Electronic)

Submitted: October, 2008

Abstract

The global community's desire for cheap, efficient, truly sustainable energy generation is ever present. Contemporary silicon based PV's are used extensively and have a present maximum experimental efficiency of $\approx 24\%$. These inorganic devices require expensive high-temperature fabrication methods and their economic considerations vary. Organic PV's have the benefit of being much cheaper and easier to fabricate and have mechanical flexibility for curved architectural applications. However, organic PV's currently have lower efficiencies than silicon PV's as well as other downside factors.

Contemporary doped silicon PV's follow pn junction theory and photocurrent generation is via the creation and flow of minority carriers. The carbon molecule C_{60} buckminsterfullerene "buckyball" was discovered in 1985 by researchers at Rice University. Buckyballs, other carbon molecule fullerenes and the related and so-named carbon nanotubes (CNT) have diameters in the order of single-digit nanometers. They also have extremely high electronic transport, tensile strength and thermal transfer characteristics as well as other unique qualities.

One type of organic PV being tested is a blend of electron-donor-type polymer and electron-accepting fullerene, where the interface between the two materials is dispersed within the active layer making up the bulk heterojunction (BHJ) device. Photocurrent is generated when excitons created by light absorption, then dissociate at an interface to become majority carriers in the respective materials. This makes the organic PV a majority carrier device in contrast to the inorganic PV as a minority carrier device.

The aim of this research project was to research respective inorganic and organic PV theory and concepts and to create MATLAB® models that may be run and altered

to observe the theoretical change in output and efficiency to enhance understanding.

An inorganic silicon PV MATLAB® model has been created and while not perfect, it appears to follow most expectations when different physical PV characteristics are altered. This model requires further refinement and development and some insight into the limitations of and the possible future direction of this model are included in this work.

The organic PV theory and concepts and the consequent MATLAB® model are incomplete. However like the inorganic PV model, the progress to date of the organic PV model and it's possible future direction and development are also included in this work.

University of Southern Queensland

Faculty of Engineering and Surveying

ENG4111/2 *Research Project*

Limitations of Use

The Council of the University of Southern Queensland, its Faculty of Engineering and Surveying, and the staff of the University of Southern Queensland, do not accept any responsibility for the truth, accuracy or completeness of material contained within or associated with this dissertation.

Persons using all or any part of this material do so at their own risk, and not at the risk of the Council of the University of Southern Queensland, its Faculty of Engineering and Surveying or the staff of the University of Southern Queensland.

This dissertation reports an educational exercise and has no purpose or validity beyond this exercise. The sole purpose of the course pair entitled "Research Project" is to contribute to the overall education within the student's chosen degree program. This document, the associated hardware, software, drawings, and other material set out in the associated appendices should not be used for any other purpose: if they are so used, it is entirely at the risk of the user.

Prof F Bullen

Dean

Faculty of Engineering and Surveying

Certification of Dissertation

I certify that the ideas, designs and experimental work, results, analyses and conclusions set out in this dissertation are entirely my own effort, except where otherwise indicated and acknowledged.
I further certify that the work is original and has not been previously submitted for assessment in any other course or institution, except where specifically stated.

Craig Gardner

0019323790

_____

Signature

_____

Date

Acknowledgments

My sincere thanks to Dr. Tony Ahfock (USQ) and Prof. Nunzio Motta (QUT) for their generous and patient guidance.

Thanks to Assoc. Prof. John Leis (USQ) for his kind assistance with all manner of things. Thanks go to the USQ Library and the USQ Faculty of Engineering and Surveying for their assistance.

Paul McCarthy deserves special mention for his unwavering support and friendship through thick and thin.

Thanks also to my Ergon Energy colleagues for their support and the Ergon Energy eLibrary in particular.

Finally, this work and the long progression towards it would not have been possible without the support of my wife Anne, my parents Pat and Snow Gardner, our extended families and our friends.

Craig Gardner

University of Southern Queensland
October 2008

Contents

List of Figures

List of Tables

Chapter 1

Introduction

The global community's desire for cheap, efficient, truly sustainable energy generation is ever present. Contemporary silicon based PV's are used extensively and have a present maximum experimental efficiency of $\approx 24\%$. These inorganic devices require expensive high-temperature fabrication methods and their economic considerations vary. Organic PV's have the benefit of being much cheaper and easier to fabricate and have mechanical flexibility for curved architectural applications. However, organic PV's currently have lower efficiencies than silicon PV's as well as other downside factors.

This work is in standard format starting with a literature review, methodology, analysis and results and finally conclusions. Each of these chapters has sections within for both the inorganic silicon PV and the organic PV theory and applications with a comparison of the two summarised within the conclusions chapter.

The science behind the silicon PV is quite mature but complex and convoluted, and as such this part of the literature review is necessarily long and hopefully informative. This work presents theory on light and it's absorption by semiconductors and the consequent photovoltaic effect and progresses to the methodology of modeling generation, collection efficiency and the various model outputs. In this, recent collection efficiency research concepts are used in the modeling. Next, is the presentation of the results and respective analysis of the various model outputs. Finally conclusions are drawn as well as a summary of the model limitations and suggested further work.

The carbon molecule C_{60} buckminsterfullerene "buckyball" was discovered in 1985 by researchers at Rice University. Buckyballs, other carbon molecule fullerenes and the related and so-named carbon nanotubes (CNT) have diameters in the order of single-digit nanometers. They also have extremely high electronic transport, tensile strength and thermal transfer characteristics as well as other unique qualities.

One type of organic PV being tested is a blend of electron-donor-type polymer and electron-accepting fullerene, where the interface between the two materials is dispersed within the active layer making up the bulk heterojunction (BHJ) device. Photocurrent is generated when excitons created by light absorption, then dissociate at an interface to become majority carriers in the respective materials. This makes the organic PV a majority carrier device in contrast to the inorganic PV as a minority carrier device.

The science behind the organic PV is quite young and research and development continues. This work presents a brief literature review on organic PV concepts and recent research efforts to simulate an organic PV with an optical and an electrical model. Recent research indicates that an organic PV may be simulated with only an electrical model. The methodology describes an interpretation of the mathematical iterative approach to find an equilibrium solution to the electrical model which could possibly show the way for future work. As the organic PV model was not complete the results and analysis contains only a reference to the code completed.

The following project aim and objectives are defined within the project specification in Appendix A.

1.1 Project Aim

The aim of this research project as originally defined is to determine the viability of carbon nanotubes (CNT) as a more effective material for photovoltaic (PV) converters and (if time permits) a material for renewable energy storage capacitors. However due to time constraints and the complexity of the task it was not possible to address CNT with respect to renewable energy storage capacitors.

In retrospect, an additional holistic aim of this project is to research respective inorganic and organic PV theory and concepts to create MATLAB® models that may be run and altered to observe the theoretical change in output and efficiency to enhance understanding.

1.2 Project Objectives

The objectives of the project are:

- Research and report on the theory behind contemporary silicon based PV converters.
- Create a MATLAB® program to model a contemporary silicon based PV converter.
- Research and report on the theory behind CNT and their potential use as a material in PV converters.
- Draw a parallel between the theories and the principles behind contemporary silicon based PV converters and those based on CNT.
- Create a MATLAB® program to model a theoretical CNT based PV converter.
- Draw conclusions on potential advantages of using CNT as as a base material for PV converters.

and if time permits to:

- Discuss the need for storage systems in renewable energy systems.
- Theory behind a potential storage capacitor based on CNT.

Chapter 2

Literature Review

2.1 Light

2.1.1 Theory of Light

The concept of light can be thought of in either of two ways. Firstly, Max Planck in 1900 established the idea that light can be described as a wide spectrum of electromagnetic waves of different wavelengths. Then, in 1905 Einstein proposed that light is made up of discrete particles (quanta) of energy (now called photons). Photovoltaic (PV) theory and characteristics utilise both of these concepts of light for different purposes which come together in the equation (referred to as particle-wave duality) for the energy of light (Wenham, Green, Watt & Corkish 2007):

$$E = h.f = \frac{h.c}{\lambda}(J) \tag{2.1}$$

where h = Plank's constant = 6.626 x $10^{-34}(J.s)$;

f = frequency of light (Hz);

c = speed of light in a vacuum = 2.998 x $10^{8}(m.s^{-1})$;

λ = wavelength of light (m).

A light source falling upon a PV may be described in terms of spectral irradiance F, radiant power density H or photon flux Φ.

2.1.2 Spectral Irradiance, Radiant Power Density and Photon Flux

Appendix B shows the interrelationship between spectral irradiance F, radiant power density H and photon flux Φ with respect to the silicon PV model.

Spectral irradiance represents power per unit area at a particular wavelength of light. Spectral irradiance can be determined for a particular wavelength if the photon flux for that wavelength is available (or vice versa) (Wenham et al. 2007):

$$F(\lambda) = \frac{\Phi(\lambda).E(\lambda)}{\lambda}(W.m^{-2}.\mu m^{-1}) \tag{2.2}$$

where $\Phi(\lambda)$ = photon flux at wavelength λ $(s^{-1}.m^{-2})$;
$E(\lambda)$ = energy at wavelength λ (J);
λ = wavelength of light (μm).

The pathlength that sunlight must take to reach the earth is referred to as Air Mass (AM). This pathlength is approximated by $1/\cos\theta$, where θ is the angle between the sun and the point directly overhead (for AM1.5, $\theta = 48.2°$) (Wenham et al. 2007).

Figure 2.1 shows spectral irradiance values of sunlight at Air Mass 1.5 (AM1.5 sun) provided by the National Renewable Energy Laboratory or NREL (NREL 2008) used extensively in the testing of PV's.

Radiant power density is the integral of spectral irradiance over a range of wavelengths of light. However, radiant power density can also be determined for a particular wavelength by using photon flux and the energy of that particular wavelength of light (Wenham et al. 2007):

$$H(\lambda) = \Phi(\lambda).E(\lambda)(W.m^{-2}) \tag{2.3}$$

where $\Phi(\lambda)$ = photon flux at wavelength λ $(s^{-1}.m^{-2})$;
$E(\lambda)$ = energy at wavelength λ (J).

Inspection of equation (2.3) shows that less high energy photons (eg. blue / violet) are required than lower energy photons (eg. red) to achieve the same radiant power

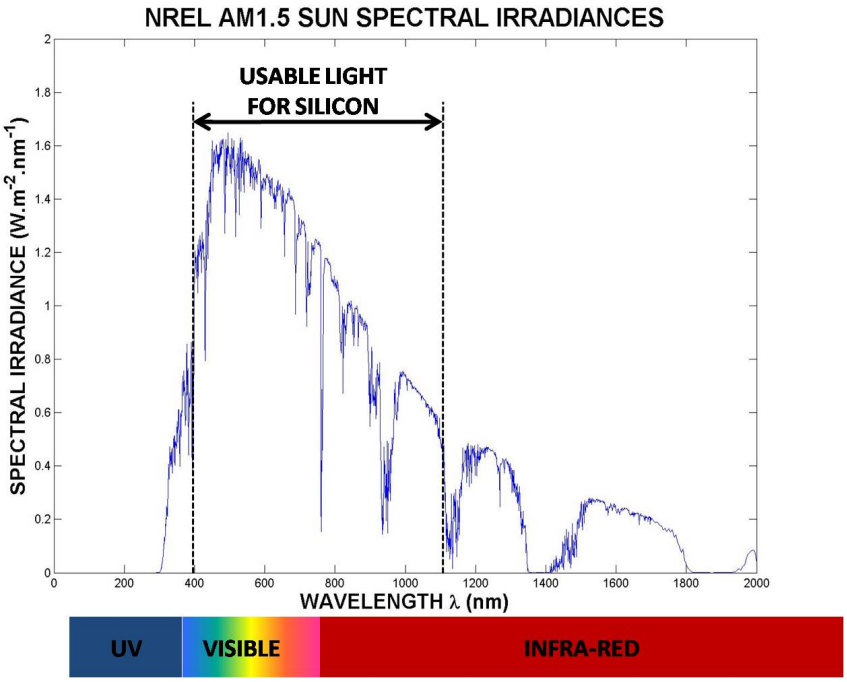

Figure 2.1: Plot of NREL AM1.5 Spectral Irradiance Figures vs Wavelength of Light

density. The radiant power density of a $AM1.5$ source integrated over all wavelengths $\approx 1kW/m^2$ (Wenham et al. 2007).

Photon flux Φ gives the number of photons per second per unit area. However, photon flux gives no information about the energy of the photons nor to what wavelength of light the photons belong - this must be specified. Photon flux is used in determining the number of electron-hole pairs that are generated (and therefore in determining light generated current) and can be calculated using the equation:

$$\Phi(\lambda) = \frac{F(\lambda).\lambda^2}{h.c}(10^{-6}.m^{-2}.s^{-1}) \tag{2.4}$$

where $F(\lambda)$ = spectral irradiance at wavelength λ $(W.m^{-2}.\mu m^{-1})$;

λ = wavelength of light (m);

h = Plank's constant = 6.626 x $10^{-34}(J.s)$;

c = speed of light in a vacuum = 2.998 x $10^8(m.s^{-1})$.

2.2 Silicon Semiconductors and Light

2.2.1 Semi-Conductor Materials

2.2.2 Intrinsic Semi-Conductors

An atom is made up of a nucleus of positively charged protons and neutral neutrons with negatively charged electrons orbiting around the nucleus in layers. These layers are of varying distance from the nucleus and electron energy increases as distance from the necleus increases. The electrons in the outer layer electrons are named valence electrons and being furthest from the nucleus hold the highest amount of energy.

III	IV	V
B	C	
Al	Si	P
Ga	Ge	As

Table 2.1: Extract from the Periodic Table

Table 2.1 shows an extract from the periodic table where each material is grouped according to the number of valence electrons within each atom of the material. Silicon is shown to be a group IV material which have four valence electrons. Covalent bonding is a chemical bonding created between atoms when valence electrons are shared between two atoms. This type of bonding is relatively strong and highly directional through mutual attraction between individual atoms creating a specific structure. Figure 2.2 shows how the silicon valence electrons interact with the neighbouring four atoms with each line representing a covalent bond. In silicon as well as other semi-conductor materials this forms a tight tetrahedral structure.

When temperature is at absolute zero ($T = 0K = -273.16°C$) each of the valence electrons are in their shared place between atoms and are at their lowest energy level. In this state, even with a small electric field applied the covalent bond between silicon atoms will hold their valence electrons in place. No free movement of electrons within the material makes silicon an insulator at $T = 0K$.

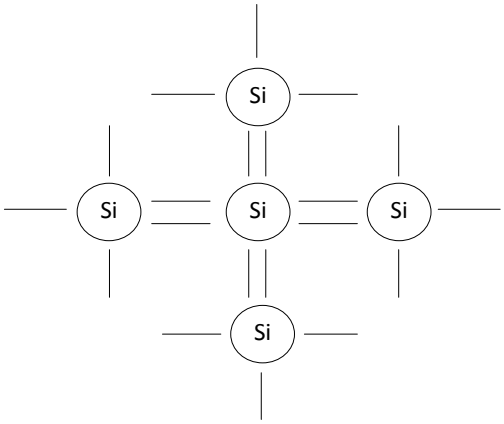

Figure 2.2: Silicon Atomic Structure

As material temperature increases, valence electrons gain thermal energy and when valence electrons reach the minimum bandgap energy level of the material E_g they leave the valence band and move to the conduction band where they are free to move within the material. As the net charge of a material is neutral this will leave behind a positively charged hole in the valence band from where the valence electron has moved. As temperature increases further, more valence electrons reach the minimum bandgap energy level, break the covalent bond, move to the conduction band and move within the material. So it is with the flow of free electrons in the conduction band (and holes within the valence band) that a capacity for current is created within the material.

The bandgap energy of a material tends to decrease marginally as the temperature increases such that (Zeghbroeck 2008):

$$E_g \approx E_g(0) - \frac{\alpha.T^2}{T+\beta} \tag{2.5}$$

where for silicon $E_g(0) = 1.166(eV)$;

$\alpha = 0.473(meV.K^{-1})$;

$\beta = 636(K)$;

$T =$ absolute temperature (K).

Using equation (2.5), a semiconductor such as silicon has a bandgap energy at room temperature in the order of $E_g(300K) = 1.12eV$ which allows a moderate amount of

free electron flow and therefore moderate current flow. Materials such as copper have a low bandgap energy at room temperature which allow more electrons to flow and are therefore classed as conductors. Conversely, materials such as porcelain with a high bandgap energy at room temperature retard electrons from flowing and are therefore insulators.

The intrinsic carrier concentration n_i of an intrinsic semiconductor material such as silicon is the number of electrons in the conduction band or holes in the valence band per unit volume. This number of carriers per unit volume depends on the bandgap and the temperature of the material. At $T = 300K$ an approximate intrinsic carrier concentration of silicon $n_i \approx 10^{10} cm^{-3}$ however an empirical fit to the measured intrinsic carrier concentration of silicon for temperature $T = 275$K to 375K is given by (Honsberg & Bowden 2008):

$$n_i \approx 9.38.10^{19} \left(\frac{T}{300}\right)^2 .exp\left(\frac{-6884}{T}\right) (cm^{-3}) \tag{2.6}$$

Inspection of equation (2.6) shows that at elevated temperatures, the intrinsic carrier concentration of a material increases which is consistent with physical expectations. Using equation (2.6) determines that at temperature $T = 25°C \approx 297K$, intrinsic carrier concentration $n_i \approx 8.6$ x $10^9 (cm^{-3})$.

Extrinsic Semi-Conductors

Intrinsic semiconductors such as silicon are a single crystal material with no other atoms within the material. The electron and hole densities of intrinsic semiconductors are approximately equal but of such relatively low concentration that allow only small currents.

As such, for an intrinsic semiconductor at equilibrium, the product of the majority and minority carrier concentrations is a constant equal to the square of the intrinsic carrier concentration:

$$n_0.p_0 = n_i^2 (cm^{-6}) \tag{2.7}$$

where n_0 = electron carrier concentration at equilibrium (cm^{-3});

p_0 = hole carrier concentration at equilibrium (cm^{-3});

n_i = intrinsic carrier concentration (cm^{-3}).

Electron or hole concentrations of intrinsic semiconductors such as silicon can be increased by adding controlled amounts of donor or acceptor impurities to provide extra electrons or holes respectively. Impurities added will enter the crystalline lattice of silicon even though the impurity atoms do not have the same number of valence electrons. This process of adding impurities to an intrinsic semiconductor to create an extrinsic semiconductor is called doping.

The doping of silicon with a donor impurity such as phosphorous (which has five valence electrons loosely bound to the phosphorous atom) donates extra electrons free to move without creating a positively charged hole. This creates an n-type material with a net negative charge. For n-type (eg. emitter in silicon PV) materials, electrons are the majority carrier and holes are the minority carrier.

The doping of silicon with an acceptor impurity such as boron (which has three valence electrons) creates positively charged holes able to accept electrons without creating the electrons. This will create an abundance of positively charged holes making it a p-type material with a net positive charge. For p-type materials (eg. base in silicon PV), holes are the majority carrier and electrons are the minority carrier.

As the doping of an intrinsic semiconductor usually creates an electron or hole concentration several orders of magnitude greater than the intrinsic carrier concentration of the material, the majority electron or hole carrier concentration approximates the doping electron or hole concentration respectively.

From this assumption come the following set of approximate equations for electron and hole carrier concentrations at equilibrium (Honsberg & Bowden 2008). For n-type:

$$n_0 = N_D, p_0 = \frac{n_i^2}{N_D}(cm^{-3}) \tag{2.8}$$

where N_D = electron doping concentration (cm^{-3});

n_i = intrinsic carrier concentration (cm^{-3}).

For p-type:

$$p_0 = N_A, n_0 = \frac{n_i^2}{N_A}(cm^{-3}) \tag{2.9}$$

where N_A = hole doping concentration (cm^{-3});

n_i = intrinsic carrier concentration (cm^{-3}).

This means that as doping of donor or acceptor impurites increases, the concentration of minority hole or electron carriers decrease respectively. This can be explained by imagining the free electrons in the conduction band of a donor doped n-type material taking up existing holes in the valence band of the undoped intrinsic material.

2.2.3 Light Absorption and Generation

Light Absorption

When light falls upon a semiconductor based PV it can be reflected, absorbed or transmitted through the semiconductor. Reflected light and light that is transmitted through the system are considered losses and play no part in the generation of electron-hole pairs within the semiconductor. Whether light is absorbed or transmitted through the system is dependent on the energy of the photons. If a photon has energy below that of the semiconductor bandgap energy then it cannot move an electron from the valence to the conduction band and is transmitted through the system as if it were transparent. However, if a photon has energy equal to the semiconductor bandgap energy then it will move an electron to the conduction band effectively generating an electron-hole pair. If a photon has energy greater than the semiconductor emitter bandgap energy then multiple electron-hole pairs will be generated dependent on the photon energy.

The absorption coefficient α determines how far into a material light of a particular wavelength can penetrate before it is absorbed to 36% (ie. $\frac{1}{e}$) of it's original energy (Honsberg & Bowden 2008). Figure 2.3 graphs the absorption coefficient data (accessed from (Honsberg & Bowden 2008) and provided in Appendix F) and it's inverse absorption depth against various wavelengths of light for crystalline silicon at 300K. Manipulating the inverse of absorption coefficient data gives the absorption depth in

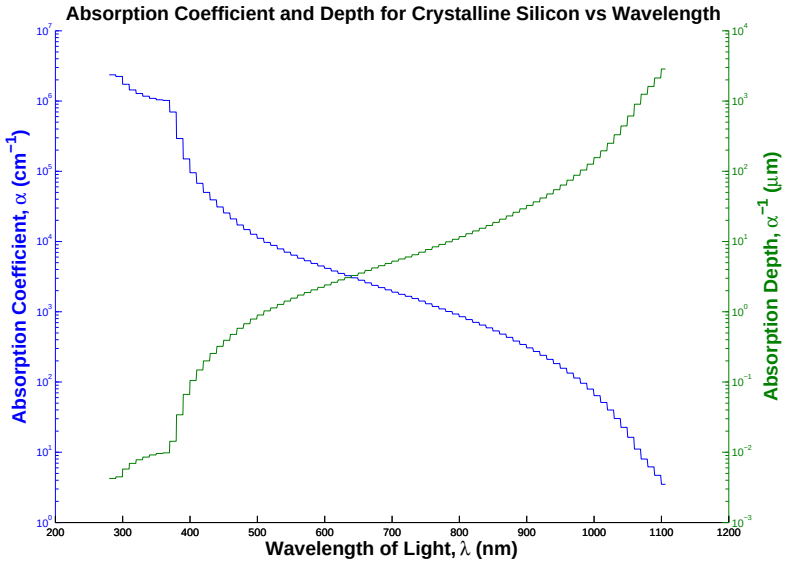

Figure 2.3: Absorption Coefficient and Absorption Depth vs Wavelength of Light

microns (ie. $(\frac{\alpha}{cm}.10^2)^{-1}.10^6 = \frac{1}{\alpha}\mu m$). This absorption depth represents the distance into crystalline silicon light will travel until it drops to 36% (ie. $\frac{1}{e}$) of it's original energy. It can be seen in Figure 2.3 that light of approximate wavelength of 510nm will travel into crystalline silicon approximately one micron until it is effectively absorbed. This means that blue/violet light at wavelength 400nm - 500nm will be absorbed in less than one micron from the surface of crystalline silicon. On the other hand red light at wavelength 620nm - 750nm will travel up to ten microns from the surface of crystalline silicon before 36% is absorbed and it can be in the hundreds of microns before it is all absorbed. If the thickness of the material is less than these values the material will be effectively appear transparent and the light of respective wavelengths will effectively pass through.

2.2.4 Recombination

Bulk Recombination

Recombination is essentially where an electron and a hole rejoin.

There are three types of recombination in the bulk of a silicon PV:

1. Radiative (band to band) recombination mainly affects direct bandgap materials (eg. GaAs) where an electron in the conduction band falls back into a hole in the valence band releasing the energy as a photon (eg. LED). Silicon however is an indirect bandgap material and consequently this type of recombination can be ignored.

2. Recombination through defect levels or Shockley-Read-Hall (SRH) recombination occurs where there are intentional impurities (eg. doping) or unintentional defects (eg. boundaries between very different doping levels) in the crystalline lattice. There are two steps in this type of recombination:

   (a) an electron (or hole) is trapped in between the valence and conduction bands in a forbidden region introduced by a defect in the crystalline lattice;

   (b) then if a hole (or electron) move up to the same forbidden region before the electron is thermally released into the conduction band by a photon - the electron and hole recombine.

   SRH (Shockley Read-Hall) is the main type of recombination in most types of silicon PV's.

3. Auger recombination involves three carriers. When an electron and a hole recombine, the energy is transferred to an electron in the conduction band rather than given off as heat or as a photon. This type of recombination is most prevalent in highly doped materials.

Minority Carrier Lifetime and Diffusion Length

Figure 2.4 shows the interrelationship between the carrier transport components including minority carrier lifetime and diffusion length.

Minority carrier lifetime (τ_n and τ_p) is a measure of the time a carrier will stay excited after electron-hole pair generation and before recombining. This may be as long as 1ms (Honsberg & Bowden 2008) and is usually measured experimentally for a particular

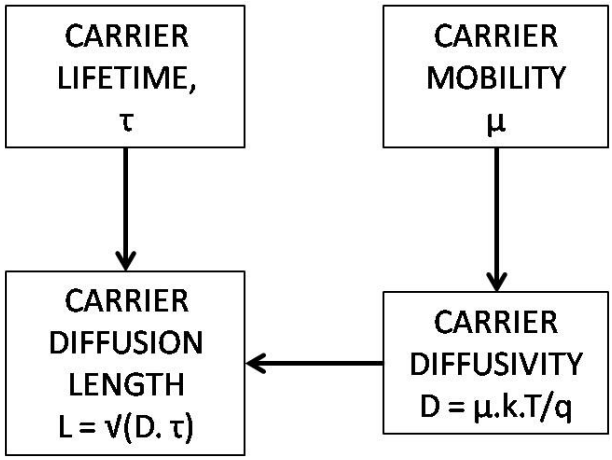

Figure 2.4: Interrelationship between Carrier Transport Components

material. A PV based on material with a long minority carrier lifetime will generally be more efficient than with a material with a short lifetime. Minority carrier lifetime is given by the equation (Honsberg & Bowden 2008):

$$\tau = \frac{\Delta n}{R}(s) \tag{2.10}$$

where Δn = the number of minority carriers generated;

R = recombination rate.

Minority carrier lifetime is usually independent of the intrinsic carrier concentration. Minority carrier lifetime within the bulk of the material is given by (Honsberg & Bowden 2008):

$$\tau_{bulk} = \frac{1}{\tau_{band}} + \frac{1}{\tau_{auger}} + \frac{1}{\tau_{SRH}} \tag{2.11}$$

where τ_{band} = lifetime due to band to band recombination;

τ_{auger} = lifetime due to auger recombination;

τ_{SRH} = lifetime due to Shockley Read-Hall recombination.

As the number of excess minority carriers is increased by the generation of electron-hole pairs, these excess numbers will decay back to equilibrium due to recombination. Therefore the recombination rate of a PV is very important as zero excess minority carriers equals zero recombination rate.

The minority carrier diffusion lengths L_n and L_p are the average distance a minority carrier can travel from where it was generated to where it recombines and is related to diffusivity D and minority carrier lifetime τ by (Honsberg & Bowden 2008):

$$L = \sqrt{D.\tau}(cm) \tag{2.12}$$

where D = diffusivity $(cm^2.s^{-1})$;
τ = lifetime (s).

Working backwards shows that both minority carrier lifetime and diffusion length are very dependent on the recombination rate which in turn is very dependent on the level of doping and fabrication of the material.

Surface Recombination

In addition to the recombination within the bulk of a PV is the surface recombination. As discussed earlier, defects and impurities promote recombination and as the surface is a disruption to the crystalline lattice the surface is a place of very high recombination. As this high rate of recombination occurs, minority carriers will be depleted at the surface. Minority carriers will then diffuse from the bulk with a higher concentration of minority carriers toward the surface with a consequent lower concentration of minority carriers in the bulk. These minority carriers travel at a surface recombination velocity (SRV) in units $cm.s^{-1}$ which limits the possible recombination rate at the surface. That is, the lower the SRV the lower the rate of minority carriers can diffuse to the surface of the emitter which results in a lower recombination rate and the higher probability majority carriers can be collected to generate current.

The surface is a disruption to the crystalline lattice which produce dangling covalent bonds as at the very surface there is no adjacent atoms on one side with which to bond. In concept, Figure 2.2 shows how dangling single bonds are created where there no adjacent atoms (on three sides of the outside four silicon atoms). Surface passivation results in the reduction of dangling bonds by growing a layer onto the surface so that there are adjacent atoms on all sides for the atoms at the surface.

2.2.5 Carrier Transport

Figure 2.4 shows the interrelationship between the carrier transport components including electron mobility μ_n and hole mobility μ_p. Electron mobility and hole mobility are different and are dependent on the level of doping and the type of impurity. A general fit equation (Zeghbroeck 2008) is given by:

$$\mu = \mu_{min} + \frac{\mu_{max} - \mu_{min}}{1 + (\frac{N}{N_r})^{\alpha}} \tag{2.13}$$

where for phosphorous doped silicon $\mu_{min} = 68.5cm^2.V^{-1}.s^{-1}$;
$\mu_{max} = 1414cm^2.V^{-1}.s^{-1}$;
$N_r = 9.2.10^{16}cm^{-3}$;
$\alpha = 0.711$;
and for boron doped silicon $\mu_{min} = 44.9cm^2.V^{-1}.s^{-1}$;
$\mu_{max} = 470.5cm^2.V^{-1}.s^{-1}$;
$N_r = 2.23.10^{17}cm^{-3}$;
$\alpha = 0.719$

Figure 2.5 shows the majority carrier mobility for both phosphorous and boron over a range of doping densities. It can be seen that the carrier mobility is relatively constant for doping density up to $10^{16}cm^{-3}$ but for higher doping beyond that concentration the carrier mobility drops away. Note that these mobilities are for the majority carriers in each type of material (ie. electrons in a donor material and holes in an acceptor material). However, minority carrier mobility can be assumed to approximate the majority carrier mobility in a doped material (Zeghbroeck 2008).

Figure 2.5 shows a general fit where as in (Kittidachachan, Markvart, Bagnall, Greef & Ensell 2007), an actual carrier mobility fit equation is provided where the mobility has been experimentally determined.

When electron-hole pairs are generated, the increase in minority carriers is high in proportion to the existing number of minority carriers therefore it is the minority carriers that are considered to create illuminated current in a silicon PV.

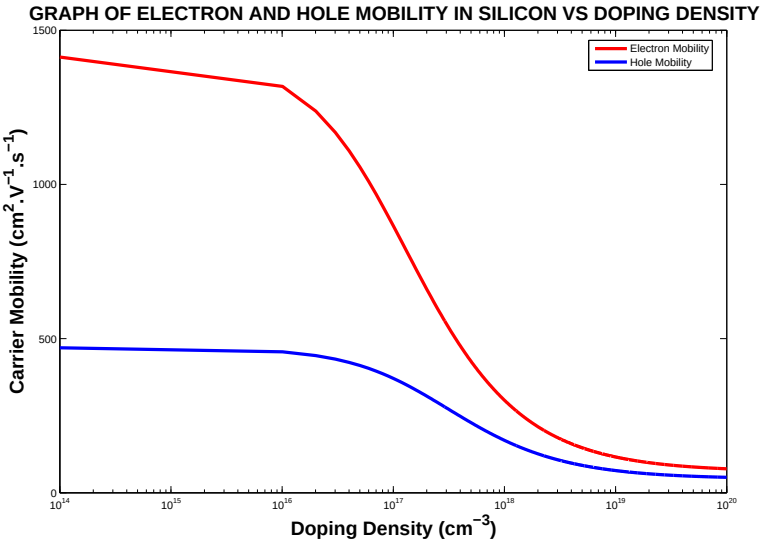

Figure 2.5: Carrier Mobility vs Doping Density

Electron and hole diffusivity (diffusion coefficient) can then be calculated using the respective carrier mobilities. The equations for electron and hole diffusivity (diffusion coefficient) are respectively:

$$D_n = \frac{k.T}{q}.\mu_n(cm^2.s^{-1}) \tag{2.14}$$

$$D_p = \frac{k.T}{q}.\mu_p(cm^2.s^{-1}) \tag{2.15}$$

where k = Boltzmann's constant = $1.380.10^{-23}(J.K^{-1})$;

T = absolute temperature (K);

q = electronic charge = $1.602.10^{-19}(C)$;

μ_n and μ_p = electron and hole mobility $(cm^2.V^{-1}.s^{-1})$.

2.2.6 p-n Junction

A silicon based PV is a single crystal device with the silicon emitter and base doped to become n-type and p-type materials respectively. The p-n junction is the crossover where the n-type and p-type materials meet and it's uniformity is dependent on the

fabrication process. The diffusion and drift of electrons and holes across the p-n junction are the two sources of current within a PV.

Diffusion

Carriers are in constant random motion and if there is an area of high carrier concentration near an area of low concentration there will be a net movement of carriers from the high concentration to the low concentration area. This can be explained in purely numerical terms where a high number of random carrier movements in the high concentration area is due to the high number of carriers. Conversely, the lower concentration area has a low amount of carriers and therefore a low amount of random movements. In this way, electrons will tend to diffuse from the high concentration n-type emitter side of the pn junction to the low concentration p-type base side to a level dependent on the electron doping profiles on both sides. Holes will naturally tend in the opposite direction from the high concentration p-type base side of the pn junction to the low concentration n-type emitter side also dependent on the hole doping profiles on both sides.

The net diffusion current density will be the difference between the electron and hole components. Diffusion current density can be given by the equation (Honsberg & Bowden 2008):

$$J = q(D_n.\frac{dn(x)}{dx} - D_p.\frac{dp(x)}{dx})(A.m^{-2}) \tag{2.16}$$

where q = electronic charge = $1.602.10^{-19}(C)$;

D_n and D_p = electron and hole diffusivity $(cm^2.s^{-1})$;

n and p = electron and hole concentration (cm^{-3});

x = distance (cm).

Drift

Drift on the other hand is the effect of an electric field to give direction to the constant random motion of carriers. This direction is in the direction of the electric field for

holes and in the opposite direction of an electric field for electrons. Like diffusion current density, the net drift current density will be the difference between the electron and hole components. The net carrier movement in the presence of an electric field is characterised by the carrier mobility (Honsberg & Bowden 2008) discussed above. Drift current density in an electric field in the x-direction is given by the one-dimensional equation (Honsberg & Bowden 2008):

$$J_x = q(n.\mu_n + p.\mu_p)E_x(A.cm^{-2}) \tag{2.17}$$

where E_x = the electric field in the x-direction ($V.cm^{-1}$);
n and p = electron and hole concentration (cm^{-3});
μ_n and μ_p = electron and hole mobility ($cm^2.V^{-1}.s^{-1}$).

Equation (2.17)can be also represented by the equation:

$$J_x = \sigma.E_x(A.cm^{-2}) \tag{2.18}$$

where σ = conductivity of the semiconductor ($\Omega^{-1}.cm^{-1}$);
E_x = the electric field in the x-direction ($V.cm^{-1}$).

Thermal Equilibrium

When a PV is in the dark with no external input (ie. no voltage applied to nor light onto a PV) it reaches thermal equilibrium with electron and hole diffusion and drift currents all canceling each other and consequently zero current flows. However, as the electrons and holes diffuse across the pn junction, a depletion (or space-charge) region forms around the pn junction the width of which is dependent on the doping level of the encapsulating and oppositely doped emitter and base.

As electrons diffuse across the pn junction from the emitter to the base they leave behind a positive ion charge within the crystalline lattice at the edge of the depletion region on the emitter side. Conversely, as holes diffuse from base to emitter, they leave behind a negative ion charge at the edge of the depletion region within the crystalline

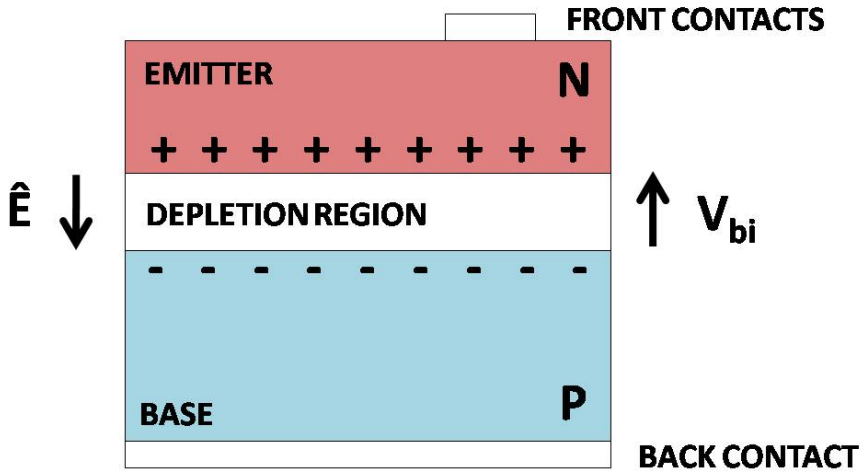

Figure 2.6: PV Thermal Equilibrium

lattice on the base side. This creates an electric field and consequent built-in voltage (assumed to be only) across the depletion region as shown in Figure 2.6.

In turn this electric field allows electrons to drift (or be swept across the depletion region as there are no free carriers in the depletion region) from base to emitter and holes to drift in the opposite direction from emitter to base. The built-in electric field tends to impede majority carriers crossing the depletion region and most return to the side from which they came. The few majority carriers that do drift across the depletion region become minority carriers on the other side and diffuse to recombine within a diffusion length.

The pn junction is where the effects of carrier generation, recombination, diffussion and drift converge (Honsberg & Bowden 2008).

Unilluminated Current Density

As the electric field across the depletion region impedes the diffusion of majority carriers it can be considered equivalent to a diode. Like a diode, if the terminals are bonded (as in Figure 2.7), a diode leakage current density J_o will flow. The drift and diffussion current density components that make up total unilluminated current density are shown in the equation for total unilluminated current density (with assumptions) (Honsberg

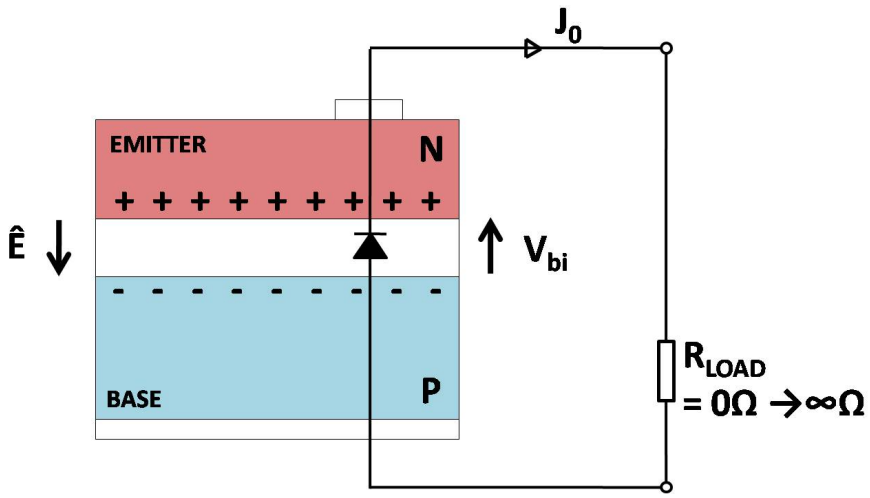

Figure 2.7: PV Unilluminated Current Density

2008):

$$J_o = [q.\frac{D_n.n_i^2}{L_n.N_A} + q.\frac{D_p.n_i^2}{L_p.N_D}](A.cm^{-2}) \tag{2.19}$$

where q = electronic charge = $1.602.10^{-19}(C)$;

D_n and D_p = electron and hole diffusivity $(cm^2.s^{-1})$;

n_i = intrinsic carrier concentration (cm^{-3});

L_n and L_p = electron and hole diffusion length (cm);

N_D and N_A = electron and hole doping concentration (cm^{-3});

2.2.7 Photovoltaic Effect

Once the PV is illuminated, the photons falling onto the PV are absorbed and electron-hole pairs are generated throughout the PV proportional to the amount of light absorbed. As the emitter is an n-type material, the number of electrons (doped and generated) to the number of holes is greater by far (although there are now proportionally more holes than electrons compared to that in the dark) giving the emitter terminal a negative charge. The opposite applies in the base as there are far more holes giving the base terminal a positive charge. This forward biases the equivalent diode of the depletion region which has two effects.

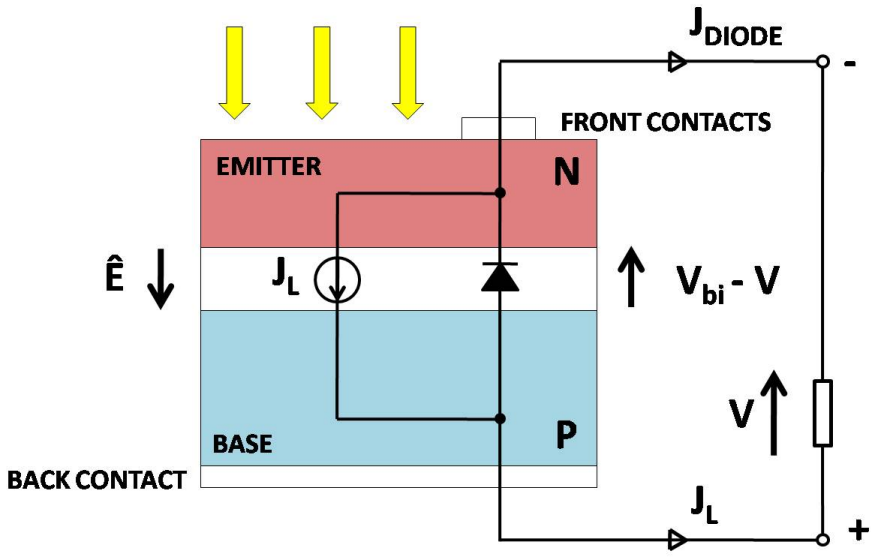

Figure 2.8: PV Photovoltaic Effect

Firstly, constant current density source J_L is generated. Secondly, unilluminated current density J_o increases as J_{Diode} as terminal voltage increases (as per equation (3.18)) in the opposing direction to the constant current density source J_L.

2.3 Organic PV Concepts

2.3.1 Buckyballs and Carbon Nanotubes

Diamond and graphite were thought be the only two forms of pure solid carbon until the carbon molecule C_{60} buckminsterfullerene "buckyball" was discovered in 1985 by Rick Smalley et al at Rice University in Houston. Figure 2.9 shows how the C_{60} buckyball is a circular cluster of 60 carbon atoms, with 32 faces of 12 pentagons and 20 hexagons much like a soccer ball.

In 1990, Rick Smalley proposed the existence of a tubular fullerene that could be made by elongating a C_{60} molecule (O'Connell 2006). In 1991, Iijima imaged multi-walled carbon nanotubes and two years later, he and others observed single-walled carbon nanotubes. Single-walled carbon nanotubes CNT are best described as a single sheet of graphene rolled into a seamless tube as shown in figure 2.10 (Wikipedia 2008). Also

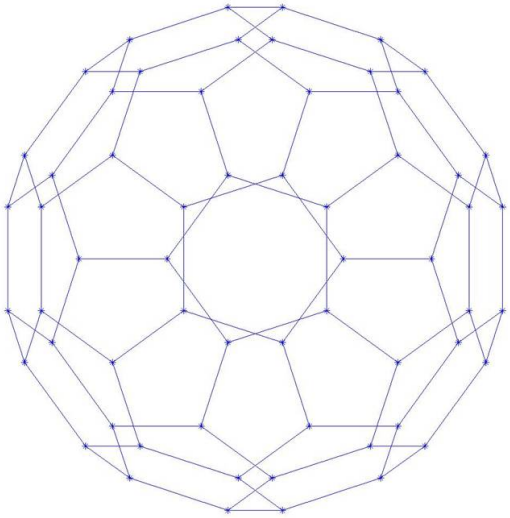

Figure 2.9: MATLAB® Plot of C_{60} Buckminsterfullerene (Buckyball)

shown in figure 2.10 (Wikipedia 2008), there are three geometries of CNT:

- armchair;
- zig-zag;
- chiral.

Figure 2.11 (Wikipedia 2008) shows that the respective geometries are dependent on the integers n and m along the axes a_1 and a_2, such that the geometry $= n.a_1 + m.a_2$. For armchair $n =$ an integer and $m = 0$, for zig-zag $n = m =$ an integer and the level of chirality is dependent on the integers n and m.

Buckyballs, other carbon molecule fullerenes and the related and so-named carbon nanotubes (CNT) have diameters in the order of single-digit nanometers. They also have extremely high electronic transport, tensile strength and thermal transfer characteristics as well as other unique qualities. These qualities includes the ability to be metallic or semiconducting depending on the geometry. The ability to be able to control whether they are created metallic or as a semiconducting is still being researched.

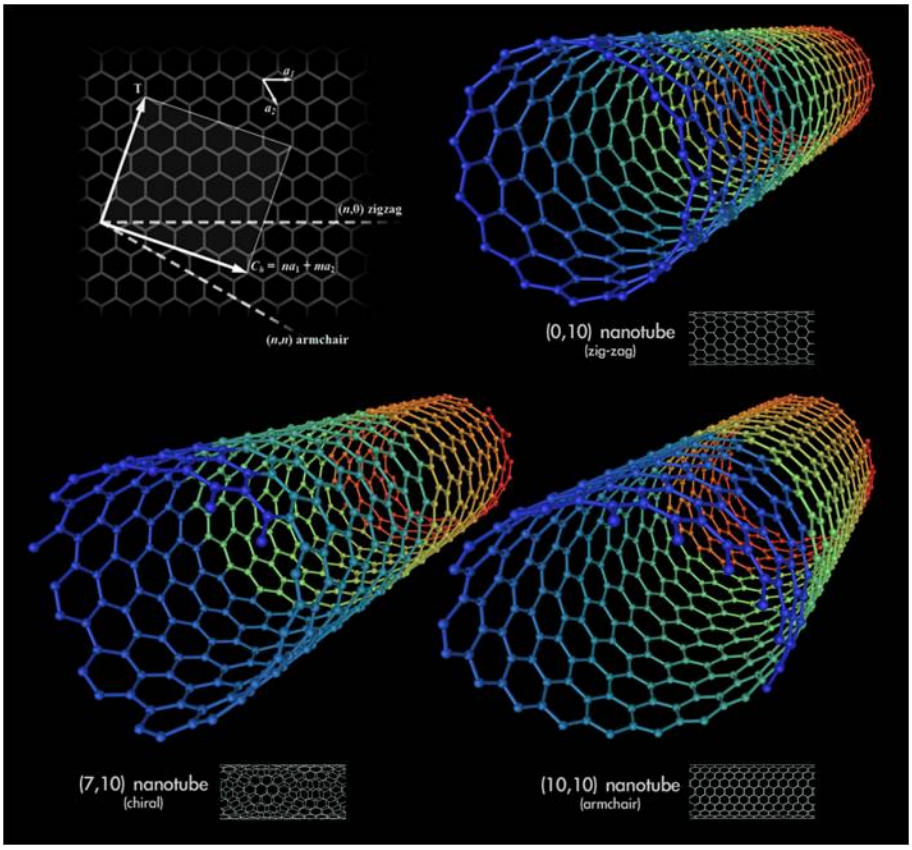

Figure 2.10: Carbon Nanotubes

2.3.2 Organic PV's

The three currently existing types of organic PV's are (Gregg & Hanna 2003):

- dye-sensitised solar cells (DSSC)
- planar (or multi-layer) organic semiconductor cells
- bulk-heterojunction (BHJ) (or high-surface-area) cells

Of these, only bulk-heterojunction (BHJ) devices are discussed here. BHJ devices consist of an optically excited, electron donating conjugated polymer and an electron conducting molecule (Sun & Sariciftci 2005) in contact with each other. One type of BHJ at the higher end of complexity and efficiency consists of vertically aligned carbon nanotubes (VA-CNT) with the conjugated polymer within the voids between the VA-CNT. This type of VA-CNT BHJ has a very high and relatively controlled amount

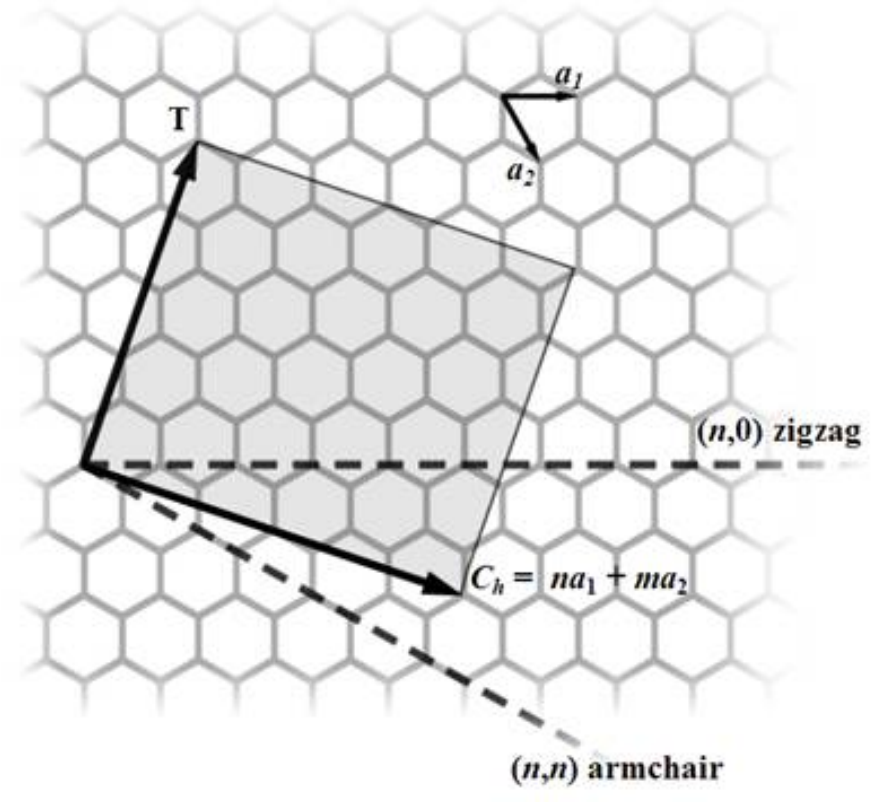

Figure 2.11: Geometry of Carbon Nanotubes

of surface area interface between the two materials but is difficult to fabricate and consequently more expensive than a more simplistic BHJ. A more simplistic type of BHJ is a random blended mix of conjugated polymer and fullerene molecule, typically at a 1:4 weight ratio. This type of BHJ also has a high surface area interface between the two materials but is easier and cheaper to fabricate and has mechanical flexibility for architectural applications.

Referring to figure 2.12, in the active layer of a BHJ light absorption in the conjugated polymer generates excitons (mobile electron-hole pairs in excited states) which then diffuse within the polymer toward an interface between the two materials. The interface needs to be within an exciton diffusion length (typically $\approx 10nm - 20nm$) for the exciton to diffuse to it where it can either dissociate (electron and hole separate) or decay back to the original ground state. If the exciton dissociates, the hole stays within the polymer and the electron transfers to the fullerene molecule to both become majority carriers within their respective materials. If the respective carriers do not recombine

they are collected to participate in generated photocurrent. This makes the organic PV a majority carrier device in contrast to the inorganic PV as a minority carrier device.

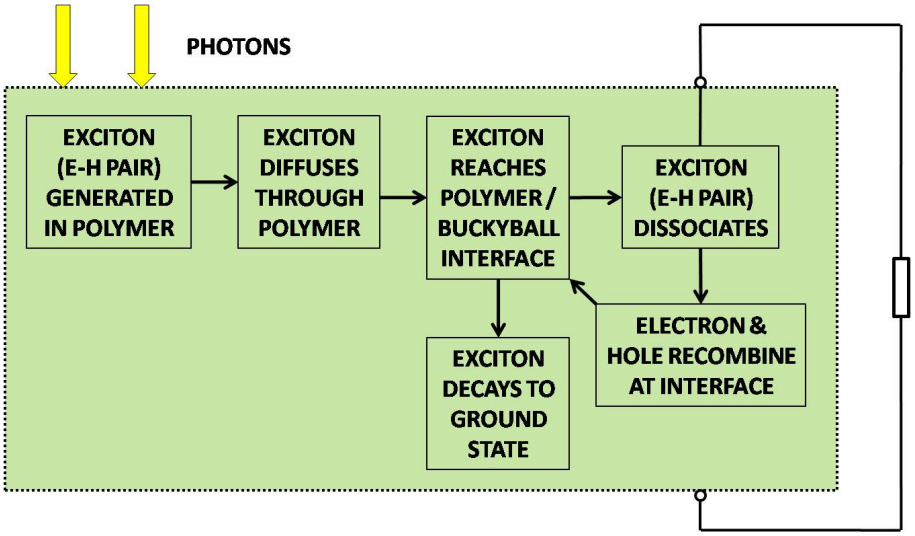

Figure 2.12: Diagram of Organic PV Active Layer

Prof. Nunzio Motta (QUT) kindly provided two recently published papers (Kanai & Grossman 2008)(Kotlarski, Blom, Koster, Lenes & Slooff 2008). The paper by (Kotlarski et al. 2008) along with it's references (Koster, Smits, Mihailetchi & Blom 2005)(L.A.A.Pettersson, Roman & Inganas 1999)(Sievers, Shrotriya & Yang 2006) was chosen as the basis on which to create an organic PV model. The experimental PV used in this research (Kotlarski et al. 2008) is a blended BHJ PV with MDMO-PPV conjugated polymer mixed with PCBM methofullerene (based on C_{61} buckyballs). In these research papers and many others accessed, modelling of the PV is consistently divided into two parts - an optical model that inputs into an electrical model.

2.3.3 Optical Model

Researchers have developed an optical model, initially for a bi-layer planar device (L.A.A.Pettersson et al. 1999) and then applied to a BHJ device (Sievers et al. 2006). This optical model relates the optical interference effects of the multiple thin film layer stack of different materials on a glass substrate (as shown in figure 3.10) and the optical absorption and thickness of the active layer to the oscillatory nature of the photogenerated short-circuit current. The output from the optical model (and input

to the electrical model) is an exciton generation rate profile through the active layer. However, (Kotlarski et al. 2008) found that while the relationship between optical interference effects and photogenerated current does appear to exist, for devices with an active layer $< 250nm$, a constant average exciton generation rate may be used instead of the optical model output exciton generation rate profile (assuming that the total generation is equal for both) to calculate photogenerated current accurately.

The theories, methods, assumptions, data and equations used to calculate the optical model can be referenced directly from published papers (L.A.A.Pettersson et al. 1999) (Sievers et al. 2006) (Kotlarski et al. 2008) or within their respective references, however the detail is not replicated here.

2.3.4 Electrical Model

Researchers have also developed an electrical model for a BHJ device that uses a constant average exciton generation rate (Koster et al. 2005) and also applied using an optical model output exciton generation rate profile (Kotlarski et al. 2008). Both applications use an iterative approach of discretising equations to converge (with stability to within a preset tolerance) towards an equilibrium solution of electric field, recombination and carrier density profiles for the given material. As with the optical model, the theories, methods, assumptions, data and equations used to calculate the electrical model can be referenced directly from published papers (Koster et al. 2005) (Kotlarski et al. 2008) or within their respective references. However, an interpretation (with some minor corrections) of the equations in these same papers is reproduced in chapter 3 and in Appendix C.

Chapter 3

Methodology

3.1 Silicon PV Model

Figure 3.1 shows the conceptual interrelationships and approach taken to the creation and coding of the silicon PV model. Appendix B shows the same interrelationships and approach but in more detail.

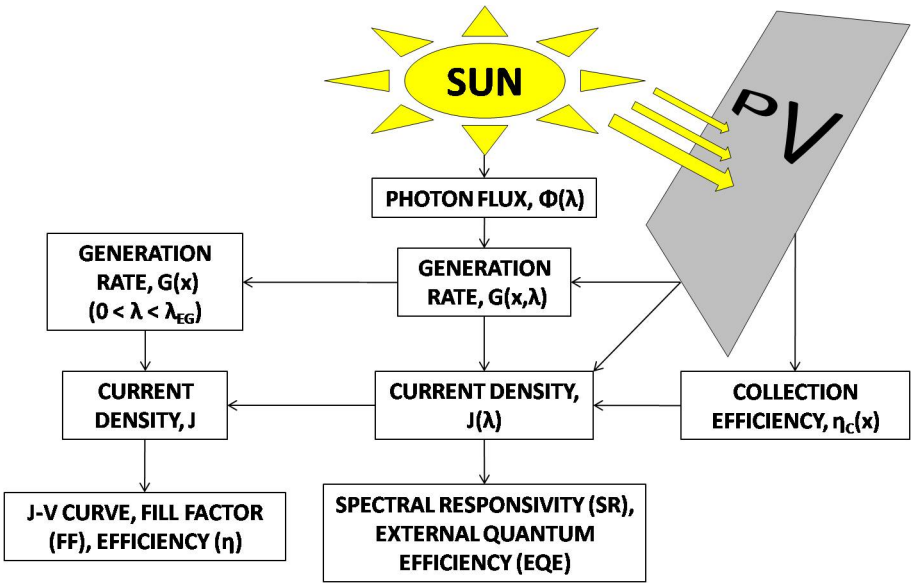

Figure 3.1: Conceptual Diagram of the Silicon PV Model

3.1.1 Generation

The generation rate G is the number of electron-hole pairs generated per unit volume per second from the absorption of photons, and is given by the equation (Honsberg & Bowden 2008):

$$G = \alpha.\Phi.exp(-\alpha.x)(m^{-3}.s^{-1}) \tag{3.1}$$

where α = absorption coefficient (m^{-1});
Φ = photon flux $(s^{-1}.m^{-2})$;
x = distance from PV surface (m).

An assumption was made that as the absorption coefficient α and photon flux Φ are different at different wavelengths of light, the generation rate at any given point in the device and at a given wavelength could be given by the equation:

$$G(x,\lambda) = \alpha(\lambda).\Phi(\lambda).exp(-\alpha(\lambda).x)(m^{-3}.s^{-1}) \tag{3.2}$$

where $\alpha(\lambda)$ = absorption coefficient at wavelength λ (m^{-1});
$\Phi(\lambda)$ = photon flux at wavelength λ $(s^{-1}.m^{-2})$;
x = distance from PV surface (m).

It is thought that the units in equation (3.2) should be modified to reflect that these same units $(m^{-3}.s^{-1})$ should appear after integration (either in the x or λ direction) but they are left at these units for lack of certainty. Figure 3.1 shows that the approach in this model is to integrate the generation rates calculated in equation (3.2) in two different directions for the two different purposes.

Firstly, the different generation rates $G(x,\lambda)$ are integrated over the full range of usable light for silicon. The lower limit wavelength of light was taken as a nominal $400nm$ below which the blue light energy is absorbed within the glass. The upper limit wavelength of light ($\lambda_{E_g} \approx 1100nm$ in this case) is that wavelength of light calculated where photon energy is equal or greater than the bandgap energy of the material.

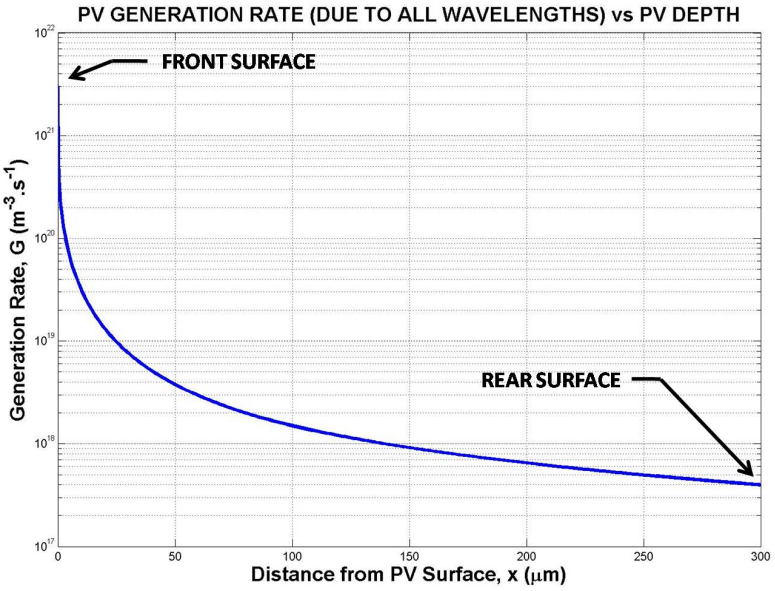

Figure 3.2: PV Generation Rate vs PV Depth

By using equations (2.1),(2.2) and (2.4), the generation rate for each given point in the PV is then given by the equation:

$$G(x) = \int_{400nm}^{\lambda_{Eg}} \alpha(\lambda).\Phi(\lambda).exp(-\alpha(\lambda).x).d\lambda(m^{-3}.s^{-1}) \tag{3.3}$$

where λ_{Eg} = upper wavelength limit of usable light for silicon (m);

$\alpha(\lambda)$ = absorption coefficient at wavelength λ (m^{-1});

$\Phi(\lambda)$ = photon flux at wavelength λ $(s^{-1}.m^{-2})$;

x = distance from PV surface (m).

Figure 3.2 shows the graphical results of equation (3.3) where the highest generation rate is at or near the surface and falls away by many orders of magnitude quite quickly. This resembles the plot in the UDEL (Honsberg & Bowden 2008) Generation Rate section and was assumed to be correct. However, the result needed to be multiplied by a term of 10^6 to get what is believed to be the correct result and it is thought to be due to integration.

Secondly, integrating equation (3.2) over all the distances x (PV is $300\mu m$ wide in this case) from the surface gives a generation rate for each wavelength:

$$G(\lambda) = \int_0^{300\mu m} \alpha(\lambda).exp(\Phi(\lambda). - \alpha(\lambda).x).dx(m^{-3}.s^{-1}) \tag{3.4}$$

As in equation (3.3), the result needed to be multiplied by a term of 10^6 to get what is believed to be the correct result and again it is thought to be due to integration.

3.1.2 Collection Efficiency (Probability)

Collection efficiency (probability) η_c represents the probability that carriers will not recombine and will be collected by the pn junction to participate in light generated current density in the PV. The numerical processes for calculating collection efficiency in the emitter and base of the PV are vastly different as described in Appendix B and is based on the published paper by (Kittidachachan et al. 2007).

For emitter collection efficiency, a normalised excess minority-carrier concentration is introduced (Kittidachachan et al. 2007) (DelAlamo & Swanson 1984):

$$u(x) = \frac{p(x) - p_0(x)}{p_0(x)} \tag{3.5}$$

where p = hole concentration (cm^{-3});

p_0 = hole carrier concentration at equilibrium (cm^{-3}).

The transport equation for the minority carriers in the dark is then written as (Kittidachachan et al. 2007):

$$-\frac{d}{dx}\left[D_p.p_0.\frac{du}{dx}\right] + \frac{D_p.p_0}{L_p^2}u = 0 \tag{3.6}$$

where D_p = hole diffusivity $(cm^2.s^{-1})$;

p_0 = hole carrier concentration at equilibrium (cm^{-3});

u = normalised excess minority-carrier concentration;

L_p = hole diffusion length (cm);

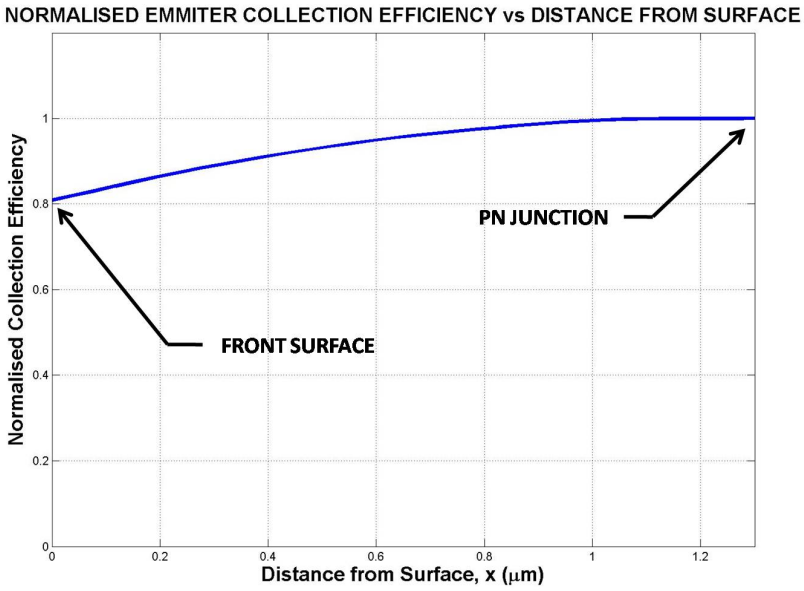

Figure 3.3: Emitter Efficiency (Probability) vs Depth from Surface

Dr Tony Ahfock gave direct assistance to numerically solve this self-adjoint Sturm-Liouville 2nd order differential equation. Converting equation (3.6) to standard Sturm-Liouville format (Ahfock 2008):

$$-(r(x).u')' + p(x).u = 0 \tag{3.7}$$

where $r(x) = D_p(x).p_0(x)$;

$p(x) = \frac{D_p(x).p_0(x)}{L_p^2(x)}$;

$x =$ position within the emitter $0 =< x =< 1.3\mu m$.

Equation (3.7) is rewritten to form the equation (Ahfock 2008):

$$-r'.u' - r.u'' + p.u = 0 \tag{3.8}$$

Equation (3.8) is then converted to the central difference equation (Ahfock 2008):

$$-\frac{(r_{k+1} - r_{k-1})}{2.\Delta x}.\frac{(u_{k+1} - u_{k-1})}{2.\Delta x} - \frac{r_k(u_{k+1} - 2.u_k + u_{k-1})}{(\Delta x)^2} + p_k.u_k = 0 \tag{3.9}$$

Equation (3.9) then becomes a set of simultaneous equations when all values of k are considered (ie. $2 < k < n - 1$) when the emitter is broken into $n - 1$ divisions.

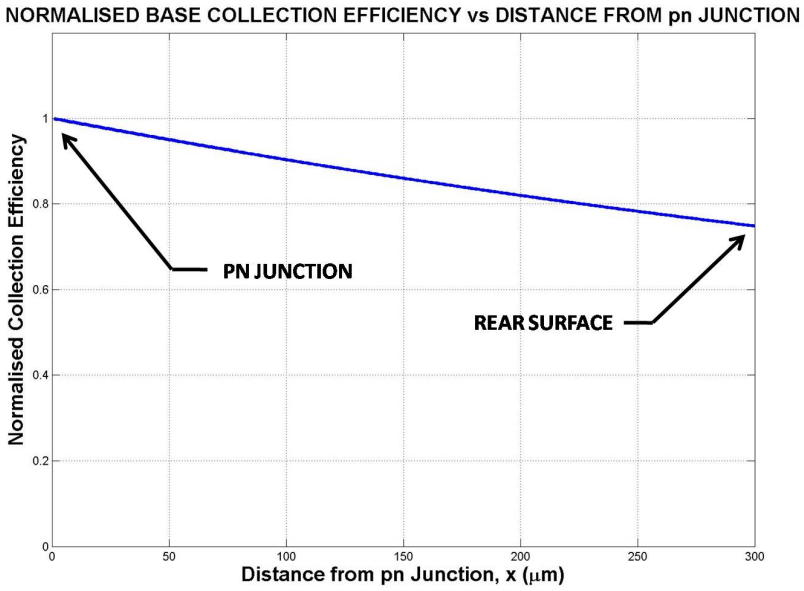

Figure 3.4: Base Efficiency (Probability) vs Depth from pn Junction

We can write (Ahfock 2008):

$$\underline{F}.\underline{U} = \underline{Z} \tag{3.10}$$

F is an n x n tri-diagonal square matrix where (Ahfock 2008):

$F(1,1) = F(n,n) = 1$;

$F(k,k) = \frac{2.r_k}{(\Delta x)^2} + p_k$ for $1 < k < n$;

$F(k,k+1) = \frac{-(r_{k+1}-r_{k-1})}{4.(\Delta x)^2} - \frac{r_k}{(\Delta x)^2}$ for $1 < k < n$;

$F(k,k-1) = \frac{(r_{k+1}-r_{k-1})}{4.(\Delta x)^2} - \frac{r_k}{(\Delta x)^2}$ for $1 < k < n$;

All other entries in $F = 0$.

U is a column vector $= [u_1, u_2, ...u_{n-1}, u_n]^T$

Z is a column vector where $Z(1)$ and $Z(n)$ are boundary values and all other entries in $Z = 0$. For the forward solution, $Z(1) = 0$ and $Z(n) = 1$. For the reverse solution, $Z(1) = 1$ and $Z(n) = 0$.

Once $\underline{F}$ and $\underline{Z}$ are constructed, $\underline{U}$ is determined (for the forward and reverse solutions) since from equation (3.10) (Ahfock 2008):

$$\underline{U} = \underline{F}^{-1}.\underline{Z} \tag{3.11}$$

In summary, equations 3.5 to 3.11 were used to calculate forward $u_f(x)$ and reverse $u_r(x)$ normalised excess minority-carrier concentration solutions (Kittidachachan et al. 2007). The forward solution has boundary conditions $u_f(0) = 0$; $u_f(W_e) = 1$ and the reverse solution has boundary conditions $u_r(0) = 1$; $u_r(W_e) = 0$; where W_e is the width of the emitter.

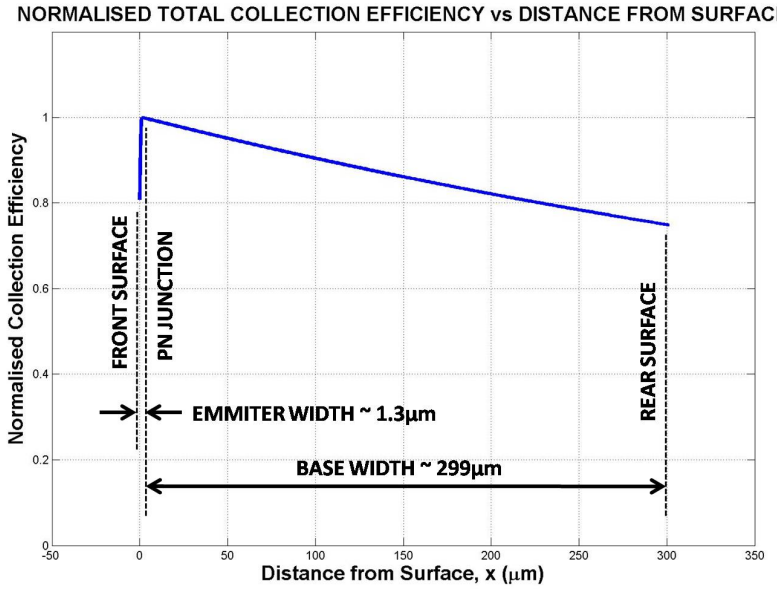

Figure 3.5: Collection Efficiency (Probability) vs Depth from Surface

These forward $u_f(x)$ and reverse $u_r(x)$ solutions were then used in the series of equations to calculate emitter collection efficiency $\eta_c(x)$ (Kittidachachan et al. 2007):

$$J_{0r} = q.D_p.p_0 \frac{du_r}{dx}\bigg|_{x=0} \tag{3.12}$$

$$\alpha_r J_{0r} = q.D_p.p_0 \frac{du_r}{dx}\bigg|_{x=W_e} \tag{3.13}$$

where q = electronic charge = $1.602.10^{-19}(C)$;

D_p = hole diffusivity $(cm^2.s^{-1})$;

p_0 = hole carrier concentration at equilibrium (cm^{-3}).

Surface saturation current density is given by:

$$J_{0Se} = \frac{q.n_{i0}^2.S_e}{N_{Deff}(0)} \tag{3.14}$$

where q = electronic charge = $1.602.10^{-19}(C)$;

n_{i0} = intrinsic carrier concentration (cm^{-3});

S_e = front surface recombination velocity $(cm.s^{-1})$;

N_{Deff} = effective doping concentration (cm^{-3}).

Emitter collection efficiency is then:

$$\eta_c(x) = u_f(x) + \frac{\alpha_r.J_{0r}}{J_{0r} + J_{0Se}}.u_r(x) \tag{3.15}$$

Figure 3.3 shows the result of the emitter collection efficiency for front (emitter) surface recombination velocity $S_e = 10^3(cm.s^{-1})$.

Base collection efficiency is relatively straight forward in comparison to emitter collection efficiency and is given by the equation (Kittidachachan et al. 2007):

$$\eta_c(x) = cosh\frac{x}{L_n} - \left[\frac{tanh\frac{W_b}{L_n} + \frac{S_b.L_n}{D_n}}{1 + \frac{S_b.L_n}{D_n}.tanh\frac{W_b}{L_n}}\right].sinh\frac{x}{L_n} \tag{3.16}$$

where x = distance from the pn junction (cm);

W_b = width of the base (cm);

L_n = electron diffusion length (cm);

S_b = back surface recombination velocity $(cm.s^{-1})$;

D_n = electron diffusivity $(cm^2.s^{-1})$;

Figure 3.4 shows the results of the base collection efficiency for rear surface recombination velocity $S_b = 10^2(cm.s^{-1})$. Figure 3.5 shows the result of plotting both the emitter and base collection efficiency together. It can be seen graphically that the emitter is thin ($\approx 1.3\mu m$) compared to the width of the base ($\approx 299\mu m$). This design feature is to allow as many holes as possible from the large number of electron-hole pairs generated near the surface to be close enough to (within a diffusion length of) the pn junction to be collected and swept across to meet up with the electrons that have flowed through the load.

3.1.3 Current Density

As described in section 2.2.7 and can be seen in figure 3.6, current density in a silicon PV is made up of two component current densities in opposite directions to each other.

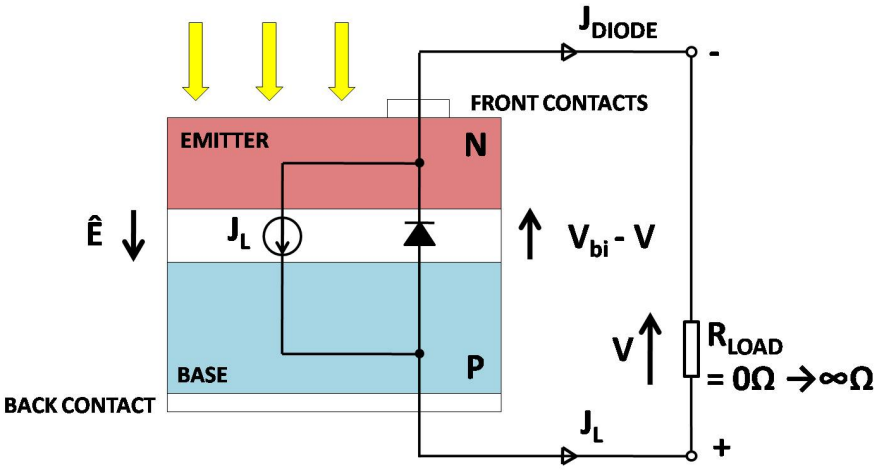

Figure 3.6: Silicon PV Diagram Overlaid with Sources of Current Densities

Firstly, there is a constant current density source J_L generated by and proportional to the amount of light absorbed by the PV. Using the results from equations (3.3), (3.15) and (3.16), the equation for the constant light generated current density J_L is (Honsberg & Bowden 2008):

$$J_L = q.\int_0^W G(x).\eta_c(x).dx(A.m^{-2}) \tag{3.17}$$

where W = width of the device (m);

$G(x)$ = generation rate $(m^{-3}.s^{-1})$;

$\eta_c(x)$ = collection efficiency.

Secondly as J_L is generated, a voltage V appears across the terminals and as V forward biases the equivalent diode of the pn junction, current density J_{Diode} increases and flows in the opposing direction to J_L. The equation for this current density through the biased equivalent diode J_{Diode} is then (Wenham et al. 2007):

$$J_{Diode} = J_0\left[exp\left(\frac{q.V}{n.k.T}\right) - 1\right](A.m^{-2}) \tag{3.18}$$

where J_0 = unilluminated current density $(A.m^{-2})$;

q = electronic charge = $1.602.10^{-19}(C)$;

V = terminal voltage (V);

n = idealty factor;

k = Boltzmann's constant = $1.380.10^{-23}(J.K^{-1})$;

T = absolute temperature (K).

Please note, a nominal J_0 (Kittidachachan et al. 2007) was used in the model as equation (2.19) (Honsberg & Bowden 2008) (Green 1992) was thought not to apply to the non-uniform doping concentration of the emitter of the PV used as the basis of the model. However, any future work could attempt to use the emitter doping concentration nearest the pn junction or depletion region in equation (2.19) to calculate J_0.

Figure 3.7 shows that when the plot is moved into the 4th quadrant, net current density J is equal to (Wenham et al. 2007):

$$J = J_L - J_{Diode}(A.m^{-2}) \tag{3.19}$$

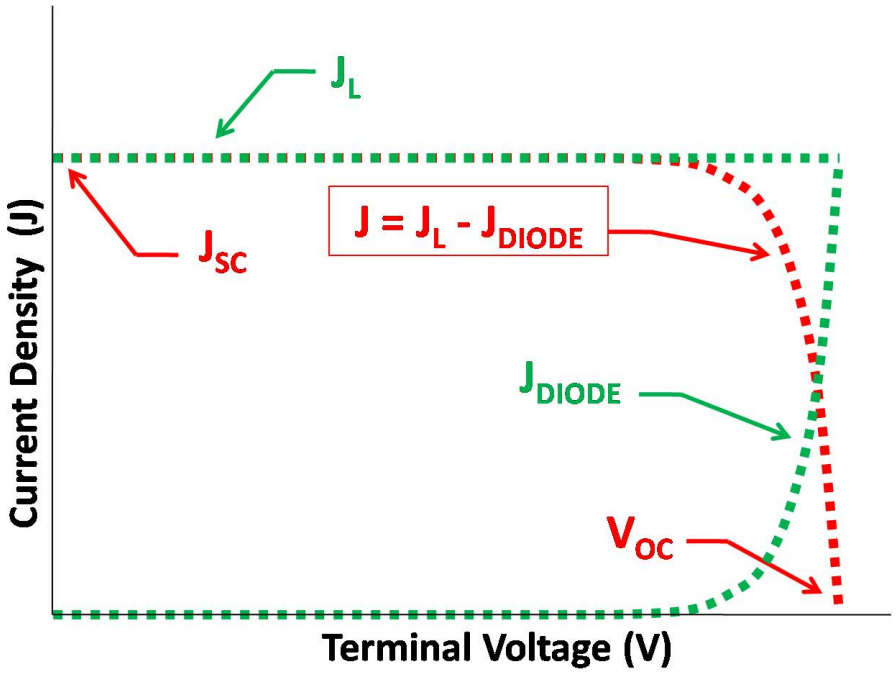

Figure 3.7: Silicon PV Plot of Current Densities vs Terminal Voltage

So, using equations (3.18) and (3.19) net current density J can be written (Wenham

et al. 2007):

$$J = J_L - J_0\left[exp\left(\frac{q.V}{n.k.T}\right) - 1\right](A.m^{-2}) \tag{3.20}$$

Once J is calculated from terminal voltage, power density can be calculated by the product:

$$PowerDensity = J.V(W.m^{-2}) \tag{3.21}$$

It should be noted that current and power densities are used extensively in PV theory and research, so that respective PV performances may be compared without the PV's being the same physical size. Current and power density values of a PV need only be multiplied by the area of a PV to calculate the respective current and power values.

3.1.4 Resistances

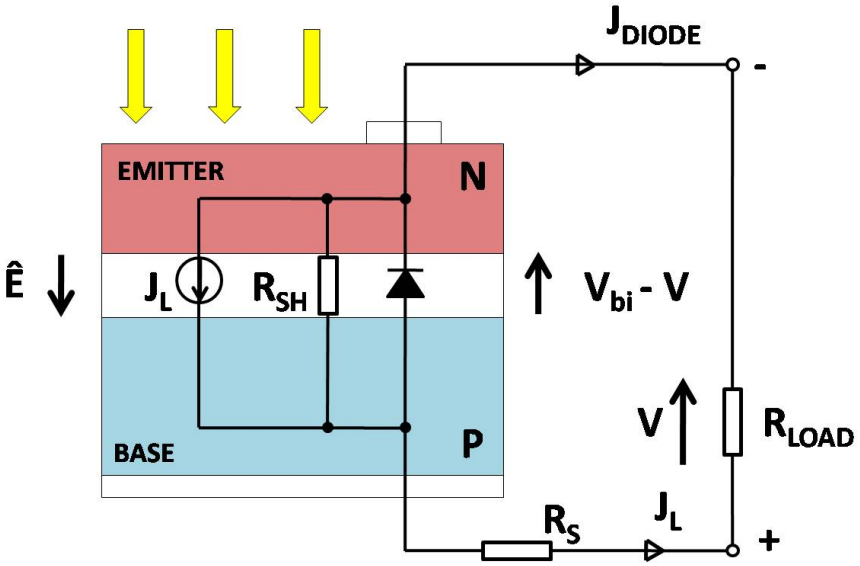

Figure 3.8: Silicon PV Diagram Overlaid with Sources of Current Densities

Figure 3.8 shows series resistance R_S and shunt resistance R_{SH} added to the silicon PV diagram. These are due to PV losses and imperfections and need to be considered when calculating actual current and power densities. Series resistance R_S represents the resistance of the bulk (mainly pn junction) of the PV added to the resistance of the front and rear contacts and interfaces. Shunt resistance R_{SH} carries current density shunted around the pn junction (equivalent diode) at the edges of the PV. This

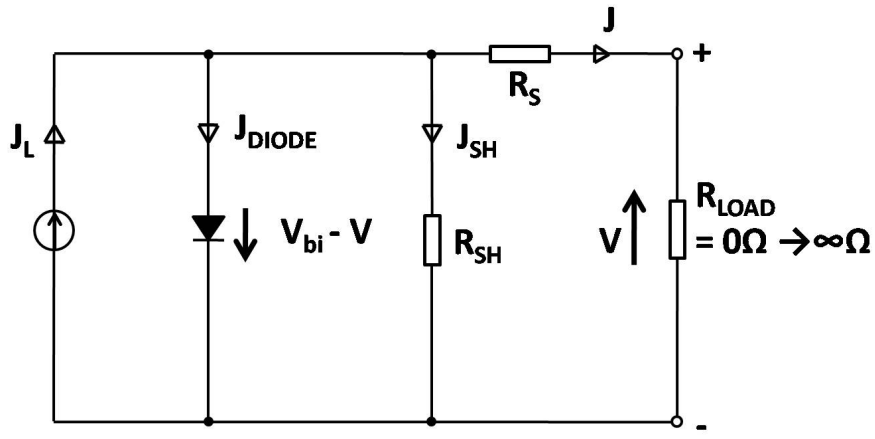

Figure 3.9: Illuminated Silicon PV Circuit Diagram

culminates in the equivalent circuit as shown in figure 3.9. Modifying the equation for current (Wenham et al. 2007) to represent current density:

$$J = J_L - J_0\left[exp\left(\frac{V + J.R_S}{(n.k.T/q)}\right) - 1\right] - \frac{V + J.R_S}{R_{SH}}(A.m^{-2}) \tag{3.22}$$

where J_L = illuminated current density $(A.m^{-2})$;

J_0 = unilluminated current density $(A.m^{-2})$;

V = terminal voltage (V);

R_S = series resistance (Ω);

R_{SH} = shunt resistance (Ω);

q = electronic charge = $1.602.10^{-19}(C)$;

n = idealty factor;

k = Boltzmann's constant = $1.380.10^{-23}(J.K^{-1})$;

T = absolute temperature (K).

However, in equation (3.22) net current density J uses itself in it's own calculation. Using nodal analysis, an attempt was made to solve equation (3.22) numerically. However, the non-linear nature of the equivalent diode compared to the linear resistances R_S and R_{SH} made it difficult to create the required series of simultaneous equations. If a PV is of sufficient quality, R_S and R_{SH} will be small and large respectively and as such J_L will not be adversely affected. Consequently, in this model J_L was substituted for J in the calculation of J, so equation (3.22) for the purpose of this model becomes:

$$J = J_L - J_0\left[exp\left(\frac{V + J_L.R_S}{(n.k.T/q)}\right) - 1\right] - \frac{V + J_L.R_S}{R_{SH}}(A.m^{-2}) \tag{3.23}$$

3.1.5 Spectral Responsivity & Quantum Efficiency

Development of the model for both spectral responsivity SR and quantum efficiency QE has required some assumptions be made and these are detailed in the following respective subsections.

Spectral Responsivity

Spectral responsivity SR of a PV is the ratio of the current generated to the power from the light incident on the PV and is given by the equations (Wenham et al. 2007):

$$SR = \frac{I_{SC}}{P_{IN}(\lambda)}(A.W^{-1}) \tag{3.24}$$

where I_{SC} = short circuit current (A);

$P_{IN}(\lambda)$ = input power at wavelength λ (W).

$$SR = \frac{q.\lambda}{h.c}.EQE(A.W^{-1}) \tag{3.25}$$

where q = electronic charge = $1.602.10^{-19}(C)$;

h = Plank's constant = 6.626 x $10^{-34}(J.s)$;

c = speed of light in a vacuum = 2.998 x $10^{8}(m.s^{-1})$;

λ = wavelength of light (m);

EQE = external quantum efficiency.

Ideally spectral responsivity of a silicon PV increases linearly with wavelength, from a theoretical $0nm$ to the upper limit bandgap energy wavelength ($\lambda_{E_g} \approx 1100nm$ in this case). A silicon PV cannot absorb all the energy from short wavelength light and in fact any energy from wavelengths below $\approx 400nm$ is mainly absorbed by the front

glass substrate and given off as heat. Consequently, spectral responsivity is calculated for wavelengths of light between these two practical limits (ie. $\approx 400nm$ to $1100nm$).

Referring to equation (3.24), the model calculates net current density J and it was assumed that current density generated by each wavelength $J(\lambda)$ was required. As shown in Appendix B, illuminated current density for each wavelength ($J_L(\lambda) = J_{SC}(\lambda) \approx J(\lambda)$ when $V = 0$) was calculated and used instead of current I_{SC}. Also, as the model input is the NREL spectral irradiances $F(\lambda)$, this was multiplied by the respective wavelength to give $P_{IN}(\lambda)$ in units Watts per unit area. Manipulating equation (3.24) with these assumptions and referring to equations (2.1) and (2.2), the equation used to calculate spectral responsivity in this model is:

$$SR(\lambda) = \frac{J_L(\lambda)}{F(\lambda).\lambda}.10^1(A.W^{-1}) \tag{3.26}$$

where $J_L(\lambda)$ = illuminated current density at wavelength λ ($mA.cm^{-2}$);
$F(\lambda)$ = spectral irradiance at wavelength λ ($W.m^{-2}.\mu m^{-1}$);
λ = wavelength of light (μm).

Please note the last term in equation (3.26) is a conversion factor in an attempt to get the result in the correct units. However, any future work may need to check the assumptions (above) that equation (3.26) is based on as well as unit conversion factors.

Quantum Efficiency

Quantum efficiency QE of a PV is defined as the number of electrons moving from the valence band to the conduction band per photon incident on the PV for each wavelength of light. External quantum efficiency EQE includes light that is consequently reflected from or transmitted through the PV where internal quantum efficiency (IQE) does not. Both external and internal quantum efficiency use the same wavelength practical limits (ie. $\approx 400nm$ to $1100nm$) and the ideal for both is unity. Only external quantum efficiency is considered in this model and can be determined in two different ways. Firstly, by rewriting equation (3.25) and using the already calculated spectral

responsivity values:

$$EQE(\lambda) = \frac{SR(\lambda).h.c}{q.\lambda} \tag{3.27}$$

Secondly, by combining equations (2.4) and (3.26) we get the equation that was used in this model:

$$EQE(\lambda) = \frac{J_L(\lambda)}{q.\Phi(\lambda)}.10^1(electron.photon^{-1}) \tag{3.28}$$

where $J_L(\lambda)$ = illuminated current density at wavelength λ $(mA.cm^{-2})$;

q = electronic charge = $1.602.10^{-19}(C)$;

$\Phi(\lambda)$ = photon flux at wavelength λ $(s^{-1}.m^{-2})$.

Please note the last term in equation (3.28) is a conversion factor in an attempt to get the result in the correct units. However, any future work may need to check the assumptions (above) that equation (3.28) is based on as well as unit conversion factors within the model.

3.2 Organic PV Model

The research paper (Koster et al. 2005) was chosen on which to base the organic PV model as it describes an electrical model that does not require an optical model - only a constant average exciton generation rate. It was thought that if a model could be created without an optical model then an optical model could be created later and then applied to the working electrical model. The main thrust of the attempt to create an organic PV model was the interpretation of this research paper (Koster et al. 2005). Figure 3.10 shows the thin film layer stack of the BHJ device on which the research was based. The olive coloured active layer is a blend of polymer / C61 Buckyball based methanofullerene with the interface between the two materials dispersed within the blend. The conceptual interpretation of the research paper electrical model (Koster et al. 2005) is shown in figure 3.11. Also shown in figure 3.11 is a conceptual interpretation of an optical model (L.A.A.Pettersson et al. 1999) (Sievers et al. 2006) (Kotlarski et al. 2008) included for completeness.

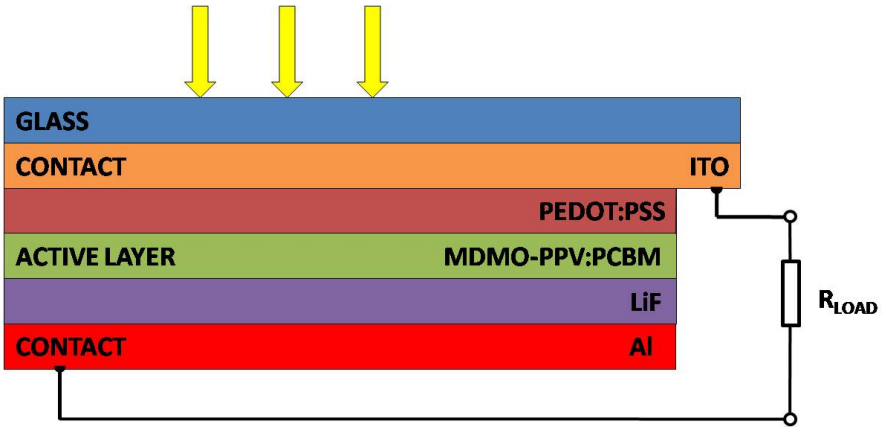

Figure 3.10: Diagram of Organic PV Layers

3.2.1 Iterative Approach

Appendix C shows a more detailed diagram of the interpretation of the research paper electrical model (Koster et al. 2005). It involves an iterative approach of discretising equations to converge (with stability to within a preset tolerance) toward an equilibrium solution of electric field $\frac{d\psi}{dx}$, recombination rate R, electron n and hole p density profiles for the given polymer. Dr Tony Ahfock (Ahfock 2008) directly assisted with attempting to find a logical approach to this problem. After numerous attempts at finding a logical approach, the following describes a rough mathematical outline of a potential solution. It is assumed that the reason for the iterative approach is that since the active layer has a blended interface, there is no possibility of measuring the carrier density n and p profiles. However, future work may confirm this or not.

Starting with known carrier density n and p profile boundaries and a guess of the profiles between these boundaries, the Poisson equation (Koster et al. 2005) is solved for the second derivative of the potential:

$$\frac{d^2}{dx^2}\psi(x) = \frac{q}{\epsilon}\left[n(x) - p(x)\right](V.m^{-2}) \tag{3.29}$$

where q = electronic charge = $1.602.10^{-19}(C)$;

ϵ = dielectric constant $(F.m^{-1})$;

n and n = electron and hole carrier concentration (m^{-3}).

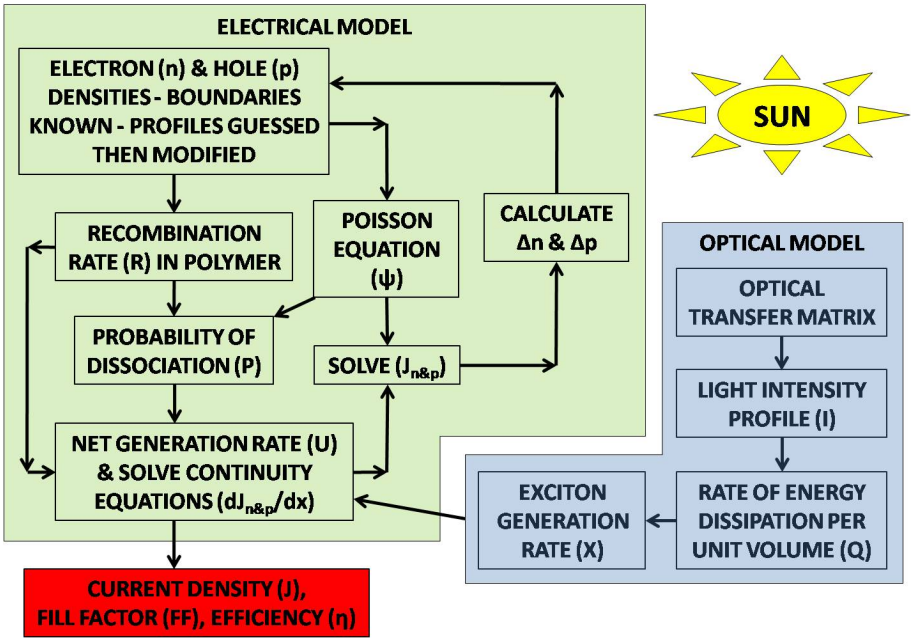

Figure 3.11: Block Diagram of Intended Approach to the Organic PV Model

Using the finite difference approach, equation 3.29 can be written as:

$$\frac{\frac{\psi_{i+1}-\psi_i}{\Delta x} - \frac{\psi_i-\psi_{i-1}}{\Delta x}}{\Delta x} = \frac{q}{\epsilon}(n_i - p_i) \tag{3.30}$$

$$\therefore \frac{\psi_{i-1} - 2.\psi_i + \psi_{i+1}}{(\Delta x)^2} = \frac{q}{\epsilon}(n_i - p_i) \tag{3.31}$$

$$\therefore \psi_{i-1} - 2.\psi_i + \psi_{i+1} = (\Delta x)^2.\frac{q}{\epsilon}(n_i - p_i) \tag{3.32}$$

Assuming:

$$A.x = b \tag{3.33}$$

A is represented by an n x n tridiagonal square matrix where:

$A(i,i) = -2$ for $1 =< i =< n$;

$A(i,i+1) = A(i+1,i) = 1$ for $1 =< i =< n-1$;

All other entries in $A = 0$.

x is a column vector $= [\psi_1, \psi_2, ...\psi_{n-1}, \psi_n]^T$

b is a column vector where:

$b(1) = -\psi(0) + (\Delta x)^2.\frac{q}{\epsilon}(n_i - p_i)$;

$b(i) = (\Delta x)^2.\frac{q}{\epsilon}(n_i - p_i)$ for $1 < i < n$;

$b(n) = -\psi(L) + (\Delta x)^2.\frac{q}{\epsilon}(n_i - p_i)$.

where boundary values $\psi(0)$ and $\psi(L)$ values are not known explicitly but the difference in their values is given (Koster et al. 2005).

Once A and b are constructed, the solution column vector x is determined for all values of $\frac{d^2}{dx^2}\psi(x)$ using:

$$x = A^{-1}.b \tag{3.34}$$

From this solution $\frac{d^2}{dx^2}\psi(x)$ profile, potential $\psi(x)$ and electric field $\frac{d}{dx}\psi(x)$ can then be calculated. The following equations are then used to solve for J_n and J_p at the boundaries:

$$J_n(x) = -q.n(x).\mu_n.\frac{d}{dx}\psi(x) + q.D_n.\frac{d}{dx}n(x) \tag{3.35}$$

$$J_p(x) = q.p(x).\mu_p.\frac{d}{dx}\psi(x) + q.D_p.\frac{d}{dx}p(x) \tag{3.36}$$

Referring to Appendix C, the solutions for J_n and J_p between the boundaries are assumed to be able to be calculated through a series of equations down the left hand side. The series of equations shown in Appendix C is replicated here, however there is some differences between the equations replicated here (and in Appendix C) and those in (Koster et al. 2005) (Mihailetchi, Koster, Hummelen & Blom 2004) and their references. This is due to an interpretation of the meaning of and some minor errors thought to exist within the equations within these research papers.

Recombination strength (Langevin) equation:

$$\gamma = \frac{q}{\langle\epsilon\rangle}.\langle\mu\rangle(m^3.s^{-1}) \tag{3.37}$$

where q = electronic charge = $1.602.10^{-19}(C)$;

$\langle\epsilon\rangle$ = spatially averaged dielectric constant $(F.m^{-1})$;

$\langle\mu\rangle$ = spatially averaged sum of electron and hole mobilities $(m^2.V^{-1}.s^{-1})$.

Intrinsic carrier concentration equation:

$$n_{int} = N_C.exp\left(\frac{-E_{gap}}{2.V_t}\right) \tag{3.38}$$

where N_C = effective density of states of both conduction and valence band;

E_{gap} = bandgap;

V_t = thermal voltage.

Please note no attempt was made to offer the units of the components of this equation as there must be a conversion factor between energy and voltage that is unclear.

Biomolecular recombination rate equation:

$$R = \gamma(n.p - n_{int}^2)(m^{-3}.s^{-1}) \tag{3.39}$$

where γ = recombination strength $(m^3.s^{-1})$;

n and n = electron and hole carrier concentration (m^{-3});

n_{int} = intrinsic carrier concentration (m^{-3}).

Constant:

$$b = \frac{q^3.F}{8.\pi.\epsilon.k^2.T^2} \tag{3.40}$$

where q = electronic charge = $1.602.10^{-19}(C)$;

F = (assumed to be) electric field $\frac{d}{dx}\psi$ calculated above $(V.m^{-1})$;

ϵ = dielectric constant $(F.m^{-1})$;

k = Boltzmann's constant = $1.380.10^{-23}(J.K^{-1})$;

T = absolute temperature (K).

Each of the following equations (3.41) to (3.44) are calculated for a range of exciton separation distances $0 < x < 4nm$ to calculate the integral in equation (3.45). However, the symbol x for exciton separation distances should not be confused with the symbol x representing distance into the organic PV.

Binding energy equation (Mihailetchi et al. 2004):

$$E_B = \frac{q^2}{4.\pi.\epsilon.x}(J) \tag{3.41}$$

where q = electronic charge = $1.602.10^{-19}(C)$;

$\epsilon = \epsilon_0.\epsilon_r$ = dielectric constant $(F.m^{-1})$;

x = exciton separation distance (m).

Dissociation rate equation:

$$k_{diss}(x,T,F) = \left(\frac{3.R}{4.\pi.x^3}\right) exp\left(\frac{-E_B}{k.T}\right)\left(1 + b + \frac{b^2}{3} + \frac{b^3}{18} + \frac{b^4}{180}\right) \tag{3.42}$$

where R = biomolecular recombination rate ($m^{-3}.s^{-1}$);

x = exciton separation distance (m);

E_B = inding energy (J);

k = Boltzmann's constant = $1.380.10^{-23}(J.K^{-1})$;

T = absolute temperature (K);

b = constant.

Probability of electron-hole pair dissociation equation:

$$p(x,T,F) = \frac{k_{diss}(x,T,F)}{k_{diss}(x,T,F) + k_f(T)} \tag{3.43}$$

where $k_{diss}(x,T,F)$ = dissociation rate at position x, temperature T and electric field F;

$k_f(T)$ = decay rate at temperature T (s^{-1}).

Normalised distribution function (for exciton separation) equation:

$$f(a,x) = \left(\frac{4}{\sqrt{\pi}.a^3}\right) x^2.exp\left(\frac{-x^2}{a^2}\right) \tag{3.44}$$

where a = highest distribution exciton separation distance (m);

x = exciton separation distance (m).

Probability electron-hole pair escape recombination equation:

$$P(a,T,F) = \int_{>0nm}^{4nm} p(x,T,F).f(a,x).dx \tag{3.45}$$

where $p(x,T,F)$ = probability of electron-hole pair dissociation;

$f(a,x)$ = normalised distribution function.

Net generation rate equation:

$$U(x) = P.G - ((1-P)R) \tag{3.46}$$

where P = probability electron-hole pair escape recombination;

G = average exciton generation rate;

R = biomolecular recombination rate.

The continuity equations can then be solved:

$$\frac{d}{dx}J_n(x) = q.U(x) \tag{3.47}$$

$$\frac{d}{dx}J_p(x) = -q.U(x) \tag{3.48}$$

With the $\frac{d}{dx}J_n(x)$ and $\frac{d}{dx}J_p(x)$ profiles and the boundaries of J_n and J_p already calculated in equation (3.35) and (3.36), the J_n and J_p profiles between the boundaries can then be calculated. However, there is uncertainty on how to calculate Δn and Δp profiles to apply to the original n and p to continue the iteration to converge with stability to a solution within a preset tolerance. Dr Tony Ahfock (Ahfock 2008) suspected a Gauss-Seidel mathematical approach could be used, however it was not possible to attempt this given time constraints. Once a current density solution is achieved, J-V curve, fill factor and efficiency calculations can be attempted.

Chapter 4

Analysis and Results

4.1 Silicon PV Model

4.1.1 J-V and Power Density Curves, Fill Factor and Efficiency

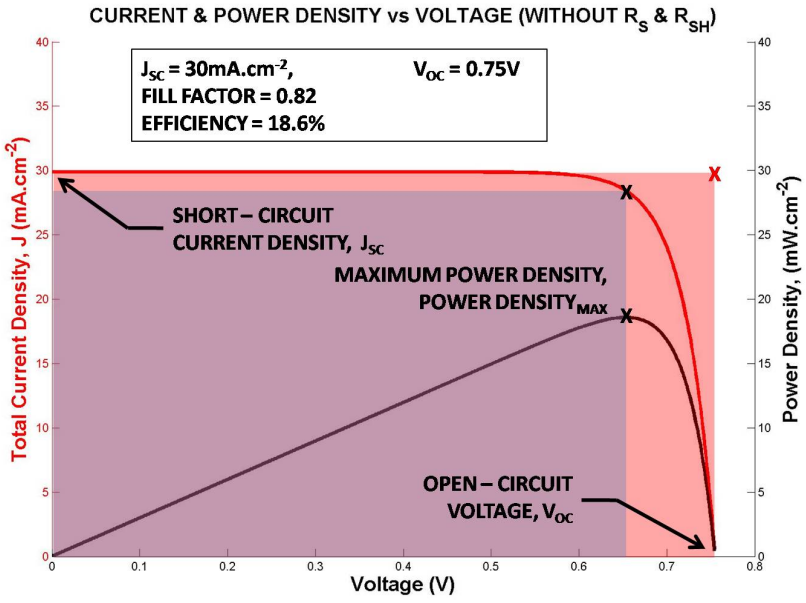

Figure 4.1: Silicon PV J-V Curve Without Considering Resistances R_S and R_{SH}

Using the theory described in section 3.1.3, figure 4.1 shows the output current density plotted against voltage ($J-V$ curve in red) of the silicon PV model without considering

resistances R_S and R_{SH} - with the y-axis on the left. Referring to figures 3.7 and 4.1, it can be seen that short circuit current density J_{SC} = light generated current density $J_L = 30mA.cm^{-2}$ when voltage $V = 0$. Open circuit voltage $V_{OC} = 0.75V$ when light generated current density $J_L = 0mA.cm^{-2}$ is also shown.

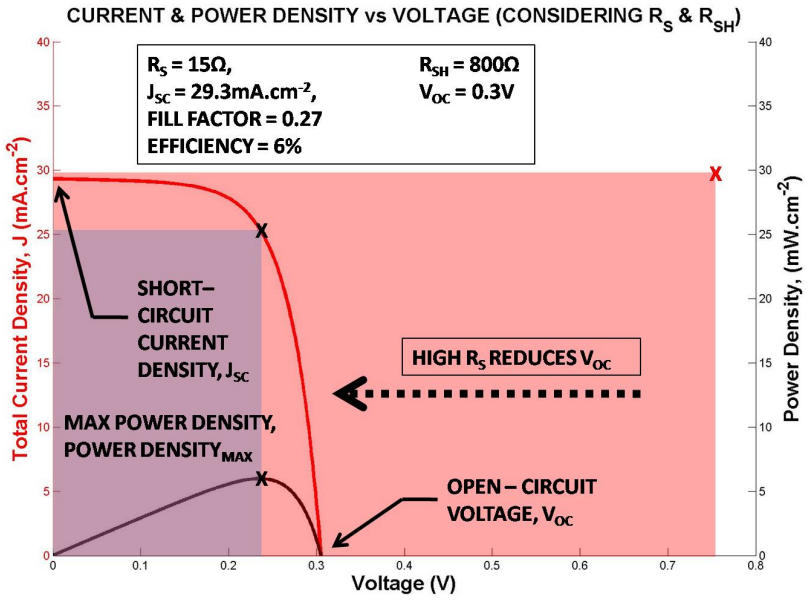

Figure 4.2: Silicon PV J-V Curve With Resistances $R_S = 15\Omega$ and $R_{SH} = 800\Omega$

The power density is also plotted against voltage in black with it's y-axis on the right. Power density is the product of the two current density and voltage axes as per the equation:

$$PowerDensity = J.V(mW.cm^{-2}) \tag{4.1}$$

where J = current density $(mA.cm^{-2})$;

V = terminal voltage (V).

The point of maximum power density $PowerDensity_{MAX}$ is also indicated in figure 4.1.

Fill factor is a standard PV ratio and is mainly a measure of the quality of the pn junction. Refering to figure 4.1 fill factor in simple terms is the ratio of the area of the purple actual maximum power density rectangle over the orange ideal maximum power

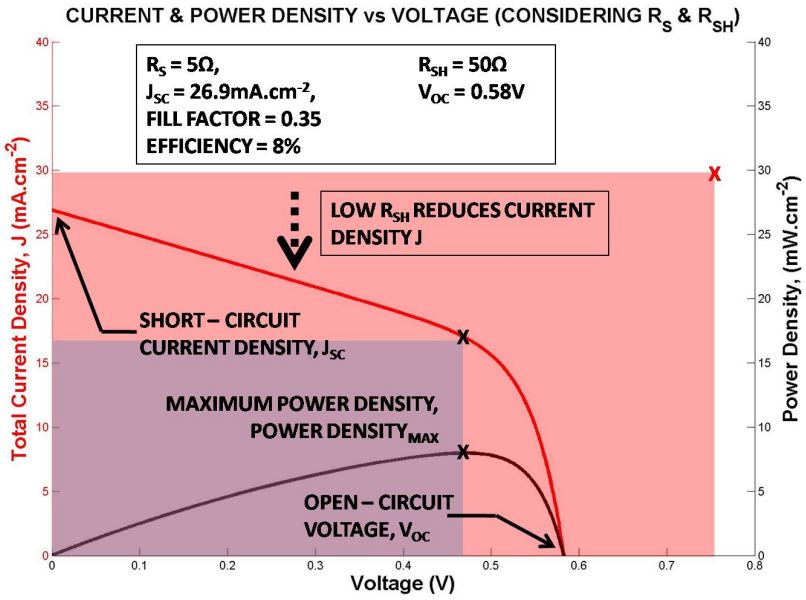

Figure 4.3: Silicon PV J-V Curve With Resistances $R_S = 5\Omega$ and $R_{SH} = 50\Omega$

density rectangle. The fill factor of the PV is calculated using the equation:

$$FF = \frac{PowerDensity_{MAX}}{(V_{OC}.J_{SC})}; \tag{4.2}$$

Referring to figure 4.1 and inspection of equation (4.2) indicates that the ideal fill factor $FF = 1$. The actual fill factor of the PV when not considering resistances = 0.82 which is quite high.

The efficiency η of the PV is a follow on from the fill factor, also using the maximum point of power density and is calculated using the equation:

$$\eta = \frac{output}{input} \tag{4.3}$$

$$\eta = \frac{PowerDensity_{MAX} * 100}{input}(\%); \tag{4.4}$$

where $PowerDensity_{MAX}$ = maximum point of power density $(mW.cm^{-2})$;

$input$ = integrated NREL AM1.5 sun (assumed) = $1kW.m^{-2} = 100mW.cm^{-2}$.

Figure 4.1 shows efficiency $\eta = 18.6\%$ when not considering resistances.

As was the intention of this project, there are numerous variables (eg. front and back surface recombination velocity) in the silicon PV model that can be altered that will

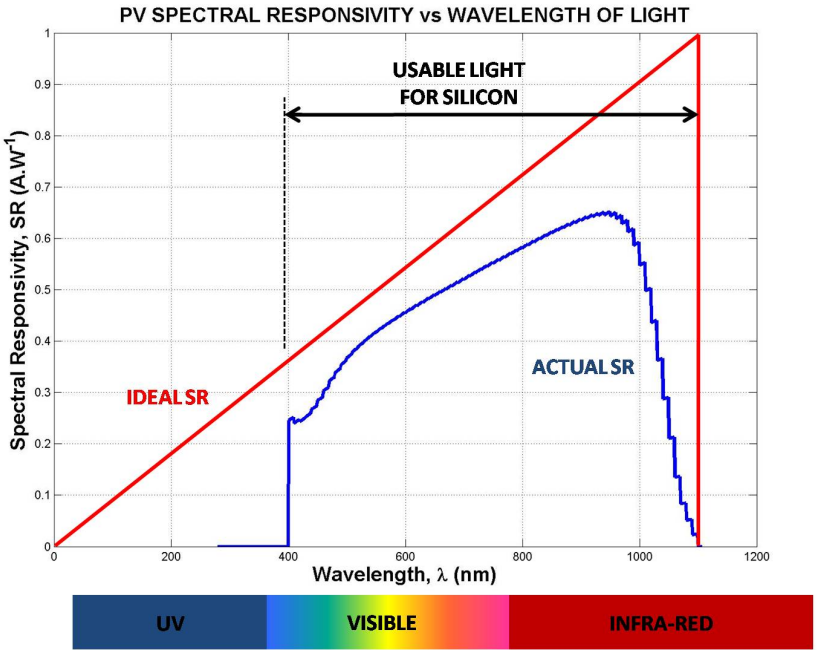

Figure 4.4: Silicon PV Ideal and Actual Spectral Responsivity

result in modifying the output in some way. Here we see the effect on output of inserting and altering series resistance R_S and shunt resistance R_{SH}. As described in section 3.1.4, these resistances describe the quality of the pn junction. So, as fill factor is a measure of the quality of the pn junction and efficiency follows on from fill factor, the expectation is that fill factor and efficiency are affected by series and shunt resistances.

Figure 4.2 shows the result of adding series resistance $R_S = 15\Omega$ and shunt resistance $R_{SH} = 800\Omega$. The relatively high series resistance causes open circuit voltage to be reduced considerably to $V_{OC} = 0.3V$ whereas the also relatively high shunt resistance allows short circuit current density to remain almost unchanged at $J_{SC} = 29.3mA.cm^{-2}$. It can also be seen that fill factor is somewhat reduced to 0.27. Consequently efficiency is also somewhat reduced to 6%.

Figure 4.3 shows the result of altering series resistance $R_S = 5\Omega$ and shunt resistance $R_{SH} = 50\Omega$. The relatively low series resistance causes open circuit voltage to increase back out to $V_{OC} = 0.58V$ whereas the unreasonably low shunt resistance drives short circuit current density down to $J_{SC} = 26.9mA.cm^{-2}$. Also illuminated current density J_L is lowered substantially by the low shunt resistance. It can also be seen that fill factor is still relatively low at 0.35. Consequently efficiency is also still somewhat low

at 8%.

From our model we can safely say that adding and altering R_S and R_{SH}, which refer to the quality of the device in different ways, affects the fill factor and efficiency of the PV as expected.

4.1.2 Spectral Responsivity

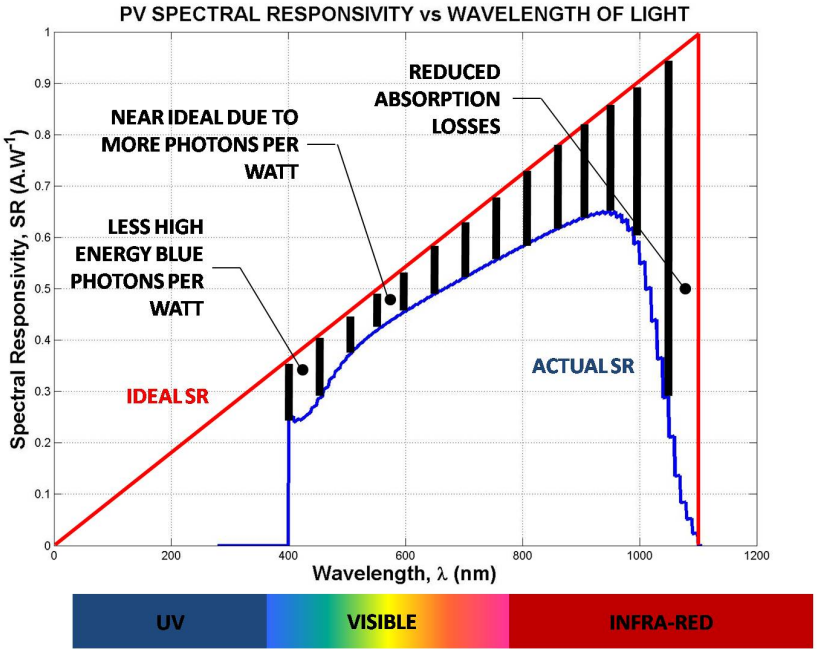

Figure 4.5: Silicon PV Spectral Responsivity With Losses

Figure 4.4 shows the model output spectral responsivity (SR) plotted in blue against each usable wavelength of light. The ideal spectral responsivity is also shown in red. The actual spectral responsivity although it is the expected shape, originally exceeded the ideal. The model was then modified to clamp the spectral responsivity to zero at the bandgap wavelength ($\lambda_{E_g} \approx 1100nm$ in this case). This bought it below ideal but as such, this part of the model needs refining.

Figure 4.5 shows the losses (ie. the difference between the actual and ideal SR) hatched and the likely causes of these losses. The losses at the lower wavelengths are mainly due to there being less high energy blue photons per watt at these wavelengths and the inability of the PV to absorb the high energy of each of those photons. As discussed in

section 3.1.5 a PV cannot absorb the high energy from photons below $\approx 400nm$. The losses at the higher wavelengths are mainly due to reduced absorption for the lower energy red photons. Here the photons are absorbed further into the PV base and consequently further than a diffusion length from the collecting pn junction. This increases the probability that the generated electrons (in the base) will recombine, rather than be collected by the pn junction and consequently not contribute to illuminated current density.

4.1.3 External Quantum Efficiency

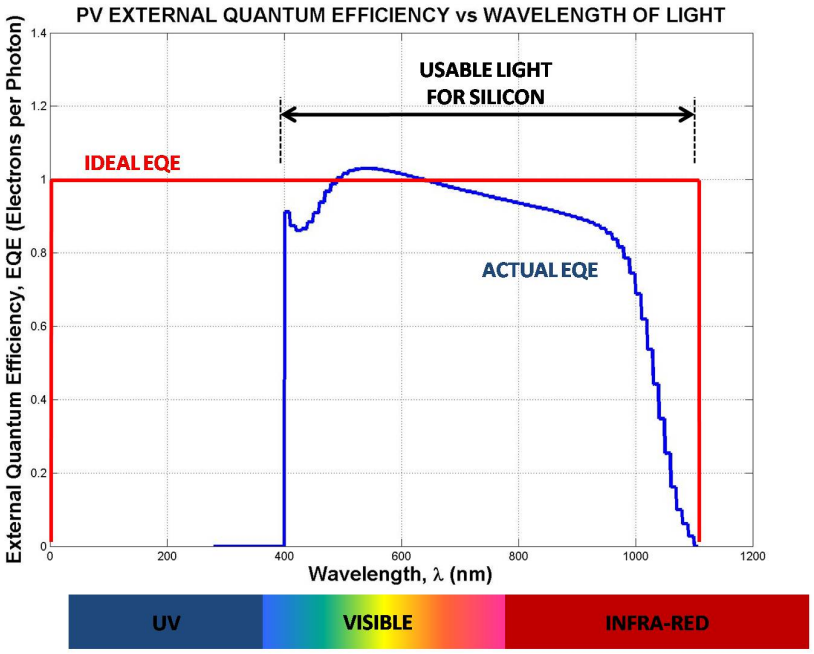

Figure 4.6: Silicon PV Ideal and Actual External Quantum Efficiency

Much like the spectral responsivity above, figure 4.6 shows the model output external quantum efficiency (EQE) plotted in blue against each usable wavelength of light. The ideal external quantum efficiency is shown in red. The actual external quantum efficiency although it is the expected shape, originally exceeded the ideal and still does. The model was modified to clamp external quantum efficiency to zero at the bandgap wavelength ($\lambda_{E_g} \approx 1100nm$ in this case). This bought the plot down somewhat but it can be seen to still exceed ideal and consequently this part of the model also needs refining.

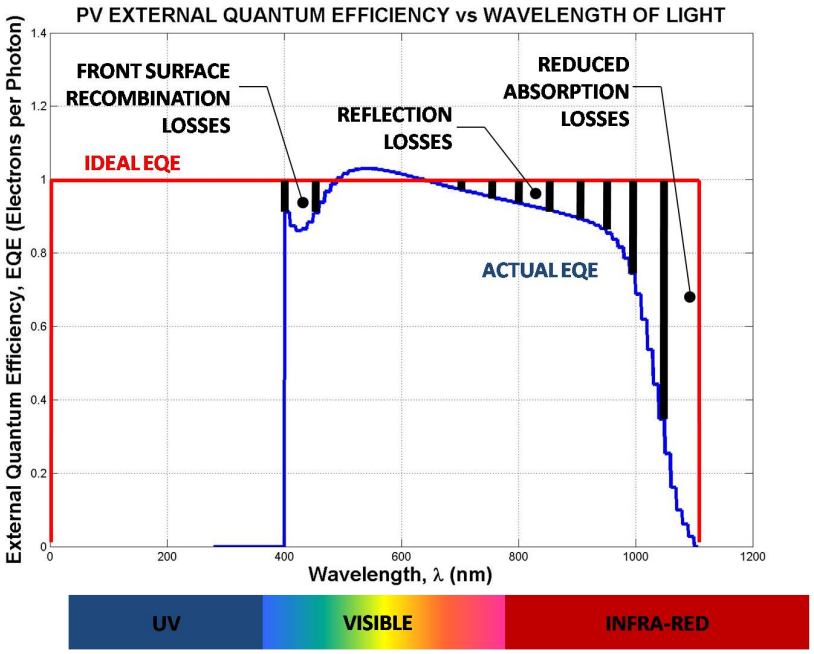

Figure 4.7: Silicon PV External Quantum Efficiency With Losses

If we imagine the external quantum efficiency plot is touching the ideal plot at it's highest point in figure 4.6 (ie. shifted down), the plot would look as it should. The losses (ie. the difference between the actual and ideal EQE) are shown hatched and briefly described in figure 4.7. The losses are due to front surface recombination losses at the shorter wavelengths, reflection losses in the middle wavelengths and again reduced absorption for the lower energy red photons at the higher wavelengths.

4.2 Organic PV Model

The code developed so far for the organic PV model is included in Appendix G. Referring to Appendix C, the code has been reduced to include only the known carrier concentration profile boundaries and the intervening guess profiles, their derivatives and solving of the Poisson equation.

Chapter 5

Conclusions

The conclusions for each of the silicon and organic PV theories and models are presented in their respective sections 5.1 and 5.2 below. This includes the respective model limitations and suggested further work. Finally, this work is concluded in section 5.3 which summarises the parallels and potential advantages of using organic PV over a silicon PV.

5.1 Silicon PV Model

A silicon PV does indeed draw on and follow existing pn junction theory. It can be seen in the theory and application in this work, that PV theory has then extended pn junction theory to become a science of it's own. That science while quite mature is constantly being researched and developed and the silicon PV model has drawn on some of that research and development and research papers published from it. The simple emitter and base silicon PV that the model is based upon, has a non-uniformly doped emitter which complicates the theory and equations. The high doping concentration at the emitter surface causes the relative increase of minority carriers to far outweigh that of majority carriers when the PV is illuminated. The emitter of this PV is very thin ($\approx 1.3\mu m$) compared to the base ($\approx 300\mu m$) to get the same minority carriers close enough to (well within a minority diffusion length), be collected by and swept

across the pn junction to become majority carriers in the base to recombine at the rear contact with the electrons that have flowed through the load. There are reciprocal effects of minority carriers from base to emitter and that of majority carriers but as has been seen, illuminated current density is generated mostly by the flow of minority carriers generated at or near the surface of a silicon PV.

The silicon PV model takes various inputs which may or may not be able to be altered to observe the effects of the model outputs. Of these, absolute temperature T cannot be altered as the absorption coefficient data used is for silicon at 300K. The inputs which can be altered include:

- emitter doping profile which has been discussed above;
- emitter width which also has been discussed above;
- front surface recombination velocity ($SRV = 10^3 cm.s^{-1}$) which as it increases from a theoretical zero, increases recombination, reduces collection efficiency and consequently reduces overall efficiency;
- base width which is relevant to the absorption of low energy red photons and distance of the generated carriers from the pn junction;
- base uniform doping level which is relevant to the formation of the depletion region and the generation of carriers;
- back surface recombination velocity like that for the front surface affects efficiency ($SRV = 10^2 cm.s^{-1}$);
- series resistance R_S reflects the quality of the pn junction and when inserted and increased, reduces fill factor and efficiency;
- shunt resistance R_{SH} also reflects the quality of the pn junction and when inserted and decreased, reduces fill factor and efficiency;
- ideality factor also reflects the quality of the pn junction and is set here to a nominal 1.3;

It has been shown in the body of this work that the effect of inserting and altering series resistance R_S and shunt resistance R_{SH} alters the fill factor and efficiency of

the device as expected. The spectral responsivity SR and external quantum efficiency EQE plot shapes resemble those published by referenced academics and researchers and so conclude the model is on the right track.

While the silicon PV model is complete to a point it is by no means perfect. The model is based on some assumptions and nominal figures and consequently it requires refinement and development to become a truly robust model of a silicon PV. Each limitation has been described in the relevant section of this work, however the known limitations and areas for improvement and further work (not necessarily in order) are summarised:

1. Assumptions were made in calculating the generation rate $G(x, \lambda)$ for each wavelength of usable light λ and at each position within the device x and the consequent integration in different directions for use in respective calculations for total light generated current density and spectral responsivity SR / external quantum efficiency EQE. While references suggest it is correct for the former, this approach needs to be checked for the latter.

2. A nominal diode leakage current J_0 was taken from (Kittidachachan et al. 2007) as the standard equations (Honsberg & Bowden 2008) (Green 1992) did not seem applicable to a non-uniformly doped emitter.

3. Illuminated current density J_L was used as a proxy for net current density J in the calculation of J. Nodal analysis and iteration could possibly be used to calculate the respective currents and voltage affected by series resistance R_S and shunt resistance R_{SH}.

4. The total radiant power density input for the efficiency calculation was assumed $= 1kW.m^{-2}$ instead of integrating the NREL spectral irradiance data over the spectrum of usable light for silicon.

5. The spectral responsivity SR and external quantum efficiency EQE plots both originally exceeded their respective ideals. Both were modified within the model to clamp each to zero at the bandgap wavelength λ_{E_g} yet the EQE still exceeds ideal.

6. Assumptions were made with respect to the calculations of spectral responsivity and external quantum efficiency and these along with conversion factors for proper units need to be checked.

7. Internal quantum efficiency IQE is quite complex in it's own right and needs to be researched, calculated and plotted.

8. Assumptions and conversion factors applied for proper output units through the entire model need to be checked.

9. The width of the depletion region was not calculated and the pn junction was assumed to be an imaginary line.

10. Modern programming facilities could be developed (eg. drop down boxes) and provided for the user to more easily alter the inputs described.

11. The reading in and manipulation of provided data could be enhanced to quicken model processing time.

5.2 Organic PV Model

Research and development continues on different types of organic PV and one type is based on vertically aligned carbon nanotubes (VA-CNT) with polymer within the voids between the VA-CNT. This type of organic PV requires high precision fabrication and therefore (at least for the moment) high cost. In retrospect, the title of this research project is a misnomer as the organic PV chosen to model is a blended mixture of polymer and C_{61} buckminsterfullerene "buckyballs" and not CNT.

The science for this type of blended bulk-heterojunction (BHJ) organic PV is quite young. Photons are absorbed within the conjugated polymer to generate exciton pairs, which then diffuse through the polymer to an interface between the two materials. At an interface, the exciton either dissociates (electron and hole separate - the hole stays within the polymer and the electron is transferred to the fullerene where they become majority carriers within their respective materials) or decays back to a ground state. If

the exciton dissociates and if the electron and hole avoid recombination at an interface they will contribute to illuminated current density.

Researchers consistently use an optical model inputing an exciton generation rate profile into an electrical model to simulate this type of organic PV. The electrical model output would be fill factor and efficiency, spectral responsivity and quantum efficiency. However, it has been shown that devices with an active layer $< 250nm$ can be adequately simulated by the electrical model alone using an average exciton generation rate. This work concentrated on creating a workable electrical model to become the basis of the organic PV model. While a model was not able to be completed, the interpretations of the mathematical concepts and ideas presented within this work may allow further work to create a working organic PV model.

5.3 Conclusion

While there are stark contrasts between the concepts of the silicon PV to those of the organic PV chosen, there are conceptual similarities as well. The most notable difference is that the organic PV is a majority carrier device in contrast to the inorganic PV as a minority carrier device. The organic PV has a two part process where an exciton is generated and then hopefully dissociates. If the respective carriers then avoid recombination they may add to illuminated current density. The silicon PV generates an electron-hole pair and if the respective minority carriers can avoid recombination may be collected by the pn junction and add to illuminated current density. Both can be seen as a two part process, recombination reduces the efficiency of both and both rely on probability calculations (collection for a silicon PV and dissociation and avoiding recombination for an organic PV) to simulate them. Consequently, there are parallels as well as differences when comparing the concepts of the silicon and organic PV.

While popular contemporary inorganic silicon based PV's have a present maximum experimental efficiency of $\approx 24\%$, they require expensive high-temperature fabrication methods and are only economically viable for specific applications. Organic blended

BHJ PV's have the benefit of being much cheaper and easier to fabricate and have mechanical flexibility for curved architectural applications. However, organic PV's currently have lower efficiencies than silicon PV's as well as other downside factors.

Although the global community's desire for cheap, efficient, truly sustainable energy generation is ever present, this work offers no definitive conclusion on which of inorganic silicon PV or organic PV is potentially superior.

References

Ahfock, A. (2008), USQ.

DelAlamo, J. A. & Swanson, R. M. (1984), 'The physics of heavily doped emitters', *IEEE Transactions on Electron Devices* **31**(12).

Green, M. A. (1992), *Solar Cells Operating Principles, Technology and System Applications*, Prentice-Hall.

Gregg, B. & Hanna, M. (2003), 'Comparing organic to inorganic photovoltaic cells: Theory, experiment and simulation', *Journal of Applied Physics* **93**(6).

Gummel, H. K. (1964), 'A self-consistent iterative scheme for one-dimensional steady state transistor calculations', *IEEE Transactions on Electron Devices* **11**(455).

Honsberg, C. (2008), *Derivation of the Ideal Diode Equation for Photovoltaics*, University of Delaware.
`http://pvcdrom.pveducation.org/`
current October 2008.

Honsberg, C. & Bowden, S. (2008), *Photovoltaics CDROM (Beta Version)*, University of Delaware.
`http://pvcdrom.pveducation.org/`
current October 2008.

Kanai, Y. & Grossman, J. (2008), 'Role of semiconducting and metallic tubes in p3ht/carbon-nanotube photovoltaic heterojunctions: Density functional theory calculations', *Nano Letters* **8**(3), 908–912.

Kittidachachan, P., Markvart, T., Bagnall, D., Greef, R. & Ensell, G. (2007), *A Detailed Study of p-n Junction Solar Cells by Means of Collection Efficiency*, National Research Council of Thailand (NRCT) and University of Southampton, UK.
`http://www.energy-based.nrct.go.th/view_res.asp?lang=en&ResId=33764`
current October 2008.

Koster, L., Smits, E., Mihailetchi, V. & Blom, P. (2005), 'Device model for the operation of polymer/fullerene bulk heterojunction solar cells', *Physical Review B* **72**(085205).

Kotlarski, J., Blom, P., Koster, L., Lenes, M. & Slooff, L. (2008), 'Combined optical and electrical modeling of polymer:fullerene bulk heterojunction solar cells', *Journal of Applied Physics* **103**(084502).

L.A.A.Pettersson, Roman, L. & Inganas, O. (1999), 'Modeling photocurrent action spectra of photovoltaic devices based on organic thin films', *Journal of Applied Physics* **86**(487).

Mihailetchi, V. D., Koster, L. J. A., Hummelen, J. C. & Blom, P. (2004), 'Photocurrent generation in polymer-fullerene bulk heterojunctions', *Physical Review Letters* **93**(21).

Motta, N. (2008), QUT.

Neamen, D. A. (2001), *Electronic Circuit Analysis and Design (2nd Edition)*, McGraw Hill.

NREL (2008), *Reference Solar Spectral Irradiance: Air Mass 1.5*, National Renewable Energy Laboratory.
`http://rredc.nrel.gov/solar/spectra/am1.5/`
current October 2008.

O'Connell, M. J. (2006), *Carbon Nanotubes Properties and Applications*, CRC Press, Taylor and Francis Group.

Sievers, D., Shrotriya, V. & Yang, Y. (2006), 'Modeling optical effects and thickness dependant current in polymer bulk-heterojunction solar cells', *Journal of Applied Physics* **100**(114509).

Sun, S. & Sariciftci, N. (2005), *Organic Photovoltaics, Mechanisms, Materials and Devices*, CRC Press, Taylor and Francis Group.

Wenham, S. R., Green, M. A., Watt, M. E. & Corkish, R. (2007), *Applied Photovoltaics*, Earthscan.

Copyright to ARC Centre for Advanced Silicon Photovoltaics and Photonics.

Wikipedia (2008), Wikipedia.

`http://en.wikipedia.org/wiki/Carbon_nanotube`

current October 2008.

Zeghbroeck, B. V. (2008), *Principles of Semiconductor Devices*, University of Colarado.

`http://ece-www.colorado.edu/~bart/book/title.htm`

current October 2008.

Appendix A

Project Specification

University of Southern Queensland

FACULTY OF ENGINEERING AND SURVEYING

ENG4111/4112 Research Project
PROJECT SPECIFICATION

FOR: Craig Gardner

TOPIC: Carbon Nanotubes (CNT) as Potentially a More Effective Material for Photovoltaic (PV) Converters and a Material for Renewable Energy Storage Capacitors.

SUPERVISOR: Dr Tony Ahfock

SPONSORHSIP: *(USQ or external body/person)* Own Project

PROJECT AIM: The project aims to determine the viability of CNT as a more effective material for PV converters and a material for renewable energy storage capacitors.

PROGRAMME: **(Issue A, 23 March 2008)**

1. Research and report on the theory behind contemporary silicon based PV converters.
2. Create a Matlab script to model a contemporary silicon based PV converter.
3. Research and report on the theory behind CNT and their potential as a useful material for PV converters.
4. Draw a parallel between the principles behind contemporary silicon based PV converters and those based on CNT.
5. Create a Matlab script to model a theoretical CNT based PV converter.
6. Draw conclusions on the potential advantages of using CNT as a base material for PV converters.
7. Discuss the need for storage in renewable energy systems.
8. Investigate and report on the theory behind a storage capacitor based on CNT.

The requirements for an "A:" grade or higher are satisfactory achievement of steps 1 to 6 and the production of an acceptable dissertation.

AGREED _____ (student) _____ (supervisor)

Date: 25/3/2008 Date: 31/3/2008

Co-examiner: _____ 1/4/08

CS

Appendix B

Silicon PV Diagram

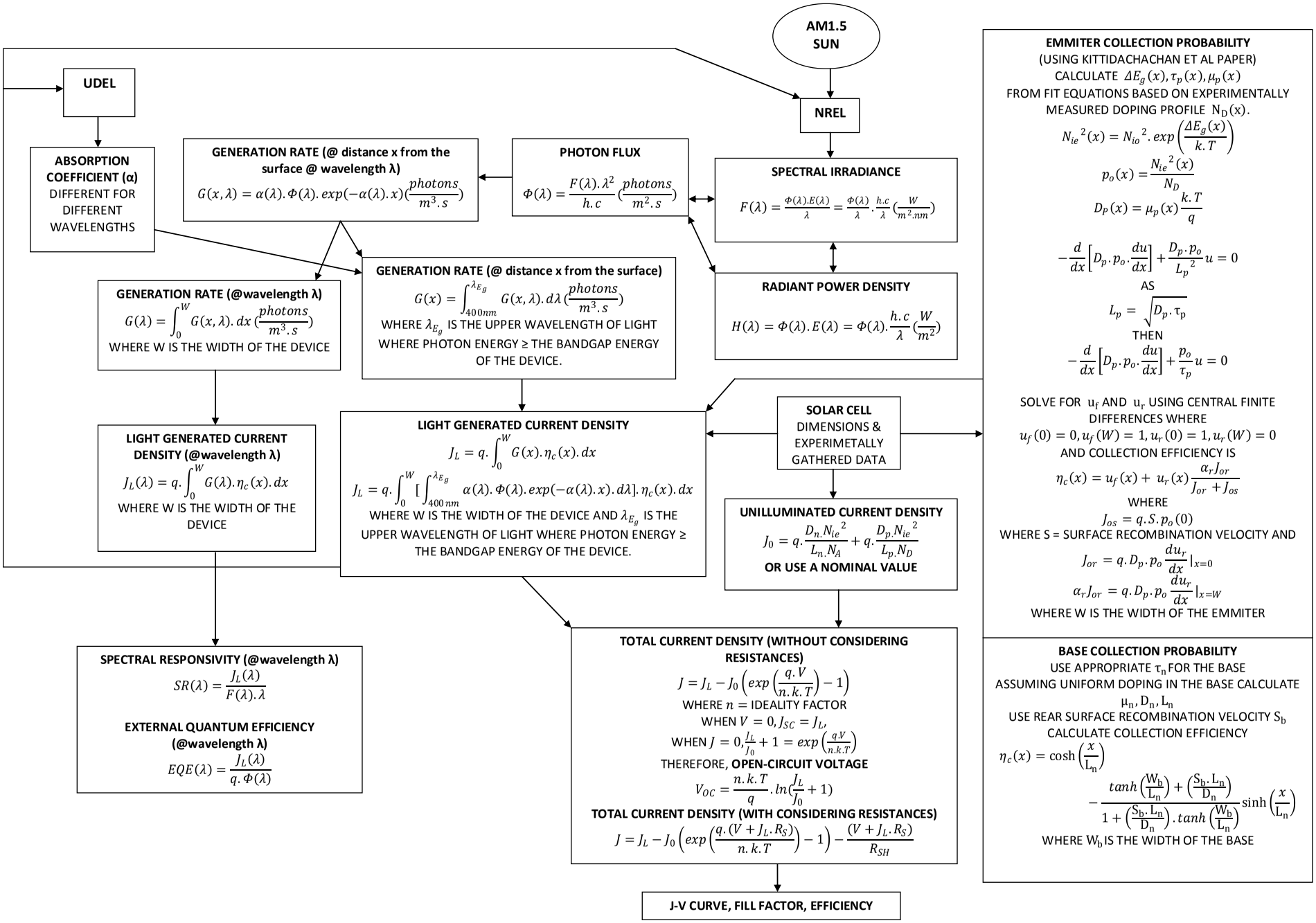
AM1.5 SUN
NREL
UDEL
ABSORPTION COEFFICIENT (α)
DIFFERENT FOR DIFFERENT WAVELENGTHS
GENERATION RATE (@ distance x from the surface @ wavelength λ)
$G(x,\lambda) = \alpha(\lambda).\Phi(\lambda).exp(-\alpha(\lambda).x)(\frac{photons}{m^3.s})$
PHOTON FLUX
$\Phi(\lambda) = \frac{F(\lambda).\lambda^2}{h.c}(\frac{photons}{m^2.s})$
SPECTRAL IRRADIANCE
$F(\lambda) = \frac{\Phi(\lambda).E(\lambda)}{\lambda} = \frac{\Phi(\lambda)}{\lambda}.\frac{h.c}{\lambda}(\frac{W}{m^2.nm})$
RADIANT POWER DENSITY
$H(\lambda) = \Phi(\lambda).E(\lambda) = \Phi(\lambda).\frac{h.c}{\lambda}(\frac{W}{m^2})$
GENERATION RATE (@wavelength λ)
$G(\lambda) = \int_0^W G(x,\lambda).dx\,(\frac{photons}{m^3.s})$
WHERE W IS THE WIDTH OF THE DEVICE
GENERATION RATE (@ distance x from the surface)
$G(x) = \int_{400nm}^{\lambda_{E_g}} G(x,\lambda).d\lambda\,(\frac{photons}{m^3.s})$
WHERE λ_{E_g} IS THE UPPER WAVELENGTH OF LIGHT WHERE PHOTON ENERGY ≥ THE BANDGAP ENERGY OF THE DEVICE.
LIGHT GENERATED CURRENT DENSITY (@wavelength λ)
$J_L(\lambda) = q.\int_0^W G(\lambda).\eta_c(x).dx$
WHERE W IS THE WIDTH OF THE DEVICE
LIGHT GENERATED CURRENT DENSITY
$J_L = q.\int_0^W G(x).\eta_c(x).dx$
$J_L = q.\int_0^W [\int_{400\,nm}^{\lambda_{E_g}} \alpha(\lambda).\Phi(\lambda).exp(-\alpha(\lambda).x).d\lambda].\eta_c(x).dx$
WHERE W IS THE WIDTH OF THE DEVICE AND λ_{E_g} IS THE UPPER WAVELENGTH OF LIGHT WHERE PHOTON ENERGY ≥ THE BANDGAP ENERGY OF THE DEVICE.
SOLAR CELL DIMENSIONS & EXPERIMETALLY GATHERED DATA
UNILLUMINATED CURRENT DENSITY
$J_0 = q.\frac{D_n.{N_{ie}}^2}{L_n.N_A} + q.\frac{D_p.{N_{ie}}^2}{L_p.N_D}$
OR USE A NOMINAL VALUE
SPECTRAL RESPONSIVITY (@wavelength λ)
$SR(\lambda) = \frac{J_L(\lambda)}{F(\lambda).\lambda}$
EXTERNAL QUANTUM EFFICIENCY (@wavelength λ)
$EQE(\lambda) = \frac{J_L(\lambda)}{q.\Phi(\lambda)}$
TOTAL CURRENT DENSITY (WITHOUT CONSIDERING RESISTANCES)
$J = J_L - J_0\left(exp\left(\frac{q.V}{n.k.T}\right) - 1\right)$
WHERE n = IDEALITY FACTOR
WHEN $V = 0, J_{SC} = J_L$,
WHEN $J = 0, \frac{J_L}{J_0} + 1 = exp\left(\frac{q.V}{n.k.T}\right)$
THEREFORE, OPEN-CIRCUIT VOLTAGE
$V_{OC} = \frac{n.k.T}{q}.ln(\frac{J_L}{J_0} + 1)$
TOTAL CURRENT DENSITY (WITH CONSIDERING RESISTANCES)
$J = J_L - J_0\left(exp\left(\frac{q.(V + J_L.R_S)}{n.k.T}\right) - 1\right) - \frac{(V + J_L.R_S)}{R_{SH}}$
J-V CURVE, FILL FACTOR, EFFICIENCY
EMMITER COLLECTION PROBABILITY
(USING KITTIDACHACHAN ET AL PAPER)
CALCULATE $\Delta E_g(x), \tau_p(x), \mu_p(x)$
FROM FIT EQUATIONS BASED ON EXPERIMENTALLY MEASURED DOPING PROFILE $N_D(x)$.
${N_{ie}}^2(x) = {N_{io}}^2.exp\left(\frac{\Delta E_g(x)}{k.T}\right)$
$p_o(x) = \frac{{N_{ie}}^2(x)}{N_D}$
$D_P(x) = \mu_p(x)\frac{k.T}{q}$
$-\frac{d}{dx}\left[D_p.p_o.\frac{du}{dx}\right] + \frac{D_p.p_o}{{L_p}^2}u = 0$
AS
$L_p = \sqrt{D_p.\tau_p}$
THEN
$-\frac{d}{dx}\left[D_p.p_o.\frac{du}{dx}\right] + \frac{p_o}{\tau_p}u = 0$
SOLVE FOR u_f AND u_r USING CENTRAL FINITE DIFFERENCES WHERE
$u_f(0) = 0, u_f(W) = 1, u_r(0) = 1, u_r(W) = 0$
AND COLLECTION EFFICIENCY IS
$\eta_c(x) = u_f(x) + u_r(x)\frac{\alpha_r J_{or}}{J_{or} + J_{os}}$
WHERE
$J_{os} = q.S.p_o(0)$
WHERE S = SURFACE RECOMBINATION VELOCITY AND
$J_{or} = q.D_p.p_o\frac{du_r}{dx}|_{x=0}$
$\alpha_r J_{or} = q.D_p.p_o\frac{du_r}{dx}|_{x=W}$
WHERE W IS THE WIDTH OF THE EMMITER
BASE COLLECTION PROBABILITY
USE APPROPRIATE τ_n FOR THE BASE
ASSUMING UNIFORM DOPING IN THE BASE CALCULATE μ_n, D_n, L_n
USE REAR SURFACE RECOMBINATION VELOCITY S_b
CALCULATE COLLECTION EFFICIENCY
$\eta_c(x) = \cosh\left(\frac{x}{L_n}\right) - \frac{tanh\left(\frac{W_b}{L_n}\right) + \left(\frac{S_b.L_n}{D_n}\right)}{1 + \left(\frac{S_b.L_n}{D_n}\right).tanh\left(\frac{W_b}{L_n}\right)}\sinh\left(\frac{x}{L_n}\right)$
WHERE W_b IS THE WIDTH OF THE BASE

Appendix C

Organic PV Concepts

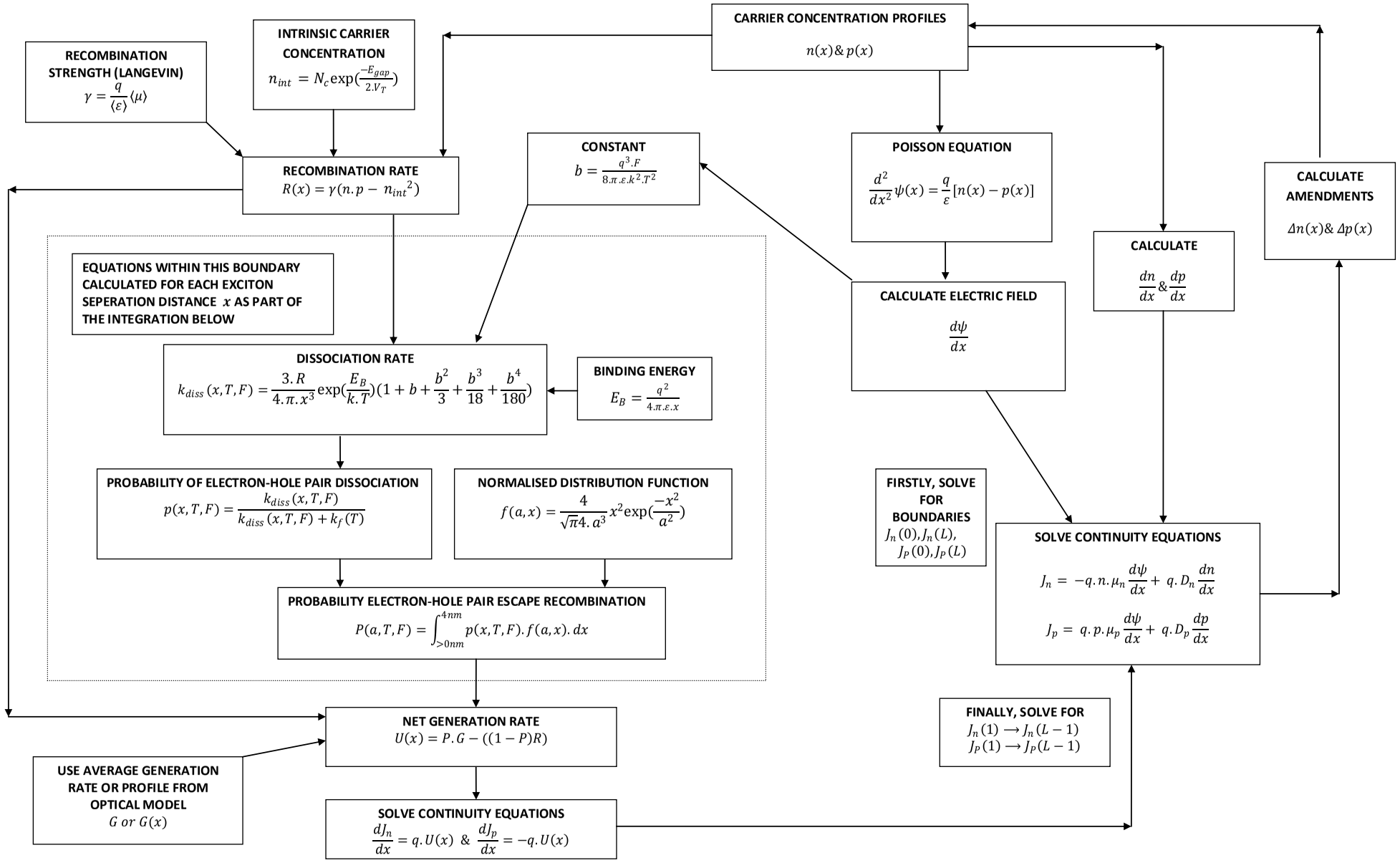
CARRIER CONCENTRATION PROFILES
$n(x)\&\,p(x)$
INTRINSIC CARRIER CONCENTRATION
$n_{int} = N_c \exp(\frac{-E_{gap}}{2.V_T})$
RECOMBINATION STRENGTH (LANGEVIN)
$\gamma = \frac{q}{\langle\varepsilon\rangle}\langle\mu\rangle$
RECOMBINATION RATE
$R(x) = \gamma(n.p - {n_{int}}^2)$
CONSTANT
$b = \frac{q^3.F}{8.\pi.\varepsilon.k^2.T^2}$
POISSON EQUATION
$\frac{d^2}{dx^2}\psi(x) = \frac{q}{\varepsilon}[n(x) - p(x)]$
CALCULATE AMENDMENTS
$\Delta n(x)\&\,\Delta p(x)$
CALCULATE
$\frac{dn}{dx}\&\frac{dp}{dx}$
EQUATIONS WITHIN THIS BOUNDARY CALCULATED FOR EACH EXCITON SEPERATION DISTANCE x AS PART OF THE INTEGRATION BELOW
CALCULATE ELECTRIC FIELD
$\frac{d\psi}{dx}$
DISSOCIATION RATE
$k_{diss}(x,T,F) = \frac{3.R}{4.\pi.x^3}\exp(\frac{E_B}{k.T})(1 + b + \frac{b^2}{3} + \frac{b^3}{18} + \frac{b^4}{180})$
BINDING ENERGY
$E_B = \frac{q^2}{4.\pi.\varepsilon.x}$
PROBABILITY OF ELECTRON-HOLE PAIR DISSOCIATION
$p(x,T,F) = \frac{k_{diss}(x,T,F)}{k_{diss}(x,T,F) + k_f(T)}$
NORMALISED DISTRIBUTION FUNCTION
$f(a,x) = \frac{4}{\sqrt{\pi}4.a^3}x^2\exp(\frac{-x^2}{a^2})$
FIRSTLY, SOLVE FOR BOUNDARIES
$J_n(0), J_n(L),$
$J_P(0), J_P(L)$
SOLVE CONTINUITY EQUATIONS
$J_n = -q.n.\mu_n\frac{d\psi}{dx} + q.D_n\frac{dn}{dx}$
$J_p = q.p.\mu_p\frac{d\psi}{dx} + q.D_p\frac{dp}{dx}$
PROBABILITY ELECTRON-HOLE PAIR ESCAPE RECOMBINATION
$P(a,T,F) = \int_{>0nm}^{4nm} p(x,T,F).f(a,x).dx$
NET GENERATION RATE
$U(x) = P.G - ((1-P)R)$
USE AVERAGE GENERATION RATE OR PROFILE FROM OPTICAL MODEL
G or $G(x)$
FINALLY, SOLVE FOR
$J_n(1) \longrightarrow J_n(L-1)$
$J_P(1) \longrightarrow J_P(L-1)$
SOLVE CONTINUITY EQUATIONS
$\frac{dJ_n}{dx} = q.U(x)$ & $\frac{dJ_p}{dx} = -q.U(x)$

Appendix D

Silicon PV Model Source Code

D.1 The SiliconPV.m MATLAB Function

Listing D.1: Silicon PV Model MATLAB function.

```
% Research Project Matlab Script for Silicon PV
% Name of function file: research_proj_silicon_pv.m

% SPECIAL NOTE: The concepts behind this Matlab code were
% derived mainly from UDEL website, UCOL website, NREL
% website, Applied Photovoltaics book (Green et al),
% Kittidachachan et al paper on collection efficiency and
% Dr Tony Ahfock.

% Purpose of function: To input a range of PV characteristics
% and output voltage, current density, power density, fill
% factor, efficiency, spectral responsivity, EQE & IQE and
% output a number of figures to screen and also output to
% individual pdf files.

% Input variables: research_proj_1_spectrum_data() is called
% to read in data (wavelengths, UDEL absorption coefficients
% and NREL spectral irradiances) from a data file
% AM15data.txt into variable spec_data.

% Output variables: none
% Written by: Craig Gardner
% Date of last revision: 18/10/08

% ------------------------------------ SETUP ------------------------------
clear all;
close all;
clc;
clf;

% ---------------------- PV SYSTEM INPUT VALUES -----------------------------
% absolute temperature K (degrees kelvin)
T = 300;
%T = 298.15; %25 deg C

% ------------------------------- EMITTER -----------------------------------
% very approximate doping profile array from
% Kittidachachan et al - gained experimentally
ND = [ 2.1e19, 2.3e19, 2.5e19, 2.4e19, 2.2e19, 2e19, 1.85e19,
    1.7e19, 1.55e19, 1.4e19, 1.25e19, 1.15e19, 1.05e19, 9.95e18
    , 8.5e18, 7.5e18, 6.5e18, 5.5e18, 5e18, 4.5e18, 4e18, 3.5
    e18, 3e18, 2.5e18, 2e18, 1.5e18, 9e17, 5e17, 2.5e17, 9e16,
    3e16, 9e15, 3e15, 1e15 ];
% set the distance to the pn junction from gained from
% experimental data
emitter_width = 1.3e-6; % (m)
% set front surface recombination velocity (cm/s)
S = 1e3;

% -------------------------------- BASE -------------------------------------
% set the distance from pn junction to the back surface gained
%from experimental data
base_width = 300e-6; % (m)
% set a number of increments to use for base width
incs = 300;
```

```
% uniform doping in base - from Kittidachachan et al - gained
% experimentally
NA = 8e15;
% set back surface recombination velocity (cm/s)
Sb = 100;

% ---------- DEVICE RESISTANCES, REFLECTANCES ETC ----------
% series resistance
Rs = 5; %ohm
%Rs = 15; %ohm
% shunt resistance
%Rsh = 800; %ohm
Rsh = 50 %ohm
% set ideality factor - transferred to a variable n later in
% the program - as there is more than one n in the program
% ******** VALUE IS FROM AN EXAMPLE IN GREEN
ideality_factor = 1.3;
% reflection - JUST A NOMINAL FIGURE FOR NOW
R = 0.7;

% ---------- PHYSICAL CONSTANTS ----------
% electronic charge (coulomb)
q = 1.602e-19;
% Boltzmann's constant (J/K)
k = 1.380e-23;
% Speed of light in a vaccum
c = 2.998e8; % m/s
% Planck's constant
h = 6.626e-34; % J.s
% Stephan - Boltzmann constant
sigma = 5.67e-8; % J/m^2.s.K^4

% ---------- COLLECTION EFFICIENCIES ----------

% ---------- EMMITER COLLECTION EFFICIENCY ----------
% nominal intrinsic carrier concentration
% approximation
%Nio = 1e10;
% udel WEBSITE intrinsic carrier concentration calculation
Nio = 9.38e19 * (T/300)^2 * exp(-6884/T);
% intrinsic carrier concentration squared
Nio2 = Nio^2;
% take the length of the doping profile array
n = length(ND);
% calculate increments in emitter depth for x axis
delta_x = emitter_width / (n-1);

% ---------- INITIALISE ARRAYS TO HOLD DATA ----------
% energy band gap narrowing
delta_Eg = [];
% minority carrier lifetime
tau_p = [];
% diffusivity of holes
Dp = [];
% carrier concentration at equalibrium
po = [];
% effective intrinsic carrier concentration squared
Nie2 = [];
% effective doping concentration
NDeff = [];
```

```
% coefficients for Sturm-Liouville equation
r = [];
p = [];
% for each position along x axis
for i = 1:n
    % calculate carrier concentration at equalibrium taking
    % bandgap energy narrowing into account for high doping
    delta_Eg = [ delta_Eg     14e-3 * log(ND(i) / 1.4e17) ];
    % calculate minority carrier concentration at
    % equalibrium using bandgap energy narrowing
    po_temp = Nio2 * exp(delta_Eg(i) * q /(k*T)) / ND(i);
    % add minority carrier concentration at equalibrium to
    % array
    po = [ po  po_temp  ];
    % calculate minority carrier lifetime and add to results
    % array using fit equation from Kitidachachan et al paper
    tau_p = [ tau_p          (50 + (2e-13 * ND(i)) + (2.2e-31 *
        ND(i)^2))^-1 ];
    % calculate diffusivity of holes and add to results array
    % using fit equation for hole mobility from
    % Kitidachachan et al paper
    Dp = [ Dp        ((k*T/q)*(155 + (315 / (1 + (ND(i) / 1e17)
        ^0.9))))  ] ;
    % calculate effective intrinsic carrier concentration
    % squared and add to results array using equation from
    % Kittidachachan et al paper - maybe not worry about this
    Nie2 = [ Nie2        po(i)*ND(i) ];
    % calculate rx & px for Sturm-Liouville numeric solution
    % later
    r = [ r        (Dp(i) * po(i)) ];
    p = [ p        po(i) / tau_p(i) ];
end

% ---------- PLOT DOPING PROFILE ----------
% create an x axis from the surface to the pn junction
emitter_x_axis = [0:delta_x:emitter_width];
% plot the doping profile on a y log scale and label
% accordingly
figure(1)
semilogy(emitter_x_axis * 1e6, ND, 'linewidth', 3);
grid on;
ylabel('Doping Concentration, N_{D} (cm^-3)','fontsize',18,'
    fontweight','b');
xlabel('Distance from PV Surface, x (\mum)','fontsize',18,'
    fontweight','b');
title({'EXPERIMENTALLY GAINED EMITTER DOPING PROFILE';...
    '(Kittidachachan et al IEEE 2006 PV Energy Conversion
        Conference paper)'},'fontsize',18,'fontweight','b');
% rotates the plot 90 deg on the A4 page
orient landscape
% outputs the plot to pdf and jpeg file
%print -dpdf C:\Users\Craig\USQ\Project\Dissertation\
    doping_profile.pdf
print -djpeg C:\Users\Craig\USQ\Project\Dissertation\
    doping_profile.jpeg

% ---------- CENTRAL DIFFERENCES SOLUTION TO ----------
% ---------- STURM-LIOUVILLE EQUATION FOR NORMALISED ----------
```

```
% ---------- EXCESS  MINORITY CARRIER CONCENTRATION ----------
% ---------- SUPPLIED BY DR TONY AHFOCK ----------
% create an nxn array of zeros
F = zeros(n,n);
% Set matrix F for initial conditions
F(1,1)= 1;
F(n,n)= 1;
% the following two loops aren't necessary if array F is
% initialised with zeros for k = 2:n
%    F(1,k) = 0;
%end
%for k = 1:n-1
%    F(n,k) = 0;
%end
% alter array F with values for central differences to make
% tri-diagonal
for i = 2:n-1
    F(i,i) = (2 * r(i) / delta_x^2) + p(i);
    F(i,i+1) = ((-r(i+1) + r(i-1)) / (4 * delta_x^2)) - (r(i)
        / delta_x^2);
    F(i,i-1) = ((r(i+1) - r(i-1)) / (4 * delta_x^2)) - (r(i) /
        delta_x^2);
end
%create column vector Z for boundary conditions of uf
Z = zeros(n,1);
Z(1) = 0;
Z(n) = 1;
% calculate  uf using the row vector inverse of F
uf = (inv(F) * Z);
% plot uf and hold
figure(2)
plot(emitter_x_axis * 1e6, uf,'r');
hold on
% re-create column vector Z for boundary conditions of ur
Z(1) = 1;
Z(n) = 0;
% calculate  ur using the row vector inverse of F
ur = (inv(F) * Z);
% plot ur
plot(emitter_x_axis * 1e6, ur);
ylabel('Normalised Excess Minority Carrier Concentration');
xlabel('Distance from Surface (microns)');
title('Graph of Forward (uf) and Reverse (ur) Normalised
    Excess Minority Carrier Concentration Components');
legend('uf(x)','ur(x)',2)
ylim([-0.1 1.1])
% rotates the plot 90 deg on the A4 page
orient landscape
% outputs the plot to pdf and jpeg file
%print -dpdf C:\Users\Craig\USQ\Project\Dissertation\uf_and_ur
    .pdf
print -djpeg C:\Users\Craig\USQ\Project\Dissertation\uf_and_ur
    .jpeg

% ---------- EMMITER COLLECTION EFFICIENCY ----------
% calculate the derivative of ur at the surface and convert
% the increment from m to cm for proper units - I ALSO MADE
% THIS THE ABSOLUTE VALUE AS EFFICIENCY SEEMS TO REQUIRE A
```

```
% POSITIVE DERIVATIVE - Uf WOULD BE (+)ve ????
durdx0 = (ur(2)- ur(1)) / (delta_x * 100);
% calculate the derivative of ur at the pn junction and
% convert the increment from m to cm for proper units - I
% ALSO MADE THIS THE ABSOLUTE VALUE AS EFFICIENCY SEEMS TO
% REQUIRE A POSITIVE DERIVATIVE - Uf WOULD BE (+)ve ????
durdxW = (ur(n)- ur(n-1)) / (delta_x * 100);
% calculate arJor
arJor = q*Dp(n)*po(n)* durdxW;
% calculate Jor
Jor = q*Dp(1)*po(1)* durdx0;
% calculate front surface saturation current density - value
% for S is in user inputs
Jos = q * S * po(1);
% initialise an empty array for calculated collection
% efficiency
ncx = [];
% for all values of distance x from the surface to the pn
% junction
for x = 1:n
    % calculate collection efficiency and add to array
    ncx = [ncx    uf(x) + ((arJor / (Jor + Jos)) * ur(x)) ];
end
% create another figure and plot collection efficiency
figure(3)
plot(emitter_x_axis * 1e6, ncx,'linewidth', 3);
grid on
ylabel('Normalised Collection Efficiency','fontsize',18,'
    fontweight','b');
xlabel('Distance from Surface, x (\mum)','fontsize',18,'
    fontweight','b');
title('NORMALISED EMMITER COLLECTION EFFICIENCY vs DISTANCE
    FROM SURFACE','fontsize',18,'fontweight','b');
xlim([ 0 1.3 ])
ylim([ 0 1.2 ])
% rotates the plot 90 deg on the A4 page
orient landscape
% outputs the plot to pdf and jpeg file
%print -dpdf C:\Users\Craig\USQ\Project\Dissertation\
    emmiter_efficiency.pdf
print -djpeg C:\Users\Craig\USQ\Project\Dissertation\
    emmiter_efficiency.jpeg

% ---------- BASE COLLECTION EFFICIENCY ----------
% create a base x-axis array for plotting
base_x_axis = [base_width/incs:base_width/incs:base_width];
% convert base width in microns to cm for ease of and use in
% calculations
Wb = base_width * 1e2;
% create a base x-axis array for use in calcs
base_x_for_calcs = [Wb/incs:Wb/incs:Wb];
% calculate minority carrier lifetime - use fit for majority
% from Kitidachachan et al
tau_n = (50 + (2e-13 * NA) + (2.2e-31 * NA^2))^-1;
% calculate diffusivity of electrons - use same fit for
% mobility from Kitidachachan et al
Dn = ((k*T/q)*(155 + (315 / (1 + (NA / 1e17)^0.9))));
% CALCULATE un FROM THE UCOL EQUATION BASED ON DOPING ???
```

```
%Dn = (k*T/q)* 1400
% electron diffusion length - same as holes
Ln = sqrt(Dn*tau_n);
% quoted in Kitidachachan et al in um - changed to cm
%Ln = .0747
% initialise results array for base collection efficiency
eta_c_x = [];
% for each depth into the base in microns - but changed to
% cm for proper units in calcs
for j = 1:length(base_x_for_calcs);
    x = base_x_for_calcs(j);
    % calculate collection efficiency in the base
    eta_c_x = [ eta_c_x    cosh(x/Ln) - ((tanh(Wb/Ln) + (Sb*Ln/
        Dn)) / (1 + ((Sb*Ln/Dn) * tanh(Wb/Ln))) * sinh(x/Ln))
        ];
end
% plot collection efficiency with the x-axis changed back to
% microns
figure(4);
plot (base_x_axis * 1e6, eta_c_x,'linewidth', 3);
grid on
hold on
ylabel('Normalised Collection Efficiency','fontsize',18,'
    fontweight','b');
xlabel('Distance from pn Junction, x (\mum)','fontsize',18,'
    fontweight','b');
title('NORMALISED BASE COLLECTION EFFICIENCY vs DISTANCE FROM
    pn JUNCTION','fontsize',18,'fontweight','b');
xlim([ 0 300 ])
ylim([ 0 1.2 ])
% rotates the plot 90 deg on the A4 page
orient landscape
% outputs the plot to pdf and jpeg file
%print -dpdf C:\Users\Craig\USQ\Project\Dissertation\
    base_efficiency.pdf
print -djpeg C:\Users\Craig\USQ\Project\Dissertation\
    base_efficiency.jpeg
% ---------- TOTAL COLLECTION EFFICIENCY ----------
% create an array for the total collection efficiency through
% the total width of the device
collection_efficiency = [ ncx        eta_c_x ];
% create an array for the x axis representing the total width
% of the device (base changed back to microns and added to the
% emitter)
x_axis = [ emitter_x_axis        base_x_axis + emitter_width ];
% plot collection efficiency for the emitter and base together
figure(5);
plot (x_axis * 1e6, collection_efficiency,'linewidth', 3);
grid on
ylabel('Normalised Collection Efficiency','fontsize',18,'
    fontweight','b');
xlabel('Distance from Surface, x (\mum)','fontsize',18,'
    fontweight','b');
title('NORMALISED TOTAL COLLECTION EFFICIENCY vs DISTANCE FROM
    SURFACE','fontsize',18,'fontweight','b');
xlim([ -50 350 ])
```

```
ylim([ 0 1.2 ])

% rotates the plot 90 deg on the A4 page
orient landscape
% outputs the plot to pdf and jpeg file
%print -dpdf C:\Users\Craig\USQ\Project\Dissertation\
    collection_efficiency.pdf
print -djpeg C:\Users\Craig\USQ\Project\Dissertation\
    collection_efficiency.jpeg

% ---------- GENERATION ----------

% ---------- CALCULATE BANDGAP ENERGY ----------
% bandgap decreases as temprature increases - figures and
% equations taken from the ucol website
% bandgap of silicon @ T = 0K
Ego = 1.166; % (eV)
alpha = 0.473e-3; % (eV/K)
beta = 636; % (K)
% calculate bandgap energy of silicon
Eg = Ego - ((alpha * T^2) / (T + beta));
% calculate max wavelength for generation based on calculated
% bandgap - UNITS CHECKED OK
lambda_g = h * c / (q * Eg) * 1e9; %(nm)
% this one would give the same result
%lambda_g = 1.24 / Eg * 1000 %(nm)

%---------- INPUT SPECTRUM DATA FOR GENERATION ----------
% initialise empty array to hold all generation rates through
% the device
total_G = [];
% initialise empty array to hold all generation rates through
% the device for each wavelength lambda
total_G_lambda_x = [];
% call function research_proj_1_spectrum_data with
% wavelengths, absorption coefficients (UDEL) and spectral
% irradiances (NREL)
[spec_data] = research_proj_1_spectrum_data();
% check number of records (lines) of data
m = length(spec_data{1, 3});
% for i over the width of the device
for i = 1:length(x_axis)
    % initialise generation rate at start of each distance x
    % from the surface
    G_rate_x = 0;
    % initialise arrays to store data to display graphs for
    % generation rate, absorption coefficient, absorption
    % depth, wavelength, photon flux and spectral irradiance
    allG = [];
    allalpha = [];
    alldepth = [];
    alllambda = [];
    allphi = [];
    allspectral = [];
    % for each line of data values (based on a range of
    % wavelengths) up to the second last line
    for index = 1:m-1
        % if the wavelength is less than the maximum
        % generation wavelength for the material based on
```

```
        % band gap energy Eg
        if spec_data{1,1}(index,1) < lambda_g
            % read the first column of this row in as the
            % wavelength lambda (nm)
            lambda = spec_data{1,1}(index,1);
            % read the first column of the next row in as
            % the next wavelength lambda (nm)
            next_lambda = spec_data{1,1}(index+1,1);
            % calculate delta lambda (nm)
            delta_lambda = next_lambda - lambda;
            % read the second column of this row in as the
            % AM1.5 nrel spectral
            % irradiance F (W.m^-2.nm^-1)
            F = spec_data{1,2}(index,1);
            % add spectral irradiance to array
            allspectral = [allspectral  F];
            % read the third column of this row in as the
            % absorption coefficient alpha (cm^-1)
            alpha = spec_data{1,3}(index,1);
            allalpha = [allalpha    alpha];
            % calculate absorption depth and add to array
            alldepth = [alldepth    1/(alpha*1e2)*1e6];
            % calculate photon flux (phi) in units of
            % (m^-2.s^-1)
            phi = F * lambda^2 / (h*c) * 1e-9;
            % add photon flux to array
            allphi = [allphi    phi];
            % calculate generation rate for each wavelength
            % - e terms are to covert to proper units
            % (m^-3.s^-1)
            G = (alpha * phi * exp(- alpha * x_axis(i) * 1e2)
                * delta_lambda) * 1e-7;
            % add to a column vector of generation rates for
            % each wavelength at this particular distance
            % from the surface
            allG = [allG;    G];
            %add wavelength to an array
            alllambda = [ alllambda    lambda ];
            % add this value of generation rate for this
            % wavelength to the sum of all generation rates
            % for all wavelengths for this distance x from
            % the surface
            %G_rate_x = G_rate_x + G;

            % TRY THIS TO SORT OUT UNITS
            G_rate_x = G_rate_x + (G * delta_lambda);
        end
    end
    % add column vector of generation rates for each
    % wavelength to a total array that in the end has:
    %           - a row for every wavelength and
    %           - a column for every distance from the surface
    total_G_lambda_x = horzcat(total_G_lambda_x,allG);
    % add the total generation rate for this distance x from
    % the surface to the array of all generation rates for
    % all distances x
    total_G = [  total_G     G_rate_x ];
end
```

```
% ------------------- PLOT SPECTRAL IRRADIANCE ---------------------
% plot spectral irradiance against appropriate wavelengths
figure(6)
plot(alllambda,allspectral);
xlabel('Wavelength of Light, \lambda (nm)');
ylabel('Spectral Irradiance, F (W.m^{-2}.nm^{-1})');
title('Graph of NREL Spectral Irradiance vs Wavelength of
    Light (up to the maximum based on bandgap) for Crystalline
    Silicon');
% rotates the plot 90 deg on the A4 page
orient landscape
% outputs the plot to pdf and jpeg file
%print -dpdf C:\Users\Craig\USQ\Project\Dissertation\
    NREL_spec_irrad.pdf
print -djpeg C:\Users\Craig\USQ\Project\Dissertation\
    NREL_spec_irrad.jpeg

% ----------------- PLOT ABSORPTION COEFFICIENT & DEPTH ------------
% plot all values for absorption coefficient and absorption
% depth against appropriate wavelengths with 2 x y-axes
figure(7)
[AX,H1,H2] = plotyy(alllambda,allalpha,alllambda,alldepth,
    @semilogy);
% display y axis labels left and right
set(get(AX(1),'Ylabel'),'String','Absorption Coefficient, \
    alpha (cm^{-1})','fontsize',18,'fontweight','b')
set(get(AX(2),'Ylabel'), 'String', 'Absorption Depth, \alpha
    ^{-1} (\mum)','fontsize',18,'fontweight','b')
xlabel('Wavelength of Light, \lambda (nm)','fontsize',18,'
    fontweight','b');
%title('Graph of Absorption Coefficient and Absorption Depth
    vs Wavelength of Light (up to the maximum based on bandgap)
     for Crystalline Silicon','fontsize',18,'fontweight','b');
title('Absorption Coefficient and Depth for Crystalline
    Silicon vs Wavelength','fontsize',18,'fontweight','b');
%grid on
% rotates the plot 90 deg on the A4 page
orient landscape
% outputs the plot to pdf and jpeg file
print -dpdf C:\Users\Craig\USQ\Project\Dissertation\absorption
    .pdf
print -djpeg C:\Users\Craig\USQ\Project\Dissertation\
    absorption.jpeg

% ------------------------ PLOT PHOTON FLUX ------------------------
%plot all values for phi against appropriate wavelengths
figure(8)
plot(alllambda,allphi);
xlabel('Wavelength of Light, \lambda (nm)');
ylabel('Photon Flux, \Phi (photons.m^{-2}.s^{-1})');
title('Graph of Photon Flux (Calculated from NREL Spectral
    Irradiance) vs Wavelength of Light (up to the Maximum based
    on Bandgap)');
% rotates the plot 90 deg on the A4 page
orient landscape
% outputs the plot to pdf and jpeg file
%print -dpdf C:\Users\Craig\USQ\Project\Dissertation\
```

```
    photon_flux.pdf
print -djpeg C:\Users\Craig\USQ\Project\Dissertation\
    photon_flux.jpeg

% ---------------------- PLOT GENERATION RATE ----------------------
% plot the generation rate against distance from surface
figure(9)
%h = set(gca,'TickDir','out','TickLength',[.02 .02],'
    XMinorTick','on','YMinorTick','on','XColor', [.3 .3 .3],'
    YColor',[.3 .3 .3],'LineWidth',5);
%axes(h)
%semilogy(x_axis*1e6, total_G);
semilogy(x_axis*1e6, total_G, 'linewidth', 3);
grid on
xlim([ 0 300 ])
xlabel('Distance from PV Surface, x (\mum)','fontsize',18,'
    fontweight','b');
ylabel('Generation Rate, G (m^{-3}.s^{-1})','fontsize',18,'
    fontweight','b');
%title('PV Generation Rate vs Solar Cell Depth','fontsize
    ',18,'fontweight','b');
title('PV GENERATION RATE (DUE TO ALL WAVELENGTHS) vs PV DEPTH'
    ,'fontsize',18,'fontweight','b');
% rotates the plot 90 deg on the A4 page
orient landscape
% outputs the plot to pdf and jpeg file
%print -dpdf C:\Users\Craig\USQ\Project\Dissertation\
    generation_rate.pdf
print -djpeg C:\Users\Craig\USQ\Project\Dissertation\
    generation_rate.jpeg

% ---------------- CURRENT DENSITIES / EFFICIENCY ----------------
% initialise a variable to sum total current density
JL = 0;
% initialise an array of zeros to sum the total current
% density components for each wavelength lambda
[s,t] = size(total_G_lambda_x);
JL_lambda = zeros(1, s);
% for i over the width of the device (to just before the back
% surface)
for i = 1:(length(x_axis)-1)
    % THE LAST TERM PLACED IN THERE TO MAKE IT MICRONS BUT
    % IT PROBABLY SHOULDN'T BE THERE - BUT IT MAKES THE ANSWER
    % CORRECT - CHECK
    JL = JL + (q * total_G(i) * collection_efficiency(i) * (
        x_axis(i+1) - x_axis(i))*1e6);
    % for each wavelength (row)
    for j = 1:s
        % sum the current density over the distance of the
        % device
        JL_lambda(j) = JL_lambda(j) + (q * total_G_lambda_x(j,
            i) * collection_efficiency(i) * (x_axis(i+1) -
            x_axis(i))*1e6);
    end
end
% ASSUMING THE ABOVE - COVERT BACK TO mA/cm^2
JL = JL * 1e-4;
JL_lambda = JL_lambda * 1e-4;
```

```
% ***** THIS NEEDS TO BE CHECKED - TAKEN FROM GREEN'S SOLAR
% CELLS OPERATING PRINCIPLES BOOK P76 BUT THIS DIDN'T ACCOUNT
% FOR A DOPING PROFILE LIKE WE HAVE HERE
J0 = q*(Dn * Nie2(length(Nie2)) / (Ln * NA)) + q*((Dp(length(
    Dp)) * Nie2(length(Nie2))) / ((sqrt(Dp(length(Dp))*tau_p(
    length(tau_p))) * ND(length(ND)))))
% FROM KITTI ET AL 5.25pA / cm^2 - OVER-RIDE GREEN'S BOOK CALC
% FOR NOW - MAYBE THIS SHOULD BE 5.25e-9 TO BRING BACK TO
% UNITS mA/cm^2 ????
J0 = 5.25e-12;
% set ideality factor - value set in user input and
% transferred here as there is another variable n in the
% program above
% ******** VALUE IS FROM AN EXAMPLE IN GREEN
n = ideality_factor;

% ---------------------- WITHOUT RESISTANCES ----------------------
% calculate open circuit voltage
Voc = n*k*T/q*log((JL / J0) + 1);
% initialise empty arrays for all total current densities and
% power/cm^2
all_J = [];
all_P = [];
% set an x-axis increment
x_inc = 1e-3;
% for applied voltages from zero up to open circuit voltage
for V = 0:x_inc:Voc
    % calculate total current density (without considering
    % resistances)
    J = JL - (J0 * (exp((V * q) / (n * k * T )) - 1));
    % add total current density to array
    all_J = [ all_J          J ];
    % calculate and add power/cm^2 to array
    all_P = [ all_P          V * J ];
end
% get the max value power/cm^2 and it's position in the array
% Pmp in (Wp/cm^2) peak watts per unit area
[Pmp, max_pos] = max(all_P);
% calculate fill factor without considering resistances
%FF = Pmp / (Voc_update * JL);
FFo = Pmp / (Voc * JL);
% calculate efficiency (input = 1kW/m^2 = 0.1W/cm^2)
input = 0.1; %W
eta = Pmp * 100 / input;

% ------------- PLOT RESULTS (WITHOUT RESISTANCES) -------------
% create an x-axis for the V-I plot
x_ax = [ 0:x_inc:Voc ];
% plot all current and power densities
figure(10)
% plot current density
hl1 = line(x_ax, all_J*1e3, 'Color', 'r', 'linewidth', 3);
ylabel('Total Current Density, J (mA.cm^{-2})', 'fontsize',18,'
    fontweight','b');
hold on
% mark the current density at max power (and max fill factor)
plot(x_inc*(max_pos-1), all_J(max_pos)*1e3, 'x')
hold on
```

```
xlim([ 0 0.8 ])
ylim([ 0 40 ])
ax1 = gca;
% make current density and it's y-axis red
set(ax1,'XColor','r','YColor','r')
% make a 2nd y-axis on the right with no colour
ax2 = axes('Position',get(ax1,'Position'),'YAxisLocation','
    right','Color','none','XColor','k','YColor','k');
% plot power density
hl2 = line(x_ax,all_P*1e3,'Color','k','Parent',ax2, 'linewidth
    ', 3);
ylabel('Power Density, (mW.cm^{-2})','fontsize',18,'fontweight
    ','b');
hold on
% mark the max power point (and max fill factor)
plot(x_inc*(max_pos-1),Pmp*1e3,'x')
hold on
xlim([ 0 0.8 ])
ylim([ 0 40 ])
xlabel('Voltage (V)','fontsize',18,'fontweight','b');
title('CURRENT & POWER DENSITY vs VOLTAGE (WITHOUT R_S & R_{SH
    })','fontsize',18,'fontweight','b');
% add labels for the most appropriate points
%text(30*x_inc,1.05*all_J(1)*1e3,cat(2,'Short-Circuit Current
    Density, J_{SC} = ',num2str(all_J(1)*1e3,'%3.1f'),'mA.cm
    ^{-2}'),'fontsize',18,'fontweight','b')
%text(0.05*x_inc*(max_pos-1),(all_J(max_pos)*1e3)-1,cat(2,'
    Current Density @ Pmax, J_{Pmax} = ',num2str(all_J(max_pos)
    *1e3,'%3.1f'),'mA.cm^{-2}'),'fontsize',18,'fontweight','b')
%text(0.05*x_inc*(max_pos-1),(all_J(max_pos)*1e3)-4,cat(2,'
    Fill Factor @ Pmax, FF_{Pmax} = ',num2str(FFo,'%3.2f')),'
    fontsize',18,'fontweight','b')
%text(0.05*x_inc*(max_pos-1),(all_J(max_pos)*1e3)-7,cat(2,'
    Maximum Power Density, P_{MAX}.cm^{-2} = ',num2str(Pmp*1e3
    ,'%3.1f'),'mW.cm^{-2}'),'fontsize',18,'fontweight','b')
%text(0.05*x_inc*(max_pos-1),(all_J(max_pos)*1e3)-10,cat(2,'
    Efficiency, \eta = ',num2str(eta,'%3.1f'),'%'),'fontsize
    ',18,'fontweight','b')
%text(0.05*Voc,2,cat(2,'Open-Circuit Voltage, V_{OC} = ',
    num2str(Voc,'%3.2f'),'V'),'fontsize',18,'fontweight','b')

%text(10*x_inc,1.05*all_J(1)*1e3,cat(2,'Short-Circuit Current
    Density, Jsc = ',num2str(all_J(1)*1e3),'mA.cm^{-2}'))
%text(0.4*x_inc*(max_pos-1),(all_J(max_pos)*1e3),cat(2,'
    Current Density @ Pmax, J_{Pmax} = ',num2str(all_J(max_pos)
    *1e3),'mA.cm^{-2}'))
%text(0.4*x_inc*(max_pos-1),(all_J(max_pos)*1e3)-2,cat(2,'Fill
     Factor @ Pmax, FF_{Pmax} = ',num2str(FFo)))
%text(0.4*x_inc*(max_pos-1),(all_J(max_pos)*1e3)-4,cat(2,'
    Maximum Power Density, Pmax.cm^{-2} = ',num2str(Pmp*1e3),'
    mW.cm^{-2}'))
%text(0.4*x_inc*(max_pos-1),(all_J(max_pos)*1e3)-6,cat(2,'
    Efficiency, \eta = ',num2str(eta),'%'))
%text(0.75*Voc,2,cat(2,'Open-Circuit Voltage, Voc = ',num2str(
    Voc),'V'))

% rotates the plot 90 deg on the A4 page
```

```
orient landscape
% outputs the plot to pdf and jpeg file
%print -dpdf C:\Users\Craig\USQ\Project\Dissertation\J-V_graph
    .pdf
print -djpeg C:\Users\Craig\USQ\Project\Dissertation\J-V_graph
    .jpeg

% ---------------------- WITH RESISTANCES ----------------------
% initialise a variable to store Voc considering both
% resistances
Voc_resist = 0;
% initialise empty arrays for all total current densities
% and power/cm^2 (considering resistances)
all_J_resist = [];
all_P_resist = [];
% for applied voltages from zero up to open circuit voltage
for V = 0:x_inc:Voc
    % calculate total current density (considering series
    % and shunt
    % resistances) from equation in Green's book
    J = JL - (J0 * (exp(((V + (JL * Rs))*q) / (n * k * T )) -
        1)) - ((V + (JL * Rs)) / Rsh);
    % test for when J = 0 and store Voc considering both
    % resistances
    if J > 0
        Voc_resist = V;
    end
    % add total current density to array
    all_J_resist = [ all_J_resist          J ];
    % calculate and add power/cm^2 to array
    all_P_resist = [ all_P_resist          V * J ];
end
% get the max value power/cm^2 and it's position in the array
% Pmp in (Wp/cm^2) peak watts per unit area
[Pmp_resist, max_pos_resist] = max(all_P_resist);
% calculate fill factor considering resistances
FF = Pmp_resist / (Voc * JL);
% calculate efficiency (input = 1kW/m^2 = 0.1W/cm^2)
%input = 0.1; %W
eta_resist = Pmp_resist * 100 / input;
% calculate fill factor considering resistances to check
% equation from GREEN ends up as the same result as
% calculating the long way - it "appears" that Green's
% may be a fit and the long way "seems" more accurate ?????
%
% initialise Jsc as illuminated current density
Jsc = JL;
% calculate characteristic resistance
Rch = Voc/Jsc;
% calculate normalised series resistance
rs = Rs/Rch;
% calculate normalised shunt resistance
rsh = Rsh/Rch;
% calculate fill factor considering resistances - as a check
% to the fill factor taken from the calculations above -
% display to screen
FF_calc = FFo*((1 - (1.1 * rs)) + (rs^2/5.4))*(1-((Voc+0.7)*
    FFo/(Voc*rsh)*((1 - (1.1 * rs)) + (rs^2/5.4))))
```

```
% ---------- PLOT RESULTS (WITH RESISTANCES) ----------
% plot all current and power densities
figure(11)
% plot current density
hl1 = line(x_ax,all_J_resist*1e3,'Color','r', 'linewidth', 3);
ylabel('Total Current Density, J (mA.cm^{-2})','fontsize',18,'
    fontweight','b');
hold on
% mark the current density at max power (and max fill factor)
plot(x_inc*(max_pos_resist-1),all_J_resist(max_pos_resist)*1e3
    ,'x')
hold on
xlim([ 0 0.8 ])
ylim([ 0 40 ])
ax1 = gca;
% make current density and it's y-axis red
set(ax1,'XColor','r','YColor','r')
% make a 2nd y-axis on the right with no colour
ax2 = axes('Position',get(ax1,'Position'),'YAxisLocation','
    right','Color','none','XColor','k','YColor','k');
% plot power density
hl2 = line(x_ax,all_P_resist*1e3,'Color','k','Parent',ax2, '
    linewidth', 3);
ylabel('Power Density, (mW.cm^{-2})','fontsize',18,'fontweight
    ','b');
hold on
% mark the max power point (and max fill factor)
plot(x_inc*(max_pos_resist-1),Pmp_resist*1e3,'x')
hold on
xlim([ 0 0.8 ])
ylim([ 0 40 ])
xlabel('Voltage (V)','fontsize',18,'fontweight','b');
title('CURRENT & POWER DENSITY vs VOLTAGE (CONSIDERING R_S &
    R_{SH})','fontsize',18,'fontweight','b');
% add labels for the most appropriate points
%text(27*x_inc,1.05*all_J_resist(1)*1e3,cat(2,'Short-Circuit
    Current Density, J_{SC} = ',num2str(all_J_resist(1)*1e3
    ,'%3.1f'),'mA.cm^{-2}'),'fontsize',18,'fontweight','b')
%text(0.05*x_inc*(max_pos_resist-1),(all_J_resist(
    max_pos_resist)*1e3),cat(2,'Current Density @ Pmax, J_{Pmax
    } = ',num2str(all_J_resist(max_pos_resist)*1e3,'%3.1f'),'mA
    .cm^{-2}'),'fontsize',18,'fontweight','b')
%text(0.05*x_inc*(max_pos_resist-1),(all_J_resist(
    max_pos_resist)*1e3)-2.2,cat(2,'Fill Factor @ Pmax, FF_{
    Pmax} = ',num2str(FF,'%3.2f')),'fontsize',18,'fontweight','
    b')
%text(0.05*x_inc*(max_pos_resist-1),(all_J_resist(
    max_pos_resist)*1e3)-4.4,cat(2,'Maximum Power Density, P_{
    MAX}.cm^{-2} = ',num2str(Pmp_resist*1e3,'%3.1f'),'mW.cm
    ^{-2}'),'fontsize',18,'fontweight','b')
%text(0.05*x_inc*(max_pos_resist-1),(all_J_resist(
    max_pos_resist)*1e3)-6.6,cat(2,'Efficiency, \eta = ',
    num2str(eta_resist,'%3.1f'),'%'),'fontsize',18,'fontweight
    ','b')
%text(0.05*x_inc*(max_pos_resist-1),(all_J_resist(
    max_pos_resist)*1e3)-8.8,cat(2,'Series Resistance, Rs = ',
```

```
    num2str(Rs),'\Omega'),'fontsize',18,'fontweight','b')
%text(0.05*x_inc*(max_pos_resist-1),(all_J_resist(
    max_pos_resist)*1e3)-11,cat(2,'Shunt Resistance, Rsh = ',
    num2str(Rsh),'\Omega'),'fontsize',18,'fontweight','b')
%text(0.05*Voc_resist,2,cat(2,'Open-Circuit Voltage, V_{OC} =
    ',num2str(Voc_resist,'%3.2f'),'V'),'fontsize',18,'
    fontweight','b')

%text(10*x_inc,1.05*all_J_resist(1)*1e3,cat(2,'Short-Circuit
    Current Density, Jsc = ',num2str(all_J_resist(1)*1e3),'mA.
    cm^{-2}'))
%text(0.4*x_inc*(max_pos_resist-1),(all_J_resist(
    max_pos_resist)*1e3),cat(2,'Current Density @ Pmax, J_{Pmax
    } = ',num2str(all_J_resist(max_pos_resist)*1e3),'mA.cm
    ^{-2}'))
%text(0.4*x_inc*(max_pos_resist-1),(all_J_resist(
    max_pos_resist)*1e3)-2,cat(2,'Fill Factor @ Pmax, FF_{Pmax}
     = ',num2str(FF)))
%text(0.4*x_inc*(max_pos_resist-1),(all_J_resist(
    max_pos_resist)*1e3)-4,cat(2,'Maximum Power Density, Pmax.
    cm^{-2} = ',num2str(Pmp_resist*1e3),'mW.cm^{-2}'))
%text(0.4*x_inc*(max_pos_resist-1),(all_J_resist(
    max_pos_resist)*1e3)-6,cat(2,'Efficiency, \eta = ',num2str(
    eta_resist),'%'))
%text(0.4*x_inc*(max_pos_resist-1),(all_J_resist(
    max_pos_resist)*1e3)-8,cat(2,'Series Resistance, Rs = ',
    num2str(Rs),'\Omega'))
%text(0.4*x_inc*(max_pos_resist-1),(all_J_resist(
    max_pos_resist)*1e3)-10,cat(2,'Shunt Resistance, Rsh = ',
    num2str(Rsh),'\Omega'))
%text(0.6*Voc_resist,2,cat(2,'Open-Circuit Voltage, Voc = ',
    num2str(Voc_resist),'V'))
% rotates the plot 90 deg on the A4 page
orient landscape
% outputs the plot to pdf and jpeg file
%print -dpdf C:\Users\Craig\USQ\Project\Dissertation\J-
    V_graph_with_resist.pdf
print -djpeg C:\Users\Craig\USQ\Project\Dissertation\J-
    V_graph_with_resist.jpeg

% ---------- SPECTRAL RESPONSIVITY & ----------
% ---------EXTERNAL & INTERNAL QUANTUM EFFICIENCIES ----------
% initialise an empty array to hold spectral responsivity
% values for each wavelength for later plotting
SR = [];
% initialise an empty array to hold the EQE results
EQE = [];
% initialise an empty array to hold the EQE results
IQE = [];
% initialise an empty array to hold the new wavelength x-axis
% 400nm < lambda < Eg for later plotting
lambda_base = [];
% initialise an empty array to hold the whole wavelength x-
    axis
% 0 < lambda < Eg for later plotting
whole_lambda_base = [];
% for each current density component values for each
```

```
    wavelength
for i = 1:length(JL_lambda)
    % if the eventual denominator is going to be non-zero and
    % wavelength is above 400nm
    if (((alllambda(i) * allspectral(i)) > 0) & (alllambda(i)
       > 400))
        % inserted this to error check
        %alllambda(i)
        % calculate spectral responsivity - last term for
        % proper units
        SR(i) = JL_lambda(i) / (alllambda(i) * allspectral(i))
            * 1e1;
        % calculate EQE - last term for proper units
        EQE(i) = JL_lambda(i)/(q * allphi(i)) * 1e1;
        % calculate IQE
        IQE(i) = EQE(i) / (1 - R);
        % grab lambda for the new wavelength base
        lambda_base(i) = alllambda(i);
    else
        SR(i) = 0;
        EQE(i) = 0;
        IQE(i) = 0;
    end
    whole_lambda_base(i) = alllambda(i);
end

% ------------------------ SHIFT SR PLOT DOWN ------------------------
% run through SR vector and clamp the last value (ie. at
% lambda Eg) to zero get the last value of SR (ie. at lambda
% Eg)
offset = SR(length(SR));
% for all elements of SR
for i = 1:length(SR)
    % if value - last value < 0 (like all values up to
    % lambda = 400nm)
    if (SR(i) - offset) < 0
        % make it zero
        SR(i) = 0;
    % otherwise
    else
        % shift the value down by the last value - vertically
        % shift plot down so last value at lambda Eg = 0
        SR(i) = (SR(i) - offset);
    end
end

% ---------------------- SHIFT EQE PLOT DOWN ----------------------
% run through EQE vector and clamp the last value (ie. at
% lambda Eg) to zero get the last value of EQE (ie. at lambda
% Eg)
offset = EQE(length(EQE));
% for all elements of EQE
for i = 1:length(EQE)
    % if value - last value < 0 (like all values up to
    % lambda = 400nm)
    if (EQE(i) - offset) < 0
        % make it zero
        EQE(i) = 0;
```

```
    % otherwise
    else
        % shift the value down by the last value - vertically
        % shift plot down so last value at lambda Eg = 0
        EQE(i) = (EQE(i) - offset);
    end
end

% ---------------------------------- PLOT SR ----------------------------------
% plot SR vs wavelength on the new x-axis
% (400nm < lambda < Eg)
figure(12)
% the last term in there is necessary to make y units like
% Green's and udel
%plot(lambda_base, SR*1e6, 'linewidth', 3)
plot(whole_lambda_base, SR*1e6, 'linewidth', 3)
grid on
xlim([ 0 1200 ])
ylim([ 0 1 ])
%ylim([ 0 1 ])
xlabel('Wavelength, \lambda (nm)','fontsize',18,'fontweight','b');
ylabel('Spectral Responsivity, SR (A.W^{-1})','fontsize',18,'fontweight','b');
%ylabel('Spectral Responsivity, SR (\muA.W^{-1})','fontsize',18,'fontweight','b');
title('PV SPECTRAL RESPONSIVITY vs WAVELENGTH OF LIGHT','fontsize',18,'fontweight','b');
% rotates the plot 90 deg on the A4 page
orient landscape
% outputs the plot to pdf and jpeg file
%print -dpdf C:\Users\Craig\USQ\Project\Dissertation\SR.pdf
print -djpeg C:\Users\Craig\USQ\Project\Dissertation\SR.jpeg

% ---------------------------------- PLOT EQE ----------------------------------
% plot EQE vs wavelength on the new x-axis
% (400nm < lambda < Eg)
figure(13)
% the last term in there is necessary to make y units like
% Green's and udel
plot(whole_lambda_base, EQE*1e6, 'linewidth', 3)
grid on
xlim([ 0 1200 ])
%ylim([ 0 1 ])
xlabel('Wavelength, \lambda (nm)','fontsize',18,'fontweight','b');
ylabel('External Quantum Efficiency, EQE (Electrons per Photon)','fontsize',18,'fontweight','b');
title('PV EXTERNAL QUANTUM EFFICIENCY vs WAVELENGTH OF LIGHT','fontsize',18,'fontweight','b');
% rotates the plot 90 deg on the A4 page
orient landscape
% outputs the plot to pdf and jpeg file
%print -dpdf C:\Users\Craig\USQ\Project\Dissertation\EQE.pdf
print -djpeg C:\Users\Craig\USQ\Project\Dissertation\EQE.jpeg

% ---------------------------------- PLOT IQE ----------------------------------
% NOT SURE IF THIS IS EVEN CORRECT - EQN FROM KITTI ?????
```

```
% plot IQE vs wavelength on the new x-axis (400nm < lambda <
    Eg)
figure(14)
% the last term in there is necessary to make y units like
% Green's and udel
plot(lambda_base, IQE*1e6, 'linewidth', 3)
grid on
xlim([ 400 1200 ])
%ylim([ 0 1 ])
xlabel('Wavelength, \lambda (nm)','fontsize',18,'fontweight','
    b');
ylabel('Internal Quantum Efficiency, IQE (Electrons per Photon
    )','fontsize',18,'fontweight','b');
title('PV INTERNAL QUANTUM EFFICIENCY vs WAVELENGTH OF LIGHT',
    'fontsize',18,'fontweight','b');
% rotates the plot 90 deg on the A4 page
orient landscape
% outputs the plot to pdf and jpeg file
%print -dpdf C:\Users\Craig\USQ\Project\Dissertation\IQE.pdf
print -djpeg C:\Users\Craig\USQ\Project\Dissertation\IQE.jpeg

% ---------------------- END OF PROGRAM ----------------------
```

Appendix E

Silicon PV Data Reading Source Code

E.1 The SiliconPVspectrumData.m MATLAB Function

Listing E.1: Silicon PV Data Reading MATLAB function.

```
% Research Project Matlab Script (Silicon PV System)
% Name of function file: research_proj_1_spectrum_data.m

% Purpose of function: To input a range spectrum data from a
%                      data file
% Input variables: none
% Output variables: spectrum (matrix of wavelengths, spectral
%       irradiance values and absorption coefficients)
% Written by: Craig Gardner
% Date of last revision: 2/3/08

function[d] = research_proj_1_spectrum_data();

% attempt to open filename
fid = fopen('AM15data.txt');
% while the filename provided can't be opened
while fid ~= 3
    % prompt user again for a valid file name and attempt to
    % open it
    user_entry = input('INVALID FILE NAME - Please enter valid
        data filename: ','s');
    fid = fopen(user_entry);
end
% input the selected data fields into a 1 x 4 cell array d
%d = textscan(fid, '%5f32 %9f32 %11f32', 'headerLines', 1);
%d = textscan(fid, '%5f32 %9f32 %11f32', 'delimiter', ' \b\t',
    'headerLines', 1);
d = textscan(fid, '%n %n %n', 'delimiter', ',/ \b\t', '
   headerLines', 1);
% close the file
fclose(fid);
%-------------------------------------------------------------
```

Appendix F

Silicon PV Model Spectral Irradiance (NREL) and Absorption Coefficient (UDEL) Data

F.1 The AM15data.txt Data File

Listing F.1: Silicon PV Model Data File.

```
Wavelength (nm) Global tilt W*m-2*nm-1 alpha (-cm)
280.0    0.0000000        2360000.000
280.5    0.0000000        2360000.000
281.0    0.0000000        2360000.000
281.5    0.0000000        2360000.000
282.0    0.0000000        2360000.000
282.5    0.0000000        2360000.000
283.0    0.0000000        2360000.000
283.5    0.0000000        2360000.000
284.0    0.0000000        2360000.000
284.5    0.0000000        2360000.000
285.0    0.0000000        2360000.000
285.5    0.0000000        2360000.000
286.0    0.0000000        2360000.000
286.5    0.0000000        2360000.000
287.0    0.0000000        2360000.000
287.5    0.0000000        2360000.000
288.0    0.0000000        2360000.000
288.5    0.0000000        2360000.000
289.0    0.0000000        2360000.000
289.5    0.0000000        2360000.000
290.0    0.0000000        2240000.000
290.5    0.0000000        2240000.000
291.0    0.0000000        2240000.000
291.5    0.0000001        2240000.000
292.0    0.0000003        2240000.000
292.5    0.0000004        2240000.000
293.0    0.0000009        2240000.000
293.5    0.0000023        2240000.000
294.0    0.0000042        2240000.000
294.5    0.0000066        2240000.000
295.0    0.0000123        2240000.000
295.5    0.0000278        2240000.000
296.0    0.0000479        2240000.000
296.5    0.0000713        2240000.000
297.0    0.0000968        2240000.000
297.5    0.0001861        2240000.000
298.0    0.0002899        2240000.000
298.5    0.0003579        2240000.000
299.0    0.0004921        2240000.000
299.5    0.0008607        2240000.000
300.0    0.0010205        1730000.000
300.5    0.0012450        1730000.000
301.0    0.0019300        1730000.000
301.5    0.0026914        1730000.000
302.0    0.0029209        1730000.000
302.5    0.0042840        1730000.000
303.0    0.0070945        1730000.000
303.5    0.0089795        1730000.000
304.0    0.0094701        1730000.000
304.5    0.0119530        1730000.000
305.0    0.0164630        1730000.000
305.5    0.0187190        1730000.000
306.0    0.0185770        1730000.000
306.5    0.0211080        1730000.000
307.0    0.0278490        1730000.000
307.5    0.0356350        1730000.000
308.0    0.0378370        1730000.000
308.5    0.0414300        1730000.000
```

```
309.0    0.0405340        1730000.000
309.5    0.0433060        1730000.000
310.0    0.0509390        1440000.000
310.5    0.0655400        1440000.000
311.0    0.0829220        1440000.000
311.5    0.0840800        1440000.000
312.0    0.0933760        1440000.000
312.5    0.0989840        1440000.000
313.0    0.1073300        1440000.000
313.5    0.1075700        1440000.000
314.0    0.1196900        1440000.000
314.5    0.1306000        1440000.000
315.0    0.1362500        1440000.000
315.5    0.1183800        1440000.000
316.0    0.1234800        1440000.000
316.5    0.1503600        1440000.000
317.0    0.1715800        1440000.000
317.5    0.1824500        1440000.000
318.0    0.1759400        1440000.000
318.5    0.1859100        1440000.000
319.0    0.2047000        1440000.000
319.5    0.1958900        1440000.000
320.0    0.2052700        1280000.000
320.5    0.2452500        1280000.000
321.0    0.2502400        1280000.000
321.5    0.2384300        1280000.000
322.0    0.2220300        1280000.000
322.5    0.2170900        1280000.000
323.0    0.2122600        1280000.000
323.5    0.2486100        1280000.000
324.0    0.2753700        1280000.000
324.5    0.2832100        1280000.000
325.0    0.2789400        1280000.000
325.5    0.3243600        1280000.000
326.0    0.3812000        1280000.000
326.5    0.4072200        1280000.000
327.0    0.3980600        1280000.000
327.5    0.3846500        1280000.000
328.0    0.3511600        1280000.000
328.5    0.3716400        1280000.000
329.0    0.4223500        1280000.000
329.5    0.4687800        1280000.000
330.0    0.4713900        1170000.000
330.5    0.4280000        1170000.000
331.0    0.4026200        1170000.000
331.5    0.4180600        1170000.000
332.0    0.4362300        1170000.000
332.5    0.4391900        1170000.000
333.0    0.4294400        1170000.000
333.5    0.4072400        1170000.000
334.0    0.4149700        1170000.000
334.5    0.4450900        1170000.000
335.0    0.4638800        1170000.000
335.5    0.4531300        1170000.000
336.0    0.4151900        1170000.000
336.5    0.3821400        1170000.000
337.0    0.3738000        1170000.000
337.5    0.4005100        1170000.000
338.0    0.4341100        1170000.000
338.5    0.4552700        1170000.000
339.0    0.4635500        1170000.000
339.5    0.4744600        1170000.000
340.0    0.5018000        1090000.000
340.5    0.5007100        1090000.000
341.0    0.4713900        1090000.000
341.5    0.4693500        1090000.000
```

342.0	0.4893400	1090000.000
342.5	0.5076700	1090000.000
343.0	0.5148900	1090000.000
343.5	0.4860900	1090000.000
344.0	0.4184300	1090000.000
344.5	0.4030700	1090000.000
345.0	0.4589800	1090000.000
345.5	0.4893200	1090000.000
346.0	0.4777800	1090000.000
346.5	0.4865700	1090000.000
347.0	0.4940400	1090000.000
347.5	0.4767400	1090000.000
348.0	0.4751100	1090000.000
348.5	0.4833600	1090000.000
349.0	0.4656400	1090000.000
349.5	0.4780500	1090000.000
350.0	0.5279800	1040000.000
350.5	0.5674100	1040000.000
351.0	0.5517200	1040000.000
351.5	0.5302200	1040000.000
352.0	0.5179100	1040000.000
352.5	0.4896200	1040000.000
353.0	0.5204000	1040000.000
353.5	0.5722800	1040000.000
354.0	0.6049800	1040000.000
354.5	0.6115600	1040000.000
355.0	0.6114000	1040000.000
355.5	0.5902800	1040000.000
356.0	0.5538700	1040000.000
356.5	0.5194200	1040000.000
357.0	0.4567300	1040000.000
357.5	0.4621500	1040000.000
358.0	0.4300600	1040000.000
358.5	0.3992600	1040000.000
359.0	0.4695300	1040000.000
359.5	0.5654900	1040000.000
360.0	0.5981700	1020000.000
360.5	0.5653100	1020000.000
361.0	0.5202400	1020000.000
361.5	0.5095600	1020000.000
362.0	0.5342000	1020000.000
362.5	0.5851000	1020000.000
363.0	0.6019100	1020000.000
363.5	0.5854100	1020000.000
364.0	0.6062800	1020000.000
364.5	0.6005800	1020000.000
365.0	0.6235900	1020000.000
365.5	0.6862800	1020000.000
366.0	0.7353200	1020000.000
366.5	0.7365800	1020000.000
367.0	0.7228500	1020000.000
367.5	0.7091400	1020000.000
368.0	0.6675900	1020000.000
368.5	0.6631000	1020000.000
369.0	0.6931500	1020000.000
369.5	0.7446900	1020000.000
370.0	0.7550700	697000.000
370.5	0.6826100	697000.000
371.0	0.6933800	697000.000
371.5	0.7205100	697000.000
372.0	0.6744400	697000.000
372.5	0.6425300	697000.000
373.0	0.6188600	697000.000
373.5	0.5578600	697000.000
374.0	0.5564000	697000.000
374.5	0.5522700	697000.000

375.0	0.5893000	697000.000
375.5	0.6516200	697000.000
376.0	0.6748000	697000.000
376.5	0.6639000	697000.000
377.0	0.7122500	697000.000
377.5	0.7945500	697000.000
378.0	0.8559500	697000.000
378.5	0.8341800	697000.000
379.0	0.7438900	697000.000
379.5	0.6668300	697000.000
380.0	0.7007700	293000.000
380.5	0.7507500	293000.000
381.0	0.7638300	293000.000
381.5	0.6883700	293000.000
382.0	0.5867800	293000.000
382.5	0.5076200	293000.000
383.0	0.4549900	293000.000
383.5	0.4404900	293000.000
384.0	0.5096800	293000.000
384.5	0.6135900	293000.000
385.0	0.6735500	293000.000
385.5	0.6436300	293000.000
386.0	0.6210000	293000.000
386.5	0.6457000	293000.000
387.0	0.6514700	293000.000
387.5	0.6420400	293000.000
388.0	0.6358200	293000.000
388.5	0.6313600	293000.000
389.0	0.6854300	293000.000
389.5	0.7597000	293000.000
390.0	0.7969900	150000.000
390.5	0.8037100	150000.000
391.0	0.8513800	150000.000
391.5	0.8634400	150000.000
392.0	0.7949300	150000.000
392.5	0.6625700	150000.000
393.0	0.4797500	150000.000
393.5	0.3815200	150000.000
394.0	0.4956700	150000.000
394.5	0.6838500	150000.000
395.0	0.8077200	150000.000
395.5	0.8603800	150000.000
396.0	0.7565500	150000.000
396.5	0.5501700	150000.000
397.0	0.4261900	150000.000
397.5	0.6294500	150000.000
398.0	0.8524900	150000.000
398.5	1.0069000	150000.000
399.0	1.0693000	150000.000
399.5	1.1021000	150000.000
400.0	1.1141000	95200.000
401.0	1.1603000	95200.000
402.0	1.2061000	95200.000
403.0	1.1613000	95200.000
404.0	1.1801000	95200.000
405.0	1.1511000	95200.000
406.0	1.1227000	95200.000
407.0	1.1026000	95200.000
408.0	1.1514000	95200.000
409.0	1.2299000	95200.000
410.0	1.0485000	67400.000
411.0	1.1738000	67400.000
412.0	1.2478000	67400.000
413.0	1.1971000	67400.000
414.0	1.1842000	67400.000
415.0	1.2258000	67400.000

416.0	1.2624000	67400.000
417.0	1.2312000	67400.000
418.0	1.1777000	67400.000
419.0	1.2258000	67400.000
420.0	1.1232000	50000.000
421.0	1.2757000	50000.000
422.0	1.2583000	50000.000
423.0	1.2184000	50000.000
424.0	1.2117000	50000.000
425.0	1.2488000	50000.000
426.0	1.2135000	50000.000
427.0	1.1724000	50000.000
428.0	1.1839000	50000.000
429.0	1.0963000	50000.000
430.0	0.8746200	39200.000
431.0	0.7939400	39200.000
432.0	1.3207000	39200.000
433.0	1.2288000	39200.000
434.0	1.1352000	39200.000
435.0	1.2452000	39200.000
436.0	1.3659000	39200.000
437.0	1.3943000	39200.000
438.0	1.2238000	39200.000
439.0	1.1775000	39200.000
440.0	1.3499000	31100.000
441.0	1.3313000	31100.000
442.0	1.4250000	31100.000
443.0	1.4453000	31100.000
444.0	1.4084000	31100.000
445.0	1.4619000	31100.000
446.0	1.3108000	31100.000
447.0	1.4903000	31100.000
448.0	1.5081000	31100.000
449.0	1.5045000	31100.000
450.0	1.5595000	25500.000
451.0	1.6173000	25500.000
452.0	1.5482000	25500.000
453.0	1.4297000	25500.000
454.0	1.5335000	25500.000
455.0	1.5224000	25500.000
456.0	1.5724000	25500.000
457.0	1.5854000	25500.000
458.0	1.5514000	25500.000
459.0	1.5391000	25500.000
460.0	1.5291000	21000.000
461.0	1.5827000	21000.000
462.0	1.5975000	21000.000
463.0	1.6031000	21000.000
464.0	1.5544000	21000.000
465.0	1.5350000	21000.000
466.0	1.5673000	21000.000
467.0	1.4973000	21000.000
468.0	1.5619000	21000.000
469.0	1.5682000	21000.000
470.0	1.5077000	17200.000
471.0	1.5331000	17200.000
472.0	1.6126000	17200.000
473.0	1.5499000	17200.000
474.0	1.5671000	17200.000
475.0	1.6185000	17200.000
476.0	1.5631000	17200.000
477.0	1.5724000	17200.000
478.0	1.6230000	17200.000
479.0	1.5916000	17200.000
480.0	1.6181000	14800.000
481.0	1.6177000	14800.000

```
482.0    1.6236000        14800.000
483.0    1.6038000        14800.000
484.0    1.5734000        14800.000
485.0    1.5683000        14800.000
486.0    1.2716000        14800.000
487.0    1.4241000        14800.000
488.0    1.5413000        14800.000
489.0    1.4519000        14800.000
490.0    1.6224000        12700.000
491.0    1.5595000        12700.000
492.0    1.4869000        12700.000
493.0    1.5903000        12700.000
494.0    1.5525000        12700.000
495.0    1.6485000        12700.000
496.0    1.5676000        12700.000
497.0    1.5944000        12700.000
498.0    1.5509000        12700.000
499.0    1.5507000        12700.000
500.0    1.5451000        11100.000
501.0    1.4978000        11100.000
502.0    1.4966000        11100.000
503.0    1.5653000        11100.000
504.0    1.4587000        11100.000
505.0    1.5635000        11100.000
506.0    1.6264000        11100.000
507.0    1.5560000        11100.000
508.0    1.5165000        11100.000
509.0    1.5893000        11100.000
510.0    1.5481000        9700.000
511.0    1.5769000        9700.000
512.0    1.6186000        9700.000
513.0    1.5206000        9700.000
514.0    1.4885000        9700.000
515.0    1.5314000        9700.000
516.0    1.5455000        9700.000
517.0    1.2594000        9700.000
518.0    1.4403000        9700.000
519.0    1.3957000        9700.000
520.0    1.5236000        8800.000
521.0    1.5346000        8800.000
522.0    1.5690000        8800.000
523.0    1.4789000        8800.000
524.0    1.5905000        8800.000
525.0    1.5781000        8800.000
526.0    1.5341000        8800.000
527.0    1.3417000        8800.000
528.0    1.5357000        8800.000
529.0    1.6071000        8800.000
530.0    1.5446000        7850.000
531.0    1.6292000        7850.000
532.0    1.5998000        7850.000
533.0    1.4286000        7850.000
534.0    1.5302000        7850.000
535.0    1.5535000        7850.000
536.0    1.6199000        7850.000
537.0    1.4989000        7850.000
538.0    1.5738000        7850.000
539.0    1.5352000        7850.000
540.0    1.4825000        7050.000
541.0    1.4251000        7050.000
542.0    1.5511000        7050.000
543.0    1.5256000        7050.000
544.0    1.5792000        7050.000
545.0    1.5435000        7050.000
546.0    1.5291000        7050.000
547.0    1.5490000        7050.000
```

```
548.0    1.5049000        7050.000
549.0    1.5520000        7050.000
550.0    1.5399000        6390.000
551.0    1.5382000        6390.000
552.0    1.5697000        6390.000
553.0    1.5250000        6390.000
554.0    1.5549000        6390.000
555.0    1.5634000        6390.000
556.0    1.5366000        6390.000
557.0    1.4988000        6390.000
558.0    1.5310000        6390.000
559.0    1.4483000        6390.000
560.0    1.4740000        5780.000
561.0    1.5595000        5780.000
562.0    1.4847000        5780.000
563.0    1.5408000        5780.000
564.0    1.5106000        5780.000
565.0    1.5201000        5780.000
566.0    1.4374000        5780.000
567.0    1.5320000        5780.000
568.0    1.5180000        5780.000
569.0    1.4807000        5780.000
570.0    1.4816000        5320.000
571.0    1.4331000        5320.000
572.0    1.5134000        5320.000
573.0    1.5198000        5320.000
574.0    1.5119000        5320.000
575.0    1.4777000        5320.000
576.0    1.4654000        5320.000
577.0    1.5023000        5320.000
578.0    1.4560000        5320.000
579.0    1.4770000        5320.000
580.0    1.5020000        4880.000
581.0    1.5089000        4880.000
582.0    1.5320000        4880.000
583.0    1.5479000        4880.000
584.0    1.5448000        4880.000
585.0    1.5324000        4880.000
586.0    1.4953000        4880.000
587.0    1.5281000        4880.000
588.0    1.4934000        4880.000
589.0    1.2894000        4880.000
590.0    1.3709000        4490.000
591.0    1.4662000        4490.000
592.0    1.4354000        4490.000
593.0    1.4561000        4490.000
594.0    1.4491000        4490.000
595.0    1.4308000        4490.000
596.0    1.4745000        4490.000
597.0    1.4788000        4490.000
598.0    1.4607000        4490.000
599.0    1.4606000        4490.000
600.0    1.4753000        4140.000
601.0    1.4579000        4140.000
602.0    1.4360000        4140.000
603.0    1.4664000        4140.000
604.0    1.4921000        4140.000
605.0    1.4895000        4140.000
606.0    1.4822000        4140.000
607.0    1.4911000        4140.000
608.0    1.4862000        4140.000
609.0    1.4749000        4140.000
610.0    1.4686000        3810.000
611.0    1.4611000        3810.000
612.0    1.4831000        3810.000
613.0    1.4621000        3810.000
```

614.0	1.4176000	3810.000
615.0	1.4697000	3810.000
616.0	1.4310000	3810.000
617.0	1.4128000	3810.000
618.0	1.4664000	3810.000
619.0	1.4733000	3810.000
620.0	1.4739000	3520.000
621.0	1.4802000	3520.000
622.0	1.4269000	3520.000
623.0	1.4165000	3520.000
624.0	1.4118000	3520.000
625.0	1.4026000	3520.000
626.0	1.4012000	3520.000
627.0	1.4417000	3520.000
628.0	1.3631000	3520.000
629.0	1.4114000	3520.000
630.0	1.3924000	3270.000
631.0	1.4161000	3270.000
632.0	1.3638000	3270.000
633.0	1.4508000	3270.000
634.0	1.4284000	3270.000
635.0	1.4458000	3270.000
636.0	1.4128000	3270.000
637.0	1.4610000	3270.000
638.0	1.4707000	3270.000
639.0	1.4646000	3270.000
640.0	1.4340000	3040.000
641.0	1.4348000	3040.000
642.0	1.4376000	3040.000
643.0	1.4525000	3040.000
644.0	1.4462000	3040.000
645.0	1.4567000	3040.000
646.0	1.4150000	3040.000
647.0	1.4086000	3040.000
648.0	1.3952000	3040.000
649.0	1.3519000	3040.000
650.0	1.3594000	2810.000
651.0	1.4447000	2810.000
652.0	1.3871000	2810.000
653.0	1.4311000	2810.000
654.0	1.4153000	2810.000
655.0	1.3499000	2810.000
656.0	1.1851000	2810.000
657.0	1.2393000	2810.000
658.0	1.3855000	2810.000
659.0	1.3905000	2810.000
660.0	1.3992000	2580.000
661.0	1.3933000	2580.000
662.0	1.3819000	2580.000
663.0	1.3844000	2580.000
664.0	1.3967000	2580.000
665.0	1.4214000	2580.000
666.0	1.4203000	2580.000
667.0	1.4102000	2580.000
668.0	1.4150000	2580.000
669.0	1.4394000	2580.000
670.0	1.4196000	2380.000
671.0	1.4169000	2380.000
672.0	1.3972000	2380.000
673.0	1.4094000	2380.000
674.0	1.4074000	2380.000
675.0	1.3958000	2380.000
676.0	1.4120000	2380.000
677.0	1.3991000	2380.000
678.0	1.4066000	2380.000
679.0	1.3947000	2380.000

680.0	1.3969000	2210.000
681.0	1.3915000	2210.000
682.0	1.3981000	2210.000
683.0	1.3830000	2210.000
684.0	1.3739000	2210.000
685.0	1.3748000	2210.000
686.0	1.3438000	2210.000
687.0	0.9682400	2210.000
688.0	1.1206000	2210.000
689.0	1.1278000	2210.000
690.0	1.1821000	2050.000
691.0	1.2333000	2050.000
692.0	1.2689000	2050.000
693.0	1.2609000	2050.000
694.0	1.2464000	2050.000
695.0	1.2714000	2050.000
696.0	1.2684000	2050.000
697.0	1.3403000	2050.000
698.0	1.3192000	2050.000
699.0	1.2918000	2050.000
700.0	1.2823000	1900.000
701.0	1.2659000	1900.000
702.0	1.2674000	1900.000
703.0	1.2747000	1900.000
704.0	1.3078000	1900.000
705.0	1.3214000	1900.000
706.0	1.3144000	1900.000
707.0	1.3090000	1900.000
708.0	1.3048000	1900.000
709.0	1.3095000	1900.000
710.0	1.3175000	1770.000
711.0	1.3155000	1770.000
712.0	1.3071000	1770.000
713.0	1.2918000	1770.000
714.0	1.3029000	1770.000
715.0	1.2587000	1770.000
716.0	1.2716000	1770.000
717.0	1.1071000	1770.000
718.0	1.0296000	1770.000
719.0	0.9231800	1770.000
720.0	0.9855000	1660.000
721.0	1.0861000	1660.000
722.0	1.2407000	1660.000
723.0	1.1444000	1660.000
724.0	1.0555000	1660.000
725.0	1.0380000	1660.000
726.0	1.0813000	1660.000
727.0	1.0850000	1660.000
728.0	1.0400000	1660.000
729.0	1.0466000	1660.000
730.0	1.1285000	1540.000
731.0	1.0703000	1540.000
732.0	1.1534000	1540.000
733.0	1.1962000	1540.000
734.0	1.2357000	1540.000
735.0	1.2178000	1540.000
736.0	1.2059000	1540.000
737.0	1.2039000	1540.000
738.0	1.2269000	1540.000
739.0	1.1905000	1540.000
740.0	1.2195000	1420.000
741.0	1.2148000	1420.000
742.0	1.2153000	1420.000
743.0	1.2405000	1420.000
744.0	1.2503000	1420.000
745.0	1.2497000	1420.000

746.0	1.2470000	1420.000
747.0	1.2477000	1420.000
748.0	1.2401000	1420.000
749.0	1.2357000	1420.000
750.0	1.2341000	1300.000
751.0	1.2286000	1300.000
752.0	1.2330000	1300.000
753.0	1.2266000	1300.000
754.0	1.2420000	1300.000
755.0	1.2383000	1300.000
756.0	1.2232000	1300.000
757.0	1.2221000	1300.000
758.0	1.2295000	1300.000
759.0	1.1945000	1300.000
760.0	0.2660400	1190.000
761.0	0.1539600	1190.000
762.0	0.6876600	1190.000
763.0	0.3795200	1190.000
764.0	0.5387800	1190.000
765.0	0.6860100	1190.000
766.0	0.8146100	1190.000
767.0	0.9741700	1190.000
768.0	1.1138000	1190.000
769.0	1.1278000	1190.000
770.0	1.1608000	1100.000
771.0	1.1686000	1100.000
772.0	1.1778000	1100.000
773.0	1.1771000	1100.000
774.0	1.1771000	1100.000
775.0	1.1771000	1100.000
776.0	1.1798000	1100.000
777.0	1.1727000	1100.000
778.0	1.1713000	1100.000
779.0	1.1765000	1100.000
780.0	1.1636000	1010.000
781.0	1.1607000	1010.000
782.0	1.1662000	1010.000
783.0	1.1614000	1010.000
784.0	1.1536000	1010.000
785.0	1.1586000	1010.000
786.0	1.1592000	1010.000
787.0	1.1450000	1010.000
788.0	1.1305000	1010.000
789.0	1.1257000	1010.000
790.0	1.0910000	928.000
791.0	1.1058000	928.000
792.0	1.0953000	928.000
793.0	1.0875000	928.000
794.0	1.0972000	928.000
795.0	1.0932000	928.000
796.0	1.0742000	928.000
797.0	1.0913000	928.000
798.0	1.1121000	928.000
799.0	1.0905000	928.000
800.0	1.0725000	850.000
801.0	1.0843000	850.000
802.0	1.0856000	850.000
803.0	1.0657000	850.000
804.0	1.0782000	850.000
805.0	1.0545000	850.000
806.0	1.0974000	850.000
807.0	1.0859000	850.000
808.0	1.0821000	850.000
809.0	1.0548000	850.000
810.0	1.0559000	775.000
811.0	1.0533000	775.000

812.0	1.0268000	775.000
813.0	1.0086000	775.000
814.0	0.9035600	775.000
815.0	0.8952300	775.000
816.0	0.8321600	775.000
817.0	0.8518300	775.000
818.0	0.8225900	775.000
819.0	0.9051900	775.000
820.0	0.8618800	707.000
821.0	0.9976400	707.000
822.0	0.9515700	707.000
823.0	0.6727100	707.000
824.0	0.9350600	707.000
825.0	0.9693500	707.000
826.0	0.9338100	707.000
827.0	0.9846500	707.000
828.0	0.8497900	707.000
829.0	0.9293000	707.000
830.0	0.9160100	647.000
831.0	0.9239200	647.000
832.0	0.8942600	647.000
833.0	0.9565000	647.000
834.0	0.9341200	647.000
835.0	1.0032000	647.000
836.0	0.9723400	647.000
837.0	1.0092000	647.000
838.0	0.9990100	647.000
839.0	1.0013000	647.000
840.0	1.0157000	591.000
841.0	1.0101000	591.000
842.0	0.9970300	591.000
843.0	1.0053000	591.000
844.0	0.9863100	591.000
845.0	1.0165000	591.000
846.0	1.0187000	591.000
847.0	0.9917000	591.000
848.0	0.9921700	591.000
849.0	0.9859600	591.000
850.0	0.8937200	535.000
851.0	0.9749300	535.000
852.0	0.9692700	535.000
853.0	0.9648600	535.000
854.0	0.8511200	535.000
855.0	0.9130000	535.000
856.0	0.9731700	535.000
857.0	0.9916600	535.000
858.0	0.9919600	535.000
859.0	0.9917100	535.000
860.0	0.9881600	480.000
861.0	0.9867900	480.000
862.0	0.9944900	480.000
863.0	1.0005000	480.000
864.0	0.9791600	480.000
865.0	0.9632400	480.000
866.0	0.8490000	480.000
867.0	0.9154600	480.000
868.0	0.9592000	480.000
869.0	0.9495600	480.000
870.0	0.9675500	432.000
871.0	0.9538700	432.000
872.0	0.9668600	432.000
873.0	0.9572100	432.000
874.0	0.9404200	432.000
875.0	0.9268700	432.000
876.0	0.9527700	432.000
877.0	0.9561500	432.000

878.0	0.9523700	432.000
879.0	0.9365600	432.000
880.0	0.9395700	383.000
881.0	0.9086100	383.000
882.0	0.9324500	383.000
883.0	0.9292700	383.000
884.0	0.9330500	383.000
885.0	0.9442300	383.000
886.0	0.9075200	383.000
887.0	0.9106200	383.000
888.0	0.9222800	383.000
889.0	0.9345500	383.000
890.0	0.9239300	343.000
891.0	0.9258400	343.000
892.0	0.9088100	343.000
893.0	0.8732700	343.000
894.0	0.8513000	343.000
895.0	0.8135700	343.000
896.0	0.7625300	343.000
897.0	0.6656600	343.000
898.0	0.7178000	343.000
899.0	0.5487100	343.000
900.0	0.7426000	306.000
901.0	0.5993300	306.000
902.0	0.6679100	306.000
903.0	0.6888900	306.000
904.0	0.8445700	306.000
905.0	0.8170900	306.000
906.0	0.7755800	306.000
907.0	0.6385400	306.000
908.0	0.6521700	306.000
909.0	0.7043100	306.000
910.0	0.6246700	272.000
911.0	0.6680800	272.000
912.0	0.6889300	272.000
913.0	0.6283400	272.000
914.0	0.6264900	272.000
915.0	0.6783600	272.000
916.0	0.5764600	272.000
917.0	0.7301700	272.000
918.0	0.5927100	272.000
919.0	0.7387700	272.000
920.0	0.7441400	240.000
921.0	0.7804900	240.000
922.0	0.7002600	240.000
923.0	0.7450400	240.000
924.0	0.7215000	240.000
925.0	0.7111000	240.000
926.0	0.7033100	240.000
927.0	0.7874200	240.000
928.0	0.5896800	240.000
929.0	0.5512700	240.000
930.0	0.4321000	210.000
931.0	0.4092100	210.000
932.0	0.3008600	210.000
933.0	0.2484100	210.000
934.0	0.1438000	210.000
935.0	0.2508400	210.000
936.0	0.1614200	210.000
937.0	0.1633800	210.000
938.0	0.2005800	210.000
939.0	0.3988700	210.000
940.0	0.4718100	183.000
941.0	0.3719500	183.000
942.0	0.4053200	183.000
943.0	0.2783400	183.000

944.0	0.2857900	183.000
945.0	0.3682100	183.000
946.0	0.1946100	183.000
947.0	0.3711200	183.000
948.0	0.2742300	183.000
949.0	0.4939600	183.000
950.0	0.1472600	157.000
951.0	0.4837800	157.000
952.0	0.2689100	157.000
953.0	0.3436200	157.000
954.0	0.4241100	157.000
955.0	0.3411700	157.000
956.0	0.3282100	157.000
957.0	0.2706700	157.000
958.0	0.4610100	157.000
959.0	0.3738500	157.000
960.0	0.4206600	134.000
961.0	0.4612000	134.000
962.0	0.4417400	134.000
963.0	0.5050300	134.000
964.0	0.4586000	134.000
965.0	0.5037400	134.000
966.0	0.5027500	134.000
967.0	0.5024000	134.000
968.0	0.6521000	134.000
969.0	0.6862200	134.000
970.0	0.6346100	114.000
971.0	0.7139700	114.000
972.0	0.6876500	114.000
973.0	0.6064800	114.000
974.0	0.5752900	114.000
975.0	0.5898700	114.000
976.0	0.5719100	114.000
977.0	0.6386400	114.000
978.0	0.6150900	114.000
979.0	0.6381500	114.000
980.0	0.6046800	95.900
981.0	0.7133800	95.900
982.0	0.6921800	95.900
983.0	0.6686500	95.900
984.0	0.7373200	95.900
985.0	0.6881700	95.900
986.0	0.7508300	95.900
987.0	0.7392800	95.900
988.0	0.7346200	95.900
989.0	0.7490600	95.900
990.0	0.7322700	79.200
991.0	0.7535800	79.200
992.0	0.7510200	79.200
993.0	0.7372800	79.200
994.0	0.7541000	79.200
995.0	0.7517600	79.200
996.0	0.7488400	79.200
997.0	0.7397100	79.200
998.0	0.7388700	79.200
999.0	0.7385700	79.200
1000.0	0.7353200	64.000
1001.0	0.7444200	64.000
1002.0	0.7280500	64.000
1003.0	0.7344200	64.000
1004.0	0.7233600	64.000
1005.0	0.6817400	64.000
1006.0	0.7125200	64.000
1007.0	0.7275300	64.000
1008.0	0.7268500	64.000
1009.0	0.7197200	64.000

1010.0	0.7191400	51.100
1011.0	0.7227800	51.100
1012.0	0.7187700	51.100
1013.0	0.7176100	51.100
1014.0	0.7206800	51.100
1015.0	0.7081700	51.100
1016.0	0.7112900	51.100
1017.0	0.7033700	51.100
1018.0	0.7142200	51.100
1019.0	0.6887800	51.100
1020.0	0.6989600	39.900
1021.0	0.7017500	39.900
1022.0	0.6897000	39.900
1023.0	0.6950800	39.900
1024.0	0.6905800	39.900
1025.0	0.6975300	39.900
1026.0	0.6963600	39.900
1027.0	0.6930500	39.900
1028.0	0.6938500	39.900
1029.0	0.6862800	39.900
1030.0	0.6905500	30.200
1031.0	0.6873600	30.200
1032.0	0.6878700	30.200
1033.0	0.6761300	30.200
1034.0	0.6801500	30.200
1035.0	0.6823400	30.200
1036.0	0.6820200	30.200
1037.0	0.6749700	30.200
1038.0	0.6717200	30.200
1039.0	0.6763600	30.200
1040.0	0.6717000	22.600
1041.0	0.6717600	22.600
1042.0	0.6720000	22.600
1043.0	0.6652500	22.600
1044.0	0.6683300	22.600
1045.0	0.6645200	22.600
1046.0	0.6471400	22.600
1047.0	0.6569400	22.600
1048.0	0.6627400	22.600
1049.0	0.6589600	22.600
1050.0	0.6546300	16.300
1051.0	0.6552100	16.300
1052.0	0.6511800	16.300
1053.0	0.6491900	16.300
1054.0	0.6464600	16.300
1055.0	0.6484700	16.300
1056.0	0.6464100	16.300
1057.0	0.6448200	16.300
1058.0	0.6381800	16.300
1059.0	0.6187500	16.300
1060.0	0.6358500	11.100
1061.0	0.6212100	11.100
1062.0	0.6326600	11.100
1063.0	0.6223900	11.100
1064.0	0.6319600	11.100
1065.0	0.6291300	11.100
1066.0	0.6171300	11.100
1067.0	0.6203200	11.100
1068.0	0.6194400	11.100
1069.0	0.5862600	11.100
1070.0	0.6046900	8.000
1071.0	0.6166100	8.000
1072.0	0.6153600	8.000
1073.0	0.6036300	8.000
1074.0	0.6215800	8.000
1075.0	0.5925200	8.000

1076.0	0.6147100	8.000
1077.0	0.6043400	8.000
1078.0	0.6032100	8.000
1079.0	0.6047400	8.000
1080.0	0.5972200	6.200
1081.0	0.5808300	6.200
1082.0	0.5894000	6.200
1083.0	0.5981400	6.200
1084.0	0.5785200	6.200
1085.0	0.5933000	6.200
1086.0	0.5541000	6.200
1087.0	0.5669700	6.200
1088.0	0.5931700	6.200
1089.0	0.5791900	6.200
1090.0	0.5557300	4.700
1091.0	0.5883500	4.700
1092.0	0.5812400	4.700
1093.0	0.5105800	4.700
1094.0	0.5396500	4.700
1095.0	0.5206700	4.700
1096.0	0.5032300	4.700
1097.0	0.5785200	4.700
1098.0	0.5029100	4.700
1099.0	0.5077200	4.700
1100.0	0.4857700	3.500
1101.0	0.4969600	3.500
1102.0	0.4688300	3.500
1103.0	0.4663700	3.500
1104.0	0.4676500	3.500
1105.0	0.5064400	3.500
1106.0	0.3979200	3.500
1107.0	0.4830400	3.500
1108.0	0.4156500	3.500
1109.0	0.4127800	3.500
1110.0	0.4789900	2.700
1111.0	0.3315400	2.700
1112.0	0.4135700	2.700
1113.0	0.2685000	2.700
1114.0	0.2998500	2.700
1115.0	0.2498700	2.700
1116.0	0.2013600	2.700
1117.0	0.0796180	2.700
1118.0	0.2175300	2.700
1119.0	0.1131700	2.700
1120.0	0.1418900	2.000
1121.0	0.1858600	2.000
1122.0	0.0816860	2.000
1123.0	0.1281700	2.000
1124.0	0.1087000	2.000
1125.0	0.1442800	2.000
1126.0	0.0515890	2.000
1127.0	0.1572500	2.000
1128.0	0.0992240	2.000
1129.0	0.1059100	2.000
1130.0	0.0705740	1.500
1131.0	0.2956000	1.500
1132.0	0.2341100	1.500
1133.0	0.1533100	1.500
1134.0	0.0417400	1.500
1135.0	0.0154620	1.500
1136.0	0.1287600	1.500
1137.0	0.2878500	1.500
1138.0	0.2032900	1.500
1139.0	0.2985000	1.500

Appendix G

Organic PV Model Source Code

G.1 The OrganicPV.m MATLAB Function

Listing G.1: Organic PV Model MATLAB function.

```
% Research Project Matlab Script for ORGANIC BHJ PV
% Name of function file: research_proj_organic_pv.m

% SPECIAL NOTE: The concepts behind this Matlab code were
% derived mainly from the Koster et al research paper and
% it's references.

% Purpose of function: To set boundary conditions and a first
% guess of carrier concentrations, to calculate it's
% derivatives and to solve the Poisson as part of the
% Gummel iterative method.

% Input variables: none
% Output variables: none
% Written by: Craig Gardner
% Date of last revision: 12/9/08

% ---------- SETUP ----------
clear all;
close all;
clc;
clf;

% ---------- PHYSICAL CONSTANTS ----------
% electronic charge (coulomb)
q = 1.602e-19;
% Boltzmann's constant (J/K)
k = 1.380e-23;
% Speed of light in a vaccum
c = 2.998e8; % m/s
% Planck's constant
h = 6.626e-34; % J.s
% Stephan - Boltzmann constant
sigma = 5.67e-8; % J/m^2.s.K^4

% ---------- PV SYSTEM INPUT VALUES ----------
% absolute temperature K (degrees kelvin)
T = 300;
%T = 298.15; %25 deg C
% thermal voltage
Vt = k*T/q; %V
% applied voltage
Va = 100;
%Va = 2.74; % ????????? - WHAT UNITS - ENERGY - VOLTAGE
% band gap energy
Egap = 1.34; %eV
% electron mobility
mu_n = 2.5e-7; % m^2/(V.s)
% hole mobility
mu_p = 3e-8; % m^2/(V.s)
% electron diffusion coefficient
Dn = mu_n * Vt; % m^2/s
% hole diffusion coefficient
Dp = mu_p * Vt; % m^2/s
```

```
% effective density of states
Nc = 2.5e25; %m^3
% AVERAGE GENERATION RATE - NEED TO CALC NET GENERATION
% RATE U(x) WITH OPTICAL MODEL
G = 1.6e27; % m^-3.s^-1
% width of active layer
layer_width = 120e-9; %120nm
% no of increments in active layer
num = 100;
%num = 1000;
% increment in the x axis
%delta_x = 0.5;
delta_x = layer_width / num;

% permittivity of free space
epsilom_o = 8.854e-12; %F/m
% relative permittivity
epsilom_r = 1; % for air
% dielectric constant - override the above equation with
% the value from Koster et al
epsilom = 3e-11; %F/m
% spatially averaged
epsilom_in_brackets = 3e-11; %F/m
% dielectric constant (E = Eo.Er)
%epsilom = epsilom_o * epsilom_in_brackets;

% ---------- CENTRAL DIFFERENCES SOLUTION TO POISSON ----------
% ---------- SUGGESTED BY DR TONY AHFOCK TO LOOK IN ----------
% ---------- & CONSQUENTLY TAKEN FROM FIELDS AND ----------
% ---------- WAVES STUDY BOOK & TEXT ----------

% psi boundary conditions
%psi_0 = 0;
psi_0 = 0;
psi_L = psi_0 + Egap - Va;

% ---------- SET UP ELECTRON & HOLE ----------
% ---------- CONCENTRATION INITIAL GUESSES ----------
% create an empty row vector for electron densities
n = [];
% fill row vector for electron densities with guesses
for i = 1:num
    % make all entries the same guesses taken from
    % Koster et al paper
    n(i) = 1e25;
end
% add start and end conditions to row vector of electron
% densities
n = [ Nc    n    (Nc * exp(-Egap/Vt)) ];
% create an empty row vector for hole densities
p = [];
% fill row vector for hole densities with guesses
for i = 1:num
    % make all entries the same guesses taken from
    % Koster et al paper
    p(i) = 1e17;
end
% add start and end conditions to row vector of hole
% densities
```

```
p = [ (Nc * exp(-Egap/Vt))   p    Nc ];

% ---------- SET UP MATRICES ----------
% A.x = b
% create a sparse nxn array A
A = sparse(num,num);
% alter array A with values for central differences to make
% tri-diagonal
for i = 1:num
    A(i,i) = -2;
    if i < num
        A(i,i+1) = 1;
    end
    if i > 1
        A(i,i-1) = 1;
    end
end
A;
% THIS WAS DONE TO CHECK THAT PSI PROFILE IS LINEAR WHEN
% SOLVED AS LAPLACE
% create a column vector b of results
%b = zeros(num,1);
%b(1) = -psi_0;
%b(num) = -psi_L;

% SOLVE AS POISSON
% create a column vector b of results
b = zeros(num,1);
b(1) = -psi_0 + delta_x^2 * q / epsilom * (n(2) - p(2));
for i = 2:num-1
    b(i) = delta_x^2 * q / epsilom * (n(i+1) - p(i+1));
end
b(num) = -psi_L + delta_x^2 * q / epsilom * (n(num+2) - p(num
    +2));

% calculate column vector of potentials
x = A\b;
% ---------- PSI RESULTS ----------
% add potential boundary conditions and transfer potential
% solution column vector to a vector psi to make more sense
psi = [ psi_0; x; psi_L ];
% set up an x axis of active layer width (nm) for this and
% following plots
x_ax = [ 0:((layer_width*1e9) / (num+1)): (layer_width*1e9) ];
length(psi);
% plot potential profile
figure(1)
plot(x_ax ,psi)
xlabel('Active Layer Width (nm)');
ylabel('Potential, \psi (V)');
title('Potential Profile in Active Layer')
xlim([ 0 (layer_width*1e9) ])

% ---------- CALCULATE d psi /dx USING CENTRAL DIFFERENCES ----
% ---------- (KOSTER ET AL) -----
% create a null vector for dpsi/dx
dpsi_dx = [];
% create the vector dpsi/dx from the psi vector using central
% differences
```

```
dpsi_dx(1) = (psi(2)-psi(1))/delta_x;
for i = 2:(length(psi)-1)
    dpsi_dx(i) = (psi(i+1)-psi(i-1))/( 2 * delta_x);
end
dpsi_dx(length(psi)) = (psi(length(psi))-psi(length(psi)-1))/
    delta_x;
length(dpsi_dx);
figure(2)
plot(x_ax ,dpsi_dx)
xlabel('Active Layer Width (nm)');
ylabel('Electric Field , F or \delta\psi/\deltam (V/m)');
title('Electric Field (Derivative of Potential) Profile in
    Active Layer')
xlim([ 0 (layer_width*1e9) ])
```